MODELLING, ANALYSIS AND SYNTHESIS OF SOME STRUCTURES FOR NETWORKED CONTROL

Teză destinată obţinerii
titlului ştiinţific de doctor inginer
la
Universitatea Politehnica Timişoara
în domeniul INGINERIA SISTEMELOR
de către

Ing. Octavian Ștefan

Conducător ştiinţific:	prof. univ. dr. ing. Toma-Leonida Dragomir
Referenţi ştiinţifici:	prof. univ. dr. ing. Ioan Dumitrache
	prof. univ. dr. ing. Hubert Roth
	prof. univ. dr. ing. Gheorghe-Daniel Andreescu

Ziua susţinerii tezei: 09 octombrie 2013

ACKNOWLEDGEMENTS

I would like to thank to all the people who have helped, supported and inspired me during my doctoral study.

First and foremost I would like to thank my supervisor Professor Toma-Leonida Dragomir for his continuous support and guidance throughout this scientific journey. I especially appreciate his wisdom and his capacity to adjust to new interdisciplinary research areas, like cyber-physical systems or biomedical systems. Professor Dragomir has distinguished himself also as a pedagogical role model, by always finding a balance between teaching and research, having endless patience and willingness in shaping future engineers. Through his meticulous approach to each scientific problem, backed up by a careful attention to every detail, he showed me what scientific rigorousness means, for which I am deeply grateful.

Next, I would like to express my appreciation to Professor Ioan Silea, Head of the Department of Automation and Applied Informatics, for introducing me to the subject of Computer Networks, thus opening the door to a fruitful collaboration from that point forth, as his student and then as a teaching assistant. Throughout my entire academic career he has been a continuous source of advice, always helping me overcome each challenge that emerged. During my doctoral study, Professor Silea facilitated my access to the department's high-tech control equipment, while also helping me with different technical advices.

Four years ago, with the help of Professor Dragomir, I had the extraordinary chance to meet a young student with an immense thirst for knowledge: Alexandru Codrean. These last years, he became my colleague and close friend. During all this time, he worked with me, side by side, around the clock, helping me overcome all the difficulties encountered. He always pushed me to go further and never let me give up. Without his help, this thesis would exist in a lesser form. For this, I am very grateful to him.

I am grateful to the staff members of the Department of Automation and Applied Informatics, especially to several colleagues with whom I had the opportunity to engage in constructive discussions: Lecturer Adrian Korodi, Lecturer Sorin Nanu, Lecturer Bogdan Groza, Teaching Assistant Gabriel Vlasiu, Teaching Assistant Cosmin Koch-Ciobotaru, Teaching Assistant Bogdan Radac, Lecturer Raul Robu, Teaching Assistant Flavius Petcut, Teaching Assistant Ana-Maria Dan, Lecturer Adriana Albu, Lecturer Loredana Stanciu. Sincere thanks go to Lecturer Dorina Popescu for providing the controlled process used for experimental results.

Also, I would like to thank all my colleagues from Agora IT&C Company for their help. I would especially like to thank my boss and my friend Mr. Mircea Preunca for his understanding and support. I would like to mention Mihai Groza for his help with the graphical material.

I would like to thank the members of my Ph.D. Committee for accepting to review my thesis and for their help and suggestions concerning my research.

Last but not least, I would like to thank my family, especially my parents Ana and Dinu who made me the person I am today, my girlfriend Cristina and her parents, Maria and Ilia, my cousin Cecilia and to my best friend Lucian Lucoaie. A special thank you goes to Cris for all the sacrifices made during my studies, for her unconditional love and support. Thank you, I love you all.

Ștefan, Octavian

MODELLING, ANALYSIS AND SYNTHESIS OF SOME STRUCTURES FOR NETWORKED CONTROL

Teze de doctorat ale UPT, Seria 12, Nr. 7, Editura Politehnica, 2013, 112 pagini, 70 figuri.

ISSN: 2068-7990

ISBN: 978-606-554-717-9

Cuvinte cheie:

Networked control, network model, switched system, disturbance observer.

Rezumat,

The Ph.D. Thesis addresses the main inherent issues in networked control systems. First, a unified and systematic framework is outlined, which captures all network transmission phenomena from an input-output perspective along with possible data handling strategies as an aid for different control solutions. Then, a mathematical model, which captures simultaneously all the identified network transmission phenomena, is developed for the analysis and synthesis of future network control structures. Finally, the thesis focuses on the design of two types of control strategies for compensating the network induced disturbances – one based on disturbance observers and the other one based on switched compensators – along with the stability analysis and performance evaluation.

TABLE OF CONTENTS

TABLE OF FIGURES

ABBREVIATIONS

CAN	Controller Area Network
CDOB	Communication Disturbance Observer
CVX	Convex Optimization Toolbox
DC	Direct Current
DCO	Disturbance Compensator
DOB	Disturbance Observer
EMF	Electromagnetic Field
FD	Forwarding Delay
GPS	Global Positioning System
ICS	Internet-based Control System
IPTSE	Integral of Powered Time-Weighted Square Error
ITAE	Integral of Time-Weighted Absolute Error
IS	Irregular Situation
ISC	Interpolative Static Characteristic
ISE	Integral of Square Error
NCS	Networked Control System
TCP/IP	Transmission Control Protocol / Internet Protocol
LAN	Local Area Network
LMI	Linear Matrix Inequality
LQ	Linear Quadratic
LQR	Linear Quadratic Regulator
LTI	Linear Time Invariant
MD	Medium Delay
MIMO	Multiple Input Multiple Output
NL	Network Latency
NTB	Network Transmission Block
NTM	Network Transmission Model
NTP	Network Time Protocol
OWD	One Way Delay

PC	Personal Computer
PD	Proportional Derivative
PrD	Propagation Delay
PI	Proportional Integral
PID	Proportional Integral Derivative
PTP	Precision Time Protocol
QD	Queuing Delay
QoC	Quality of Control
QoS	Quality of Service
RTT	Round Trip Time
SD	Serialization Delay
SISO	Single Input Single Output
SS	Signal Speed
TD	Transmission Delay
UDP	User Datagram Protocol
VF	Velocity Factor
WAN	Wide Area Network

1. INTRODUCTION

1.1. Networked Control Systems

A networked control system (NCS) is a feedback control system where information between the components of the control loop is transferred using electronic real-time networks ([1]). To the basic control system from Fig. 1.1, the NCS from Fig. 1.2 can be associated from a functional point of view. Here, data from the sensors to the controller and from the controller to the actuator is sent using communication networks.

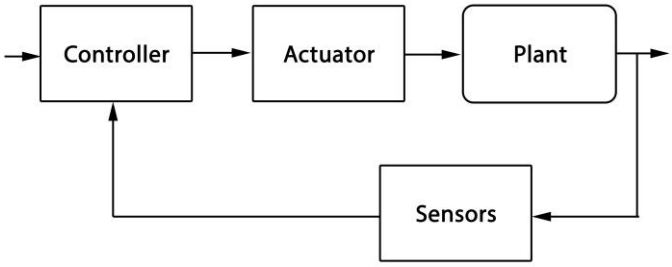

Fig. 1.1 - Generic control system

The increase in data processing power and the decrease of equipment costs have facilitated an extraordinary expansion of computer networks in the last years. Low cost, high fault tolerance and reliability of today's networks opened a new perspective in the field of control structure design. The main advantages of a NCS are reduced costs and wiring, modularity, high reliability and flexibility, robustness to failure, ease of re-configurability, maintenance and diagnostics ([2], [3]).

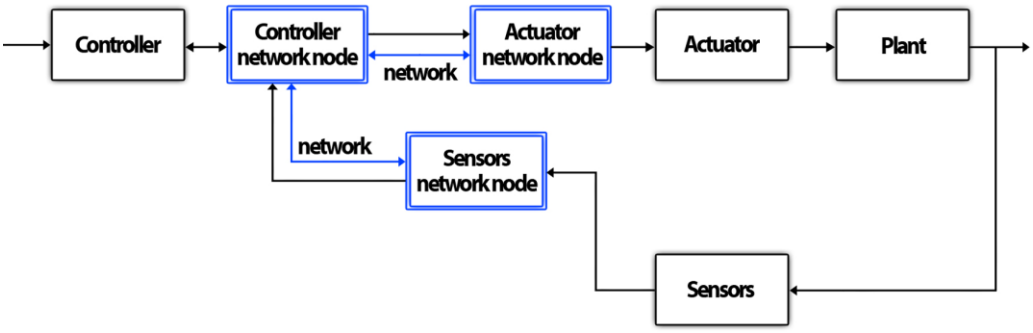

Fig. 1.2 - Generic NCS

The idea of using computer networks for control systems is receiving more and more attention from the scientific community. The research direction is of an interdisciplinary nature, involving knowledge from control theory, computer science, communication networks and information theory ([4]).

The increased interest in NCSs is sustained by their large area of applicability, several examples being: automotive industry ([5]), teleoperation ([6]), remote surgery ([7]) and unmanned vehicles ([8]).

Although it has a lot of advantages, a NCS has also some shortcomings, induced by the network components, like time varying delays and data loss, which need to be overcome before the NCS can be largely implemented in industrial applications ([9]).

1.2. Networked Control System Types

Depending on the distance between the control equipment parts there are two types of NCSs: local NCSs or shared-medium control systems and remote NCSs or teleoperation systems ([10]).

1.2.1. Local Networked Control Systems

Shared-medium control systems use the same local area network to connect all the control system's components (Fig. 1.3). The main advantages of this type of networked control are: reduced wire complexity, reduced cost, high reliability and flexibility. Furthermore, the usage of the same network permits data sharing between the control loops. This setup is often used in automotive industry and industrial process automation.

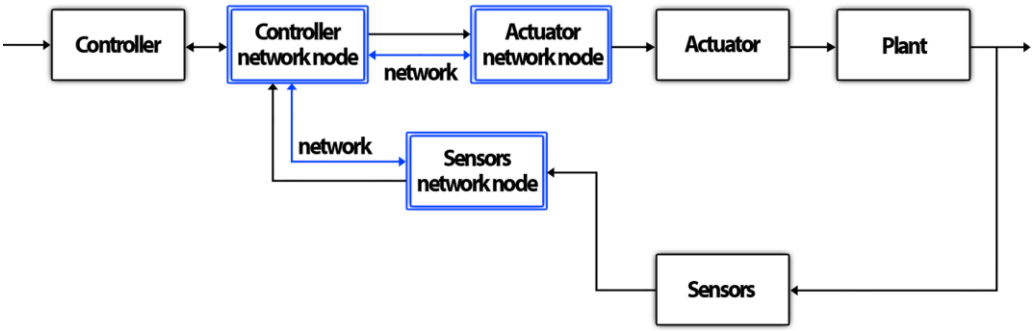

Fig. 1.3 – Local NCS

1.2.2. Remote Networked Control Systems

A remote NCS is a NCS where the main controller is located far away from the plant and it is connected to the rest of system using communication networks. There are several different structures for remote NCSs. A first approach (hierarchical structure) has a central controller and several control subsystems, each containing a local controller, sensors and actuators (Fig. 1.4). Each subsystem receives a control signal from the central controller, signal used as reference by the local controller and sends as feedback signal the data from the sensors or a status signal from the local controller. A second approach (direct structure) contains only one control loop and uses a remote controller to control through the network a local plant (Fig. 1.5). Several other hybrid structures exist that combine the direct and hierarchical structures.

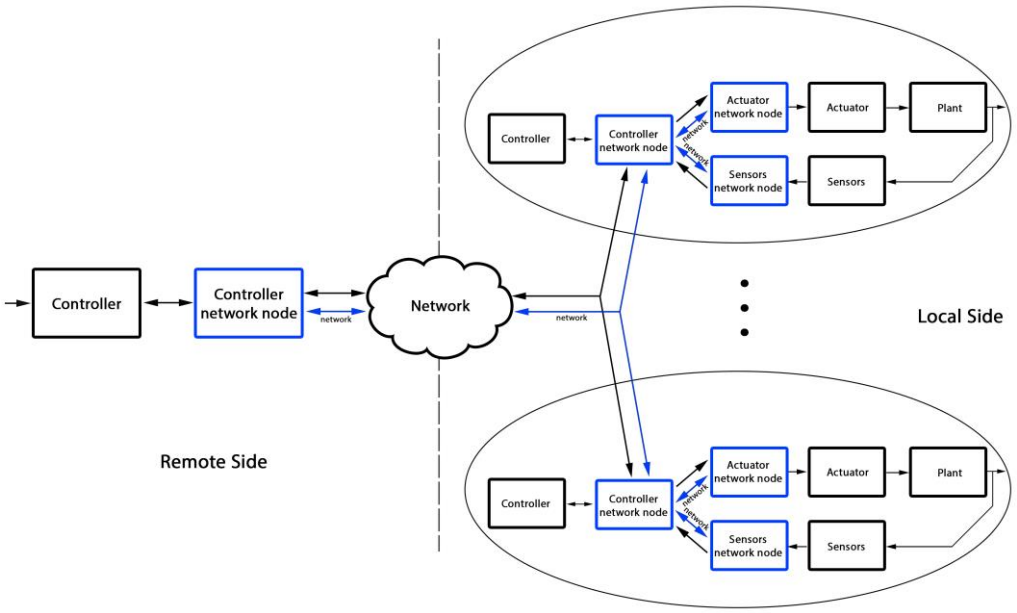

Fig. 1.4 – Remote NCS – hierarchical structure

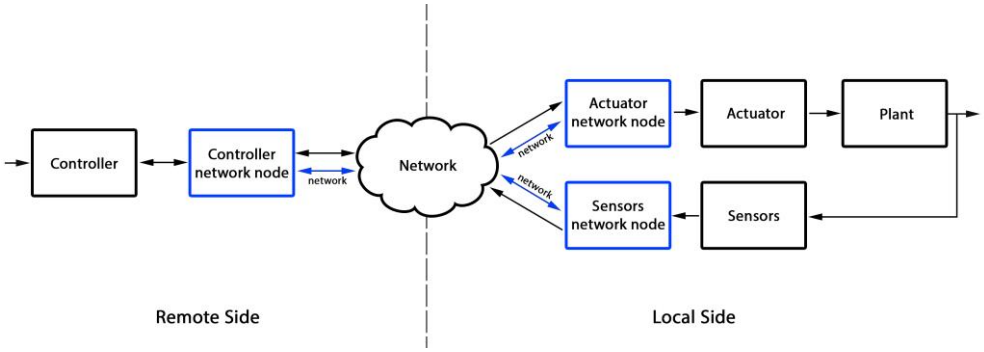

Fig. 1.5 – Remote NCS – direct structure

1.3. Issues of Networked Control Systems

The design methods from classical control theory use several idealizations as working hypothesis: instantaneous signal transmissions between the control system's components, infinite computational and transmission capacity, synchronized subsystems and constant sampling rate, no energy constraints, assured data integrity and security ([11], [12], [13], [14], [15], [16]). Depending on the type of the control application, the network induced issues can have a critical impact on the system's performance and cannot be ignored. So, when designing NCSs, the idealizations from classic theory do not always apply. In this context, the analysis of the most important issues which influence the behaviour of the NCS is necessary.

For a better understanding of the effect of network induced issues on a NCS, an example is presented in Appendix 1. As one can see, the time varying delay and information loss lead to oscillations in the system's response and sometimes even to the instability of the controlled system.

1.3.1. Time Delay

1.3.1.1. Time Delay Inducing Operations in Networked Control Systems

In a NCS, data transmission delays can be divided into two categories: device delays and network delays ([17]).

When transferring data from sensors to the controller we can identify four main time consuming operations:

- acquisition of sensors data and analog-to-digital conversion of this data which will require a time we will call Δt^{a*};
- data processing at the sensors level will consume a time Δt^{b*};
- network transmission will have a delay time Δt^{c*};
- data processing at the controller level will consume a time Δt^{d*}.

The first time amount Δt^{a*} depends on the sensors and converter's properties and it is specified by the producer, while the amount of the other three times, depends on quantity of data, processing speed and network delay time.

According to Fig. 1.6, we define the moments: t^a – when the acquisition of sensors data starts, t^b - when digital data enter the system after acquisition and analog-to-digital conversion, t^c - when data processing at sensors level is over and it is ready for network transmission, t^d - when data arrives at controller level and t^e - when network data is ready for use after being processed at the controller level. Consequently, the sensors-controller transfer delay time can be defined by $\Delta t^* = \Delta t^{a*} + \Delta t^{b*} + \Delta t^{c*} + \Delta t^{d*} = t^e - t^a$.

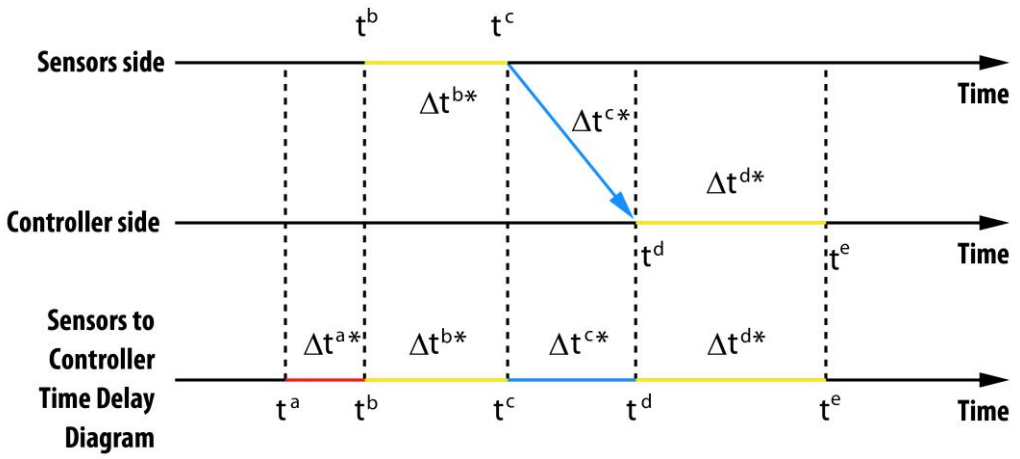

Fig. 1.6 - Delay components

Similarly, for the controller-actuators path, we will consider $\Delta t^{**} = \Delta t^{a**} + \Delta t^{b**} + \Delta t^{c**} + \Delta t^{d**}$, where Δt^{a**} and Δt^{c**} are the data processing

times at the controller and actuator sides, Δt^{b}** is the network delay and Δt^{d}** is the digital-to-analog conversion time.

1.3.1.1.1. Network Delay

Network delay or latency (NL) represents the finite amount of time needed to transfer a specific amount of data over the network between certain network nodes. Network jitter is a measure of the network latency variation ([18]).

When using packet switched networks, NL is defined as the time needed to transfer a packet of data over the digital network between the source and the destination network nodes. NL depends on the quantity of data that needs to be transferred, the network capacity, distance between transferring nodes, the number of hops to destination and the performance of hardware and software equipment involved in data transfer. It can be defined as a sum of various different constant and varying delay components.

Medium access delay (MD) defines the time needed by a network node to gain access to the network for data transmission. Depending on the network type and technology used, there are different techniques for medium access and for data collision avoidance (e.g. random access with collision detection or collision avoidance, time-division multiplexed with token passing or master-slave). MD can be constant or variable depending on the network technology used ([17]).

Serialization delay (SD) represents the finite amount of time it takes a network interface to perform bitwise transmission of a packet of data over the communication channel ([18]). SD is direct proportional to the packet size and inverse proportional to the transmission rate of the network interface (e.g. a data packet of 1500 bytes is serialized on a 56 Kbps modem link in 0.214 ms ([19]). If the transmission rate is constant, the SD of the same packet is constant also.

Propagation delay (PrD) represents the time needed by the electric, electromagnetic or optic data signal to travel through the medium between the source and the destination. The highest speed at which the data signal can travel is the speed of light in ether $c \cong 3x10^{8}$ m/s. When using other transmission mediums the signal speed (ss) is slower depending on the physical properties of that medium. The velocity factor (vf) determines the speed of the signal passing through the medium relatively to the speed of light in ether: $ss=vf \cdot c$, $vf<1$ (e.g. the speed of a light pulse in a fiber channel is typically 2/3 the speed of light in ether so the fiber channel's vf=0.67) ([19]). The PrD is directly proportional to the distance between source and destination and inverse proportional to the data signal speed. Using the same network, if the distance between the source and the destination nodes is constant, the PrD is constant.

Forwarding delay (FD) defines the time needed by network equipment (routers, switches, etc.) to pass a data packet from one physical network segment to another ([20], [21]). This delay is usually constant for a network equipment and depends on the type of technology used by the equipment and its hardware and software performances.

Queuing delay (QD) equals the total amount of time a packet stays in the hardware equipment's queues as it travels between the source and destination ([18]). QD depends on the network load so it varies greatly in time.

Transmission protocols delay (TD) represents the additional delay induced by the network transmission protocols (e.g. TCP data retransmission induced delay) ([22]). TD depends on the type, design and implementation of each specific protocol. Depending on the data traffic conditions and the protocols used for network transmission TD can vary considerably in time.

Consequently, NL = MD + SD + PrD + FD + QD+TD.

1.3.1.1.2. Computational Delay

The usage of computer networks in NCSs implies an analog to digital conversion of data for network transmission which automatically recommends a digital implementation of the controller. Most of the times in order to obtain a certain degree of performance real-time computing systems have to be used ([23]). A real-time computational system is one where the correction of a computation depends on both the logical result and the time at which the result is available for usage ([24]). Data processing in real-time systems can be done sequential or concurrent. The computational delay is deterministic in sequential processing and stochastic in concurrent processing, with the actual value depending on the performance of hardware and software resources available.

1.3.1.1.3. Synchronization Delay

When measuring time delays of operations involving different components of a NCS, a time offset between the internal clocks of different components would induce additional time delays. So, when designing distributed systems, one problem is to obtain clock synchronization between the internal clocks of different computational components.

Basically, an electronic clock is composed of a frequency oscillator and a counter. The oscillator frequency depends on its quality and usage period and also on the external conditions affecting the oscillator (e.g. ambient temperature). The variation of the oscillator frequency affects a clock accuracy making it, in time, drift away from another clock considered as reference and determining a time offset between them. In [25], the time offset of an electronic clock compared to an ideal reference at a current moment t is expressed as:

$$T(t) = T(t_0) + R(t - t_0) + D(t - t_0)^2 + x(t) \quad (1.1)$$

where t_0 is an initial moment, T is the time offset, R is the frequency offset, D is the oscillator aging drift and x is a stochastic error term.

In order to minimize the additional time delay values induced by clock drifts, a proper method of clock synchronization between different NCS components is required. Depending on the method, different accuracy of synchronization can be obtained. A method of synchronization can be obtained using the network time protocol (NTP) or precision time protocol (PTP). Using specialized hardware and software equipment, based on atomic/GPS clocks and NTP, nanosecond accuracy can be obtained ([25]) (Fig. 1.7).

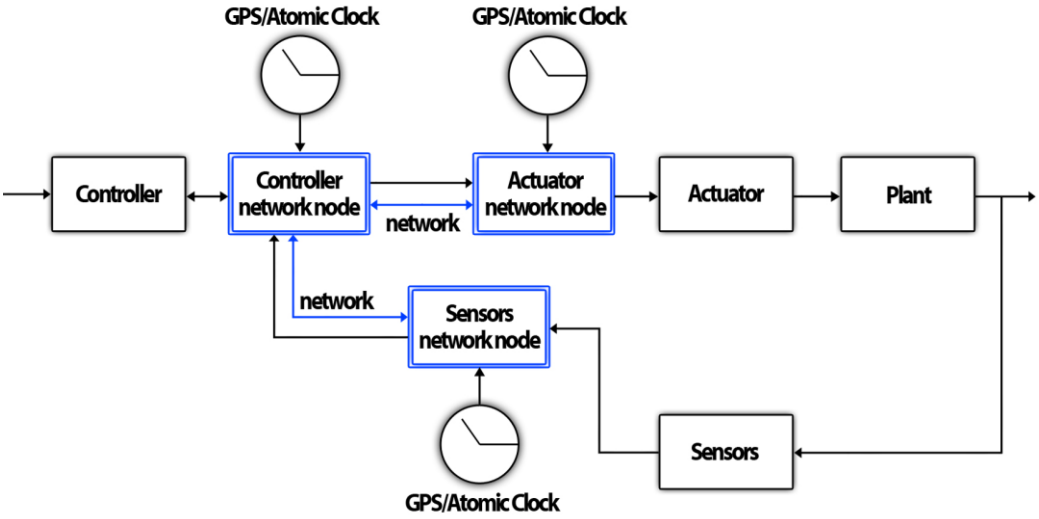

Fig. 1.7 – GPS/Atomic clock synchronized system

1.3.2. Irregular Situations

In relation to a constant sampling time operating regime, assuming a sampling period h for the NCS, depending on the time delay values two possible situations may occur:

- time delay values are smaller than the sampling period h;
- time delay values are bigger than the sampling period h.

In relation to the delay components defined in Fig. 1.6 for the feedback path of a NCS, the nominal case for data transmissions over the network is further defined as the one in Fig. 1.8 where the time delay value is smaller than the sampling period and the packet always arrives at the destination.

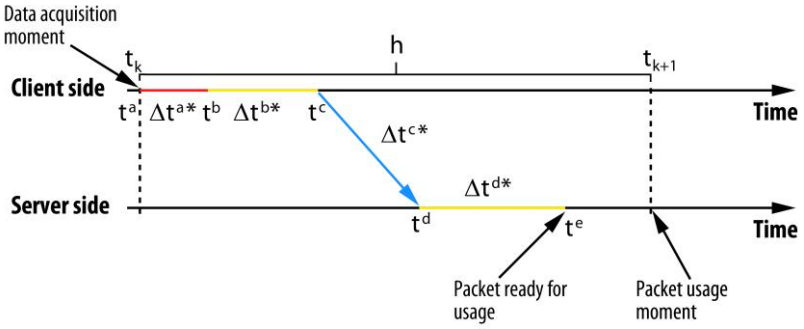

Fig. 1.8 – Data transmission – nominal case

In practice, for network transmissions using connectionless protocols, besides the nominal situation from Fig. 1.8, a series of particular undesired situations could emerge and have to be taken into account. Those situations are caused by

irregularities which may appear in the data packet transmission process. These irregular situations can be grouped in three main cases:

IS1: No data packets arrive in one sample period (e.g. Fig. 1.9).

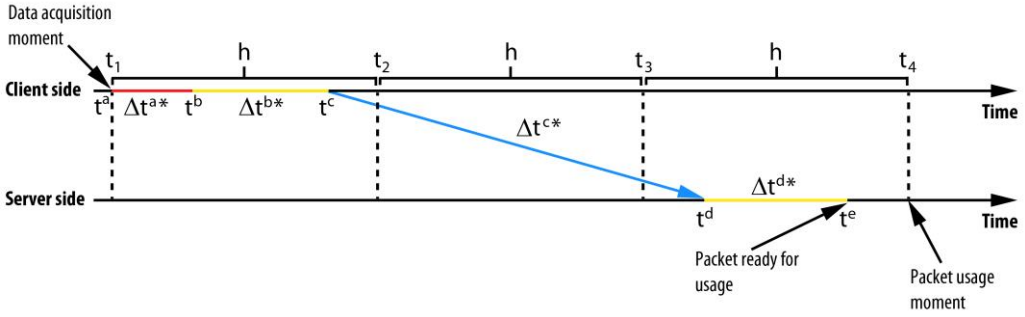

Fig. 1.9 – An example of IS1

IS2: Two or more data packets arrive at the controller side in the same sample period (e.g. Fig. 1.10).

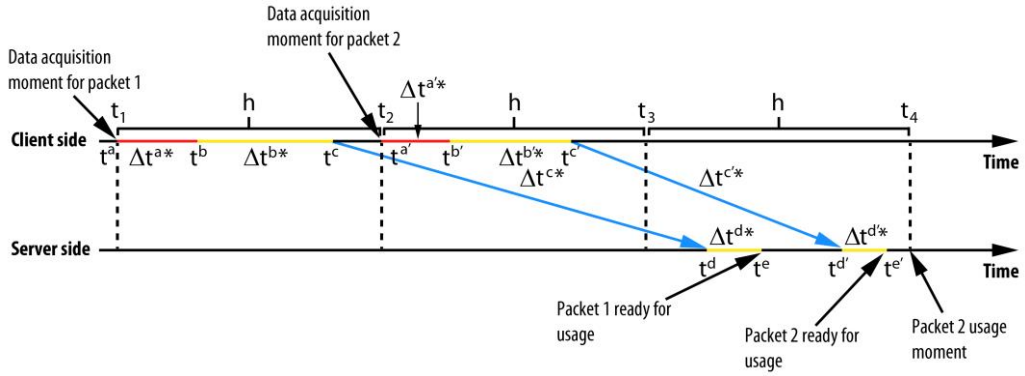

Fig. 1.10 – An example of IS2

IS3: A data packet arrives after a later packet has arrived and has been already used (e.g. Fig. 1.11).

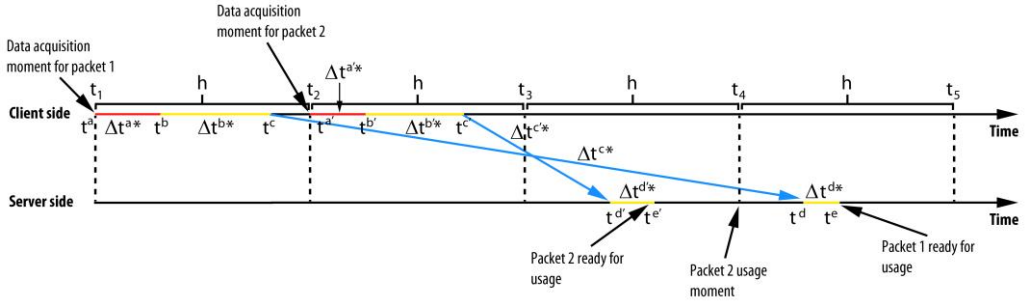

Fig. 1.11 – An example of IS3

In order to assure optimal control performances, handling strategies for this irregular situations need to be developed.

1.3.3. Data Integrity and Security

1.3.3.1. Information Loss

In typical packet switched networks there are mainly two causes for information loss:

- *packet loss* caused by transmission errors;
- *packet dropout* caused by data corruption, buffer overflow of network equipment, exceeded timeout.

Different models (deterministic or stochastic) have been proposed for information loss in order to study its effect on control system's performance and stability ([3]). Some methods consider information loss as additional transmission time delays ([2]).

A simple method of handling information loss on the receiver side in NCS is to extrapolate the previous received value in the following manner:

$$y_r[k] = p[k] \cdot y_s[k] + (1 - p[k]) \cdot y_r[k-1] \tag{1.2}$$

where y is the data value that needs to be received, r index denotes the receiver, s the sender level network node and k is the index of the current sampling period; p[k] is the packet loss flag that can take two values: 1 for an arrived packet and 0 is the packet is lost/dropped.

1.3.3.2. Security

The usage of networks in NCSs automatically extends any security issue involving computer networks also to the field of control systems. Any publicly accessible network, especially wireless networks are susceptible and possible vulnerable to cyber-attacks. Attacks to computer networks can vary from denial of service, informational theft, to partial or even entire system compromise. Several reported incidents have been mentioned in the literature [26] and solutions to different types of vulnerabilities are being proposed. Although the study of security issues in NCSs is in its infancy, the research is rapidly progressing because most of the solutions already proposed in the communication theory can be adapted for usage in NCSs.

1.3.4. Limited Communication

According to Nyquist-Shannon sampling theorem, complete signal reconstruction can be assured on a digital communication channel only if the bandwidth of the channel is beyond a certain limit. Recent studies are concerned with defining the minimum channel capacity at which system performance and stability are maintained ([27], [28]). Work has been done in improving the efficiency of data quantization for network transmissions ([29]).

1.4. Internet-based Control Systems

The extraordinary Internet expansion made TCP/IP based networks the mostly used networks of today, making them a good candidate for usage in NCSs. The way control signals are affected when transferred through a TCP/IP network depends on the network hardware components and also on the software protocols used for data transmissions. Data can be transmitted over the network using connectionless or connection oriented protocols ([30]). Both options can be used for data transmissions in a NCS, but most of the time, because of the imposed sample time restrictions (e.g. the telecontrol system presented in Appendix 1), connectionless protocols are the only valid choice. In this context, Internet-based control systems (ICSs) usually use UDP as transport protocol. Although it assures the best performances in terms of delay, UDP being an unreliable protocol introduces supplemental issues for NCS design.

1.5. Control Solutions in Networked Control Systems

1.5.1. Control of Networks

Control of networks studies how different network quality of service (QoS) parameters influences the quality of control (QoC). This research direction has been somehow neglected by the control community and has just recently started to be taken into consideration ([31]).

1.5.2. Control Over Networks

Control over networks refers to the control techniques used in NCSs for dealing with the network induced issues. In Chapter 3, several different control strategies used in NCSs are presented.

1.6. Motivation and Objectives

The extensive development of digital network technologies and the rapid global expansion of the Internet triggered the interest of scientists and engineers towards teleoperation based applications. Such applications are of an interdisciplinary nature, and imply close collaboration between specialists in control systems, computer science and communication theory. However the development of such applications is impeded by the network induced issues from a control perspective, which have the tendency to impair the control performances and may even lead to system instability.

In this context, for a simple practical teleoperation example, an attempt was made to reveal the control problems that emerge using different network transmission scenarios over the Internet. Different transmission issues were identified (time varying delays, packet loss, irregular situations, limited bandwidth capacity) and some empirical attempts to compensate them were made – see Appendix 1. The obtained results provided the starting point of this study. Consequently, several objectives emerged:

- The outline of a unified and systematic framework which captures all network transmission phenomena from an input-output perspective along with possible data handling strategies as an aid for different control strategies.

- The development of a mathematical model which captures simultaneously all the identified network transmission phenomena (due to the lack of such models in the specialized literature), for the analysis and / or synthesis of future network control structures.
- The design of different control strategies for compensating the network induced disturbances, along with the stability analysis and performance evaluation.

1.7. Thesis Structure

The remainder of this thesis is structured as follows.

Chapter 2 presents different modelling approaches for network transmissions in a NCS. First, some existing models from the specialized literature are mentioned. In order to overcome the limitations of the existing models, a novel nonlinear network transmission model is proposed that incorporates all network transmission phenomena. Next, the proposed model is recasted as a switched linear system. Finally, an associated algorithm is developed, that can be used as a network emulator.

Chapter 3 addresses different control methodologies for NCSs. After a short overview of available control strategies from the literature, two novel control solutions for time delay compensation are presented: the first uses an observer based delay compensation approach and the second relies on a switched PD delay compensator.

Chapter 4 describes in detail the design and analysis of the two control solutions for time delay compensation. Firstly, the observer based delay compensation structure is extended for second order benchmark processes. A detailed analysis is conducted on the behaviour of the full order observer versus the reduced order one, along with possible practical limitations of the approach. The results are validated through simulations and experiments. Secondly, switched networked control structures are proposed for addressing the stabilization and tracking problems. For stabilization the control structure is based on a remotely placed switched state feedback controller, while for tracking a state feedback controller is placed remotely and a PD adaptive delay compensator is placed locally along the plant. The stability analysis is addressed for both structures and simulation results further validates the solutions.

The final chapter states the thesis summary together with the main contributions and suggestions for future work.

1.8. Publications

This thesis is mostly based on the following published articles:

- **O. Stefan**, T.-L. Dragomir, A. Codrean, and I. Silea, "Issues of identifying, estimating and using delay times in telecontrol systems based on TCP/IP networks," in Proc. 2nd IFAC Symposium on Telematics Applications, Timisoara, 2010, pp. 143-148.

- **O. Stefan**, A. Codrean, T.-L. Dragomir, and I. Silea, "Time delay and information loss compensation in a network control system for a DC motor,"

in IEEE International Symposium on Applied Computational Intelligence and Informatics, Timisoara, 2011, pp. 131-135.

- **O. Stefan**, A. Codrean, and T.-L. Dragomir, "A Nonlinear State Space Model of Network Transmissions in a Network Control System," Journal of Control Engineering and Applied Informatics, vol. 13, no. 4, pp. 58-63, 2011.

- A. Codrean, **O. Stefan**, and T.-L. Dragomir, "Design, analysis and validation of an observer-based delay compensation structure for a Network Control System," in Mediterranean Conference on Control & Automation, Barcelona, 2012, pp. 928-934.

- **O. Stefan**, A. Codrean, and T.-L. Dragomir, "Stability analysis and control synthesis for a Network Control System using a nonlinear Network Transmission Model-a switched system approach," in IEEE International Conference on Control Applications, Dubrovnik, 2012, pp. 885-890.

- **O. Stefan**, A. Codrean, and T.-L. Dragomir, "Design and analysis of a network control structure with a switched PD compensator," in International Conference on Methods and Models in Automation and Robotics, Międzyzdroje, 2012, pp. 403-408.

- **O. Stefan**, A. Codrean, and T.-L. Dragomir, "A Network Control Structure with a Switched PD Delay Compensator and a Nonlinear Network Model," in American Control Conference, Washington, 2013, pp. 758-764.

2. MODELLING NETWORK TRANSMISSIONS IN A NETWORKED CONTROL SYSTEM

Extensive research has been done in order to overcome the problems introduced by the network in a NCS and some solutions have been proposed ([32]). In order to design and analyse a NCS in the context of real network complexity, a practical approach would be to model the network system from the signal processing point of view. In other words, what interests is the way in which an input signal is deformed when transmitted through a real network. For this purpose, several network models which take into account time delays and/or packet losses have been proposed in the control literature (see for example [33], [34], [35], [36], [37], [38], [39], [40], [41] and the review papers [3] and [2] along with the references within). The time delays are considered either constant, deterministic time varying (e.g. periodic) or stochastic time varying (e.g. Markov chains, random uniform distribution). Packet dropouts are modelled either in a deterministic (e.g. time average, worse case bound) or in a stochastic (e.g. Markov chains, Bernoulli distribution, Poison distribution) manner.

On the other hand, before solutions can be implemented and used in real life applications, they have to be tested in a controlled environment. The simulation of system behaviour under some imposed conditions is one method largely used by engineers for testing a design pattern. Current simulation environments, like Matlab/Simulink or Maple, provide, in their standard libraries, only ideal time-varying delay blocks which do not permit additional constraints, like the ones specific to network transmissions.

In this chapter, a new model is proposed by the author which complements existing models in literature, and can be used both for analysis and design, respectively simulation studies.

2.1. A State Space Model of Network Transmissions in a TCP/IP-based Networked Control System

The increase in data processing power and the decrease of equipment costs determined an extraordinary expansion of the Internet in the last years. Low cost, high fault tolerance and reliability of today's TCP/IP networks opened a new perspective in the field of networked control structure design. The way control signals are affected when transferred through a TCP/IP network depends on the network hardware equipment and on the software protocols used for data transmissions. A TCP/IP network implements both connectionless or connection oriented protocols for data transport ([30]). When dealing with fast dynamics processes, because of the imposed sample time restrictions, connectionless protocols are the only valid choice for a NCS implementation. In this context, the following study will focus on TCP/IP networks using UDP as a transport protocol, regardless of topology and areal coverage.

Network transmissions can be modelled from a systemic point of view as an input-output signal processing. In case of TCP/IP networks, when using UDP as a

transport protocol, because the dynamics of network transmissions involves time varying delays and sudden jumps due to packet loss, the signals that pass through the network can be delayed and deformed.

The network can be considered as a pair of discreet-time transfer elements in the control system (Fig. 2.1) composed of a forward communication path (input uc and output ud) and a feedback communication path (input y_d and output y_c). Control signals are transferred through the network using data packets. Although the adopted connectionless transmission is usually faster, it has the disadvantage of being unreliable: data packet integrity and availability is not assured. These lead to possible information loss additional to the network time varying delay and to the necessity to adopt at the receiver level a handling strategy for the arrived packets.

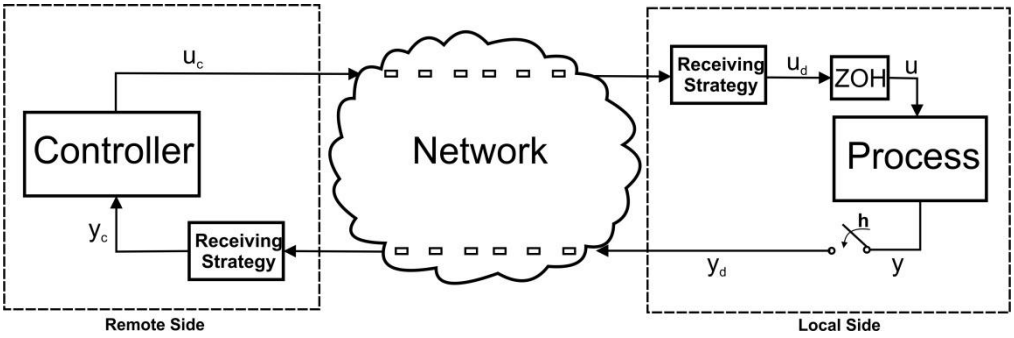

Fig. 2.1 - Structure of a NCS

The conceptual and mathematical models associated to the network, from the point of view of how it interferes with the control system's dynamics, depends on the description level of the signal transmission process and receiving processing operations. In this context, a conceptual model is further considered for the receiving strategy.

A constant sampling time operating regime with a sampling period h is assumed, so that, in both directions, the signal transmissions are synchronized with the beginning of every sampling period. Also, it is considered that, from the control point of view, when transmitting data through the network (one packet at every sample rate), three irregular situations are identified and handled as follows ([42]):

IS1: No data packets arrive during the current sampling period at the receiving end of a network path. In this case, the last valid information received is used as output of the network.

IS2: Two or more packets arrive during the current sampling period at the receiving end of a network path. In this case, only the latest information will be used as output of the network.

IS3: A data packet arrives during the current sampling period at the receiving end of a network path after a subsequent packet arrived and it had been already used. In such case, the packet is discarded and the latest valid information is used as output of the network block.

The handling manner flowchart of these irregular situations is synthesized by the logic diagram from Fig. 2.2. The algorithm associated to the diagram is executed at the beginning of each sampling period.

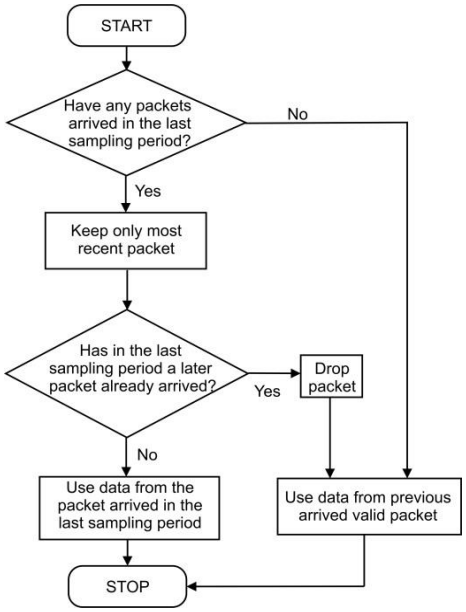

Fig. 2.2 - Logic diagram for handling the irregular situations

The development of a model for the network element which includes all the aspects mentioned above regarding data transmission would be required in most cases for the analysis and synthesis of a NCS. Most modelling approaches found in the literature (like the ones previously presented), only partially address the characteristics of data transmission (time varying delay, packet loss and irregular situations together with their handling strategies).

In this context, in [43] the author proposed a new model that takes into account all the above possible situations, simulating in a simplified manner the behaviour of a real life network. Moreover, the model can be easily implemented in simulation environments like Matlab/Simulink. This addresses the observed lack, in the specialized literature, of models that emulate, in terms of input-output signal alterations, the behaviour of a real network spanning from local to wide intercontinental areal. An interesting implementation of a real time network is presented in [44], a Matlab toolbox, but it is limited only to local area networks and to time delay induced by layer 1 and 2 protocols.

2.1.1. Nonlinear Network Transmission Model

Let u be the input data signal for a communication channel of the network system, y the output signal of the same channel, h the sampling period (the network system being considered as a discrete system) and k represents the index of discrete sample times. The time delay of a packet needed to pass through a communication channel, including packet processing time at network nodes, varies from a sampling instant to another sampling instant, therefore it is a time varying delay τ_k. Because in the considered discrete time processing systems data is used only at sample instants kh, τ_k is a multiple of h. Therefore, in the following, the notation y[k], u[k], τ[k] may be used with the same meaning as y(kh), u(kh), τ_k.

In order to develop a model for network transmissions, a simple example will be chosen (Fig. 2.3), which includes all three types of situations that occur during data transmissions (varying delay, packet loss and irregular situations). Fig. 2.3 expresses the time moments at which data packets are generated by the sender and when they arrive at the receiver. During the time window of more consecutive sample moments beginning with *k-2*, besides each packet's delay, a packet is lost at moment *k+1* and the following irregular situations appear: IS_1 at {*k-1*, *k+1*, *k+2*,*k+5*}, IS_2 at {*k*, *k+6*} and IS_3 at *k+4*. Based on the handling strategy represented in Fig. 2.2 the input sequence u should be transformed by the network system into the output sequence *y* as shown in Fig. 2.4 (receiver's operational level).

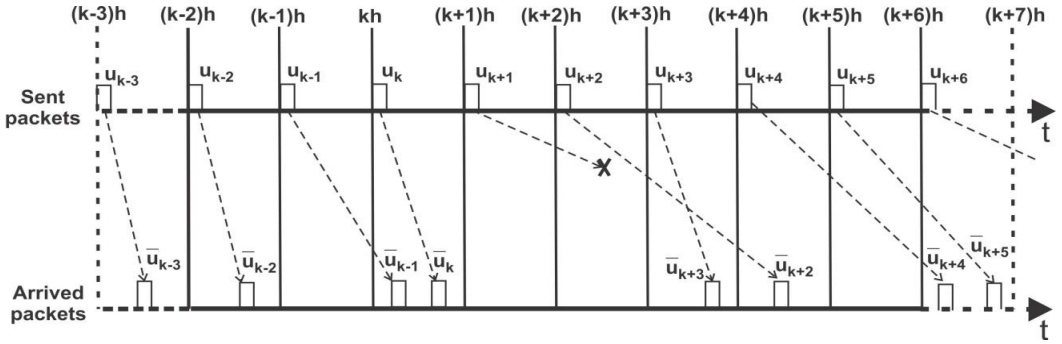

Fig. 2.3 - Network transmission example – packet arrival sequence

In order to motivate the need of a new model that describe the input-output dependency $u \rightarrow y$, first, the classic time-varying delay model, already implemented in Matlab/Simulink library ([45]), will be considered:

$$y(kh) = u(kh - \tau_k) \tag{2.1}$$

Using model (2.1) to generate the output sequence *y*[k] for the example from Fig. 2.3 the following result is obtained (absolute time):

$$\begin{cases} \tau_{k-2} = h \rightarrow & y[k-2] = u[k-3] \\ \tau_{k-1} = 2h \rightarrow & y[k-1] = u[k-3] \\ \tau_k = h \rightarrow & y[k] = u[k-1] \\ \tau_{k+1} = \infty \rightarrow & y[k+1] = u[-\infty] \\ \tau_{k+2} = 3h \rightarrow & y[k+2] = u[k-1] \\ \tau_{k+3} = h \rightarrow & y[k+3] = u[k+2] \\ \tau_{k+4} = 3h \rightarrow & y[k+4] = u[k+1] \\ \tau_{k+5} = 2h \rightarrow & y[k+5] = u[k+3] \end{cases} \tag{2.2}$$

On the operational level (2.2) becomes (the time variable refers to the current sampling instance):

$$\begin{cases} y[t] = u[t-1], & for\ t = k-2 \\ y[t] = u[t-2], & for\ t = k-1 \\ y[t] = u[t-1], & for\ t = k \\ y[t] = u[-\infty], & for\ t = k+1 \\ y[t] = u[t-3], & for\ t = k+2 \\ y[t] = u[t-1], & for\ t = k+3 \\ y[t] = u[t-3], & for\ t = k+4 \\ y[t] = u[t-2], & for\ t = k+5 \end{cases} \tag{2.3}$$

These results are illustrated in Fig. 2.5. As it can be observed, they differ from the ones shown in Fig. 2.4.

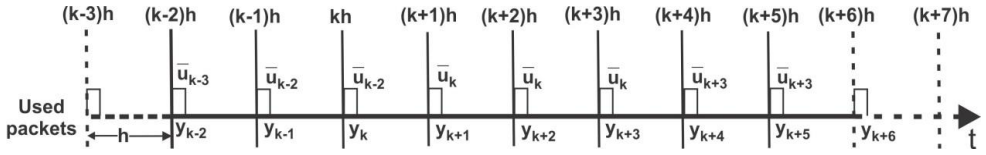

Fig. 2.4 - Network transmission example – proposed packet handling strategy

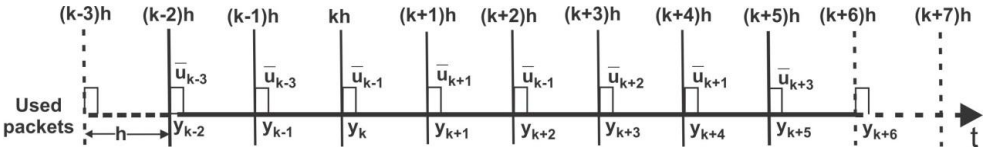

Fig. 2.5 - Network transmission example – packet handling using (2.1)

It can be noticed that packet loss situations, as well as the situations when the packets are not used, cannot be captured by model (2.1). Such packets don't appear on the right side of equations (2.3). It should be observed that by permitting the delay value to increase or decrease, the irregular situations cannot be addressed, so the principle of using the latest available packet at each sample time is not respected.

As a different approach, considering that a discrete time delay is a finite dimensional system, a state space model could be addressed. Fig. 2.6 defines the Network Transmission Block (NTB), with its inputs and outputs. Here, u is the input data signal for the NTB and y is the output data signal. τ and p are two additional input signals referring to the time varying delay and to the packet loss flag. These two input signals can be generated according to certain patterns (e.g. probability distributions) or can be obtained directly from measurements on a real TCP/IP network. At a given sample instant k, τ[k] takes as value a multiple of the sampling period {1, 2, 3, ..., τ_{max}}. The delay of a lost packet is adopted as τ_{max}.

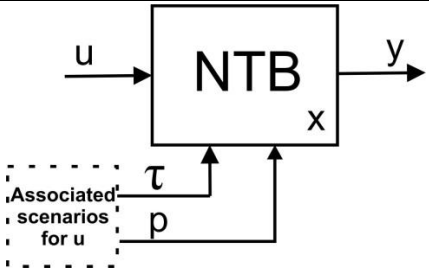

Fig. 2.6 - Network Transmission Block

A number of n states of the NTB , $x_1[k]$, $x_2[k]$… $x_n[k]$, corresponding to the data values of the input signal u, memorized in the network at the instant moment k, are represented through the vector variable $\underline{x}$, where n is given by the maximum varying delay allowed by the model, $n = \tau_{max}$. Data packets that arrive with superior delays will be considered as lost packets. The minimum time delay is limited to a sample period. Thus, a first component of the state vector has the form:

$$\underline{x}[k] = \begin{bmatrix} x_1[k] \\ \vdots \\ x_n[k] \end{bmatrix} \tag{2.4}$$

First, in order to build the model, the input is redefined as an n-dimensional vector:

$$\bar{\underline{u}}[k] = \begin{bmatrix} 0 \\ \vdots \\ 0 \\ u[k] \\ 0 \\ \vdots \\ 0 \end{bmatrix} \begin{matrix} \} \tau[k] \\ \\ \\ \\ \} n - \tau[k] \end{matrix} \tag{2.5}$$

where $\bar{\underline{u}}[k]$ now actually depends on the u[k] and τ[k] signals. Defining $\bar{\underline{u}}$ limits the possibility to express the value of zero for the input signal u[k], so another value has to be adopted as a convention for it. At any sample time the signal p[k] can take one of two values: 1 if the data packet has arrived or 0 if the packet is lost.

Based on the input defined in (2.5), the state vector $\underline{x}$ at the next sample time $k+1$ is obtained as:

$$\underline{x}[k+1] = \left(p[k] \cdot \underline{f}_n(\tau[k]) + (1 - p[k]) \cdot \underline{I}_n\right) \cdot \underline{I}_{sn} \cdot \underline{x}[k] + p[k] \cdot \bar{\underline{u}}[k] \tag{2.6}$$

with the function $\underline{f}_n : N \to N^{nxn}$ defined as:

$$\underline{f}_n(\tau[k]) = diag(\sigma(\tau[k] - 2), .., \sigma(\tau[k] - n - 1)) \tag{2.7}$$

Here $\underline{I}_n$ is the unitary matrix, while the unitary step function σ and the $n \times n$ matrix $\underline{I}_{sn}$ are defined by:

$$\sigma(x)=\begin{cases}0, x<0\\ 1, x\geq 0\end{cases},\ \underline{I}_{sn}=\begin{bmatrix}0 & 1 & 0 & \cdots & \cdots & 0\\ \vdots & \ddots & \ddots & \ddots & & \vdots\\ \vdots & & \ddots & \ddots & \ddots & \vdots\\ \vdots & & & \ddots & \ddots & 0\\ \vdots & & & & \ddots & 1\\ 0 & \cdots & \cdots & \cdots & \cdots & 0\end{bmatrix} \tag{2.8}$$

The equations (2.6)-(2.8) calculate the state vector for the next sampling period. First, $\underline{I}_{sn}$ shifts the state vector upwards with one position (the value from x_1 is eliminated because it was already used, while zero is inserted at position x_n). Second, $\underline{f}_n$ sets to zero all the state values at positions beyond τ[k]-*1* (the values are no longer needed because newer data has arrived). If a packet is lost (p[k]=0) the state vector is modified only through the shift operation ($\underline{I}_{sn}$). Third, the new value of the input signal u modifies the state vector through $\overline{\underline{u}}$.

Next, an additional state x_a is defined as:

$$x_a[k+1]=\overline{u}_1[k]+\sigma(\tau[k]-2)\cdot x_2[k]+(1-g(x_2[k]))\cdot(1-g(\overline{u}_1[k]))\cdot x_a[k] \tag{2.9}$$

where $\overline{u}_1$ is the first element of $\overline{\underline{u}}$ and

$$g(x)=\begin{cases}0, x=0\\ 1, x\neq 0\end{cases} \tag{2.10}$$

The x_a state is used in order to maintain at the output the value from the last valid arrived packet. If both $\overline{u}_1$ and x_2 are zero then the value of the state x_a is maintained the same for the next sample period by function g. If $\overline{u}_1$ is non-zero, which implies τ[k]=*1*, the value of x_2 is invalidated through the σ function.

The output y at each sample time is given by the value of the state x_a:

$$y[k]=x_a[k] \tag{2.11}$$

Equations (2.4)-(2.11) can be lumped together into a state space model by defining a global state vector

$$\overline{\underline{x}}[k]=\left[\underline{x}^T[k]\quad x_a[k]\right]^T \tag{2.12}$$

the matrix

$$\underline{A}[k]=p[k]\cdot\left(\underline{f}_n(\tau[k])-\underline{I}_n\right)\cdot\underline{I}_{sn}+\underline{I}_{sn} \tag{2.13}$$

a function

$$\tilde{g}[k]=(1-g(x_2[k]))\cdot(1-g(\overline{u}_1[k])) \tag{2.14}$$

and the additional $1\times n$ vectors:

$$\begin{aligned} \underline{v}^T &= [0 \quad \sigma(\tau[k]-2) \quad 0 \quad \cdots \quad 0] \\ \underline{w}^T &= [1 \quad 0 \quad 0 \quad \cdots \quad 0] \\ \underline{c}^T &= [0 \quad 0 \quad \cdots \quad 0 \quad 1] \end{aligned} \tag{2.15}$$

The following state space model is obtained:

$$\begin{cases} \bar{\underline{x}}[k+1] = \begin{bmatrix} \underline{A}[k] & \underline{0}_{n\times 1} \\ \underline{v}^T & \tilde{g}[k] \end{bmatrix} \cdot \bar{\underline{x}}[k] + \begin{bmatrix} \underline{I}_n \\ \underline{w}^T \end{bmatrix} \cdot p[k] \cdot \bar{\underline{u}}[k] \\ y[k] = \underline{c}^T \bar{\underline{x}}[k] \end{cases} \tag{2.16}$$

Next, using the model (2.16) to generate the output sequence y[k] for the example from Fig. 2.3 the following results are obtained:

$$\begin{cases} \tau_{k-2} = h \quad \rightarrow \quad y[k-2] = u[k-3] \\ \tau_{k-1} = 2h \quad \rightarrow \quad y[k-1] = u[k-2] \\ \tau_k = h \quad \rightarrow \quad y[k] = u[k-2] \\ \tau_{k+1} = \tau_{max} \rightarrow \quad y[k+1] = u[k] \\ \tau_{k+2} = 3h \quad \rightarrow \quad y[k+2] = u[k] \\ \tau_{k+3} = h \quad \rightarrow \quad y[k+3] = u[k] \\ \tau_{k+4} = 3h \quad \rightarrow \quad y[k+4] = u[k+3] \\ \tau_{k+5} = 2h \quad \rightarrow \quad y[k+5] = u[k+3] \end{cases} \tag{2.17}$$

The results from (2.17) are the same with those presented in Fig. 2.4 and they are in agreement with the proposed packet handling methodology described in Fig. 2.2.

Finally, as seen in the example above, model (2.16) manages to completely characterize network transmissions. The model behaves as a buffer which is continuously shifted, filled and emptied at each sample time, according to the time varying delay, the handling of the irregular situations and the packet loss flag. The shift corresponds to the passing of a new sample instance, the filling corresponds to a new data packet arrival which will be released according to the scheduled delay, and the emptying corresponds to packets that arrive too late and are dropped because newer data has already arrived (irregular situation).

The SISO model from (2.16) can be extended to the following MIMO form:

$$\begin{cases} \begin{bmatrix} \underline{x}_N[k+1] \\ \underline{x}_{Na}[k+1] \end{bmatrix} = \begin{bmatrix} \underline{E}_x(\tau,p)\underline{I}_{srn} & \underline{0}_{rn\times n} \\ \underline{E}_{ax}(\tau) & \underline{E}_a(\tau,\underline{x}_{N2}) \end{bmatrix} \overbrace{\begin{bmatrix} \underline{x}_N[k] \\ \underline{x}_{Na}[k] \end{bmatrix}}^{\tilde{\underline{x}}_N[k]} + \\ \qquad\qquad + \begin{bmatrix} \underline{E}_u(p) \\ \underline{E}_{au}(\tau) \end{bmatrix} \underline{E}_{uT}(\tau)\underline{u}_N[k] \\ \underline{y}_N[k] = \begin{bmatrix} \underline{0}_{n\times rn} & \underline{I}_n \end{bmatrix} \begin{bmatrix} \underline{x}_N[k] \\ \underline{x}_{Na}[k] \end{bmatrix} \end{cases} \tag{2.18}$$

where $\underline{x}_N \in \Re^{rn\times 1}$, $\underline{x}_N[k] = \left[\underline{x}_{N1}^T[k] \cdots \underline{x}_{Nr}^T[k]\right]^T$, $\underline{x}_{N1}, \ldots, \underline{x}_{Nr} \in \Re^{n\times 1}$, $\underline{x}_{Na} \in \Re^{n\times 1}$, $\underline{u}_N \in \Re^{n\times 1}$, $\underline{y}_N \in \Re^{n\times 1}$, $r = \tau_{max} \in \mathbb{N}^*$, τ is the time-varying delay, p is the packet loss flag, and the remainder notations stand for:

$$
\begin{aligned}
&\underline{E}_x = p[k]\cdot \underline{f}_{rn}(\tau[k]) + (1-p[k])\cdot \underline{I}_{rn}\\
&\underline{f}_{rn}(\tau[k]) = diag\left(\underline{\sigma}(\tau[k]-2),..,\underline{\sigma}(\tau[k]-r-1)\right)\\
&\underline{I}_{srn} = \begin{bmatrix} \underline{0}_n & \underline{I}_n & \underline{0}_n & \cdots & \cdots & \underline{0}_n \\ \vdots & \ddots & \ddots & \ddots & & \vdots \\ \vdots & & \ddots & \ddots & \ddots & \vdots \\ \vdots & & & \ddots & \ddots & \underline{0}_n \\ \vdots & & & & \ddots & \underline{I}_n \\ \underline{0}_n & \cdots & \cdots & \cdots & \cdots & \underline{0}_n \end{bmatrix}\\
&\underline{E}_{ax} = \begin{bmatrix} \underline{0}_n & \underline{\sigma}(\tau[k]-2) & \underline{0}_n & \cdots & \underline{0}_n \end{bmatrix}\\
&\underline{E}_a = \underline{I}_n\left(1-g\left(\underline{x}_{N2}[k]\right)\right)\cdot\left(1-g\left(\underline{E}_{u\tau}^1\right)\right)\\
&\underline{E}_{u\tau} = \begin{bmatrix} \underline{E}_{u\tau}^1 \\ \underbrace{\underline{0}_n}\\ \vdots \\ \underline{0}_n \\ \underline{I}_n \\ \underline{0}_n \\ \vdots \\ \underline{0}_n \end{bmatrix} \begin{matrix} \\ \\ \\ \\ \\ \\ \\ \end{matrix} \begin{matrix} \\ \\ \\ \\ \\ \\ \\ \end{matrix} \begin{matrix} \\ \\ n\tau[k] \\ \\ \\ \\ rn-n\tau[k] \end{matrix}, \underline{E}_u = \underline{I}_{rn}p[k]\\
&\underline{E}_{au} = \begin{bmatrix} \underline{E}_{u\tau}^1 & \underline{0}_n & \underline{0}_n & \cdots & \underline{0}_n \end{bmatrix}\\
&\underline{\sigma}(v) = \begin{cases} \underline{0}_n, v<0 \\ \underline{I}_n, v\geq 0 \end{cases}, \quad g(\underline{\mathbf{v}}) = \begin{cases} 0, \underline{\mathbf{v}} = \underline{0}_{n\times 1} \\ 1, \underline{\mathbf{v}} \neq \underline{0}_{n\times 1} \end{cases}
\end{aligned}
\tag{2.19}
$$

Here $\underline{I}_n$ and $\underline{I}_{rn}$ are unitary matrices, $\underline{I}_{srn}$ is defined as an rn order quadratic matrix, $\underline{\sigma}$ is the unitary matrix step function of scalar variable v and $\underline{0}_n$ is the quadratic zero matrix of order n.

The model (2.18) - (2.19) characterizes network transmissions as signal time shifts and deformation processes (i.e. time delay and packet loss) and captures the irregular situations along with their associated handling strategy. It behaves as a buffer which is continuously shifted (passing of a new sampling instance), filled (new data packet arrival) and emptied (packet drop). The state vector $\underline{x}_N$ is shifted upwards with one position by $\underline{I}_{srn}$ (the value from $\underline{x}_{N1}$ is eliminated because it has been already used while null values are inserted at position $\underline{x}_{Nr}$). The vector function $\underline{f}_{rn}$ sets to zero all the state values at positions beyond τ[k]-1 (the values are no longer needed because newer data has arrived). If a packet is lost (p[k]=0) $\underline{x}_N$ is modified only through the shift operation ($\underline{I}_{srn}$). When a new value for the input signal $\underline{u}_N$ arrives, the state vector $\underline{x}_N$ is modified through $\underline{E}_{u\tau}$. Finally, the state $\underline{x}_{Na}$ is used in order to

maintain at the output the value of the last valid arrived packet (according to the handling strategy for the irregular situations).

Further on, in order to facilitate the analysis and the design of NCSs, the nonlinear network transmissions model, it is brought to a switched linear form (see [46], [47]).

2.1.2. Switched System Network Transmission Model

Let $\Omega_1=\{1, 2, 3, ..., \tau_{max}\}$ be the set of possible values (multiples of the sampling period, for reasons detailed in [42]) taken by $\tau[k]$ at a given sample instant k. The value $\tau[k]=\tau_{max}$ is assigned to a lost packet. Because for a transmitted packet $p[k]=1$ and $\tau[k]< \tau_{max}$ and for a lost packet $p[k]=0$ and $\tau[k]=\tau_{max}$, the packet loss flag p can be defined as a function of τ.

Taking into account the finite number of elements of Ω_1 and the bivalent set $\Omega_2=\{0,1\}$ of values of the auxiliary function $g^*(\underline{\tilde{x}}_N[k]) = 0\cdot g(\underline{x}_{N1}[k]) + 1\cdot g(\underline{x}_{N2}[k]) + \cdots + 0\cdot g(\underline{x}_{Nr}[k]) + 0\cdot g(\underline{x}_{Na}[k])$ the following two switching functions, α and γ, can be adopted: $\alpha:\mathbb{N}\rightarrow\Omega_1$, with $\alpha[k]=\tau[k]$, defined on a discrete set, $\gamma: \Re^{rn+n}\rightarrow\Omega_2$, with $\gamma(\underline{\tilde{x}}_N) = g^*(\underline{\tilde{x}}_N)$, defined on a continuous set. Consequently, the nonlinear model (2.18) - (2.19) can be further transformed into a switched linear system with α and γ as switching signals.

$$\begin{cases} \begin{bmatrix} \underline{x}_N[k+1] \\ \underline{x}_{Na}[k+1] \end{bmatrix} = \overbrace{\begin{bmatrix} \tilde{\underline{E}}_x I_{srn} & \underline{0}_{rn\times n} \\ \tilde{\underline{E}}_{ax} & \tilde{\underline{E}}_a \end{bmatrix}}^{\underline{A}_\alpha[k],\gamma(\underline{\tilde{x}}_N)} \overbrace{\begin{bmatrix} \underline{x}_N[k] \\ \underline{x}_{Na}[k] \end{bmatrix}}^{\underline{\tilde{x}}_N[k]} + \overbrace{\begin{bmatrix} \tilde{\underline{E}}_u \\ \tilde{\underline{E}}_{au} \end{bmatrix}}^{\underline{B}_\alpha[k]} \underline{E}_{u\alpha}\underline{u}_N[k] \\ \underline{y}_N[k] = \overbrace{\begin{bmatrix} \underline{0}_{n\times rn} & \underline{I}_n \end{bmatrix}}^{\underline{C}} \begin{bmatrix} \underline{x}_N[k] \\ \underline{x}_{Na}[k] \end{bmatrix} \end{cases} \tag{2.20}$$

with

$$\begin{aligned} \tilde{\underline{E}}_x &= \sigma(\tau_{max} - a[k] - 1)\cdot \underline{f}_{rn}(a[k]) + \\ &\quad + [1 - \sigma(\tau_{max} - a[k] - 1)]\cdot \underline{I}_{rn} \\ \tilde{\underline{E}}_{ax} &= \gamma(\underline{\tilde{x}}_N)\cdot [\underline{0}_n \quad \underline{\sigma}(a[k]-2) \quad \underline{0}_n \quad \cdots \quad \underline{0}_n] \\ \tilde{\underline{E}}_a &= \gamma(\underline{\tilde{x}}_N)\cdot \sigma(a[k]-2)\cdot \underline{I}_n \\ \tilde{\underline{E}}_u &= \sigma(\tau_{max} - a[k] - 1)\cdot \underline{I}_{rn} \end{aligned} \tag{2.21}$$

$$\underline{\underline{\tilde{E}}}_{au} = \sigma(\tau_{max} - a[k] - 1) \cdot \sigma(1 - a[k]) \cdot \cdot \left[\underline{\underline{E}}_{ua}^{1} \quad \underline{\underline{0}}_n \quad \underline{\underline{0}}_n \quad \cdots \quad \underline{\underline{0}}_n \right]$$

$$\underline{\underline{E}}_{ua} = \begin{bmatrix} \underline{\underline{E}}_{ua}^{1} \\ \underbrace{\underline{\underline{0}}_n \\ \vdots}_{na[k]} \\ \underline{\underline{0}}_n \\ \underline{\underline{I}}_n \\ \underline{\underline{0}}_n \\ \underbrace{\vdots}_{rn - na[k]} \\ \underline{\underline{0}}_n \end{bmatrix} \quad , \quad \sigma(v) = \begin{cases} 0, v < 0 \\ 1, v \geq 0 \end{cases} \tag{2.22}$$

The signal α will induce a time-dependent switching while signal γ will induce a state-dependent switching. However, if a exogenous time dependent switching function can be identified which assures a one-to-one correspondence with the operating regions of the state space, so that the state and time dependent switched systems have a common trajectory (solution) - [48], the system can be reduced to a time dependent switched system. For arbitrary switching, which is the case considered in this study, a time dependent switched system is obtained by adopting the time dependent switching signal $\delta: \mathbb{N} \rightarrow \Omega_2$, which at each sampling instance k takes just the values $\gamma(\underline{\tilde{x}}_N[k])$, i.e. $\delta[k] = \gamma(\underline{\tilde{x}}_N[k])$. As a result, the switched network model (2.20) takes the form:

$$\begin{cases} \underline{\tilde{x}}_N[k+1] = \underline{A}_{a[k],\delta[k]} \underline{\tilde{x}}_N[k] + \underline{B}_{a[k]} \underline{u}_N[k] \\ \underline{y}_N[k] = \underline{C} \underline{\tilde{x}}_N[k] \end{cases} \tag{2.23}$$

2.1.3. Implementation Algorithm

From the point of view of the implementation, the model (2.4)–(2.16) for the NTB can be described through the following algorithm:

Initialization:

- *define maximum allowed delay τ_{max}*;
- *initialize buffer x*;
- *initialize y_0*;

Repeat at each sample time k:

Step1: read inputs u_k, τ_k and p_k;

Step2: if $\tau_k > \tau_{max}$ or $p_k = 0$ jump at Step5;

Step3: rewrite value at position $\tau_k + 1$ in buffer x with u_k;

Step4: delete all buffer values from the positions to the right of position $\tau_k + 1$;

Step5: if the value from the first position of buffer x is non-zero, write it to output y_k, else y_k becomes y_{k-1};

Step6: shift buffer x with one position to the left.

The following section will present simulation results obtained with an implementation of this algorithm in Matlab/Simulink.

2.1.4. Simulations

The system from Fig. 2.6 will be considered as case study for testing the proposed algorithm. The NTB is considered to be a discrete time system with sampling period *h* of 1 ms. Three scenarios will be considered.

First, the scenario corresponding to the example from Fig. 2.3 will be addressed. The first sample instance *(k-3)h* of the considered time window is adopted as 0.010 s. The values for the input *u* are the ones from Fig. 2.7. Time delay τ varies as in Fig. 2.8, where at moment 0.014 s τ gets infinitely large due to a packet loss ($p=0$). The output *y* obtained with the model (2.1) implemented as the standard time varying delay Simulink block is illustrated in Fig. 2.9. It can be observed that the time variance pattern of the input signal is significantly altered. As opposed to the result from Fig. 2.9, by using the proposed algorithm in this paper, the output signal manages to reproduce the input signal pattern (Fig. 2.10).

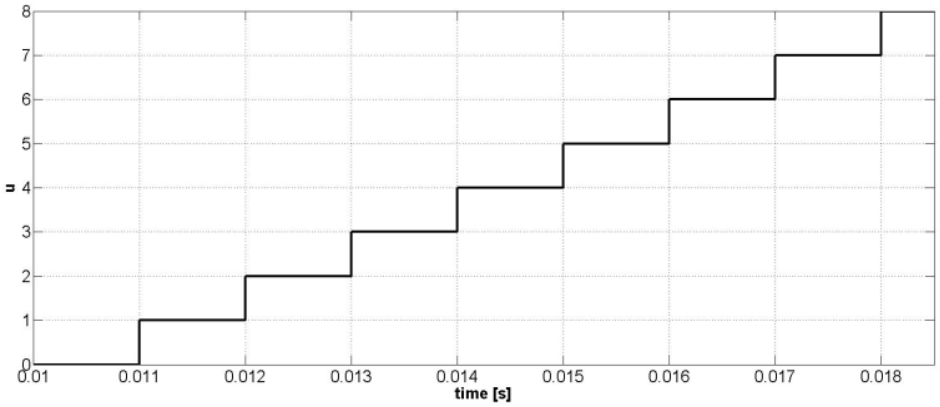

Fig. 2.7 - Input signal u

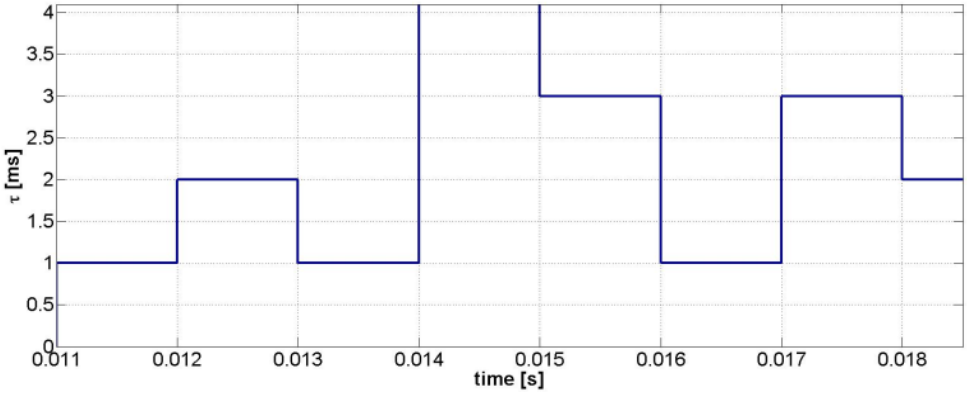

Fig. 2.8 - Time varying delay signal τ

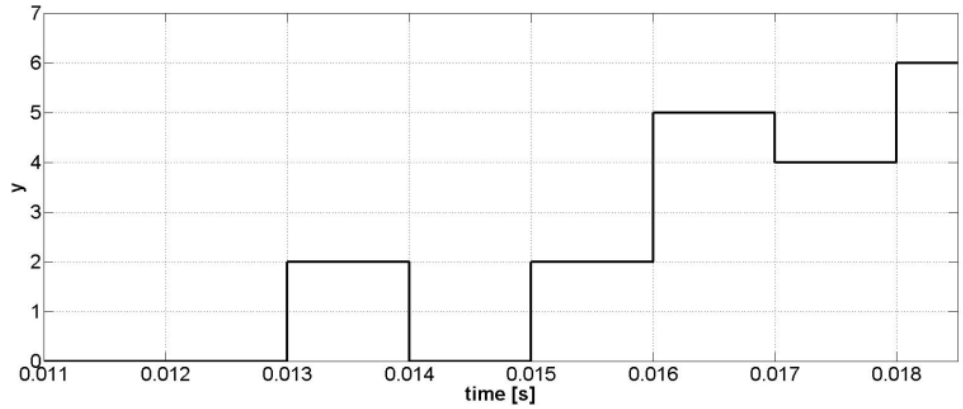

Fig. 2.9 - Output signal y for time varying delay model (2.1)

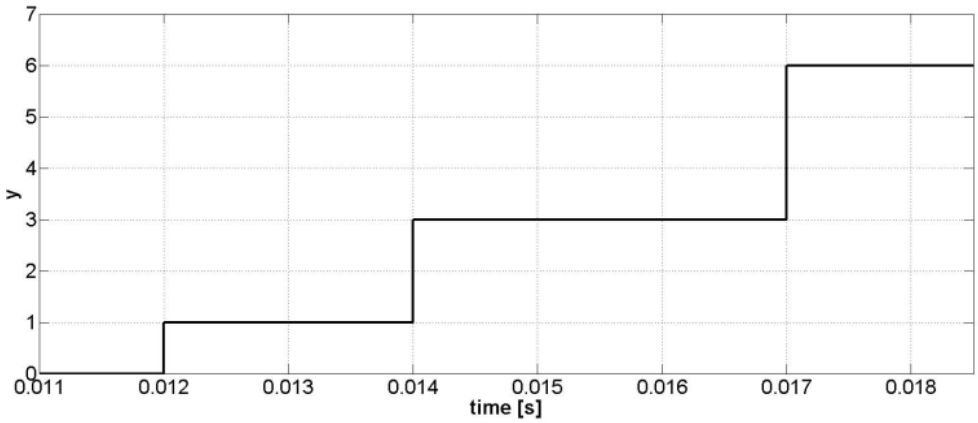

Fig. 2.10 - Output signal y for the proposed NTB model (2.16)

In the following two scenarios the inputs τ and p are generated as uniformly distributed pseudorandom numbers in a given range.

The second scenario corresponds to a discrete ramp input signal u. Fig. 2.11 shows the results obtained on a two second window, while Fig. 2.12 shows a zoomed version on a 0.2 second window. On a large time scale (2 s), it appears that the output y maintains a constant time shift in respect to the input u due to the mean value of the delay. However, by taking a look at a smaller time scale (0.2 s), it can be observed that actually the signal is significantly deformed because of packets which arrive too late or which are lost.

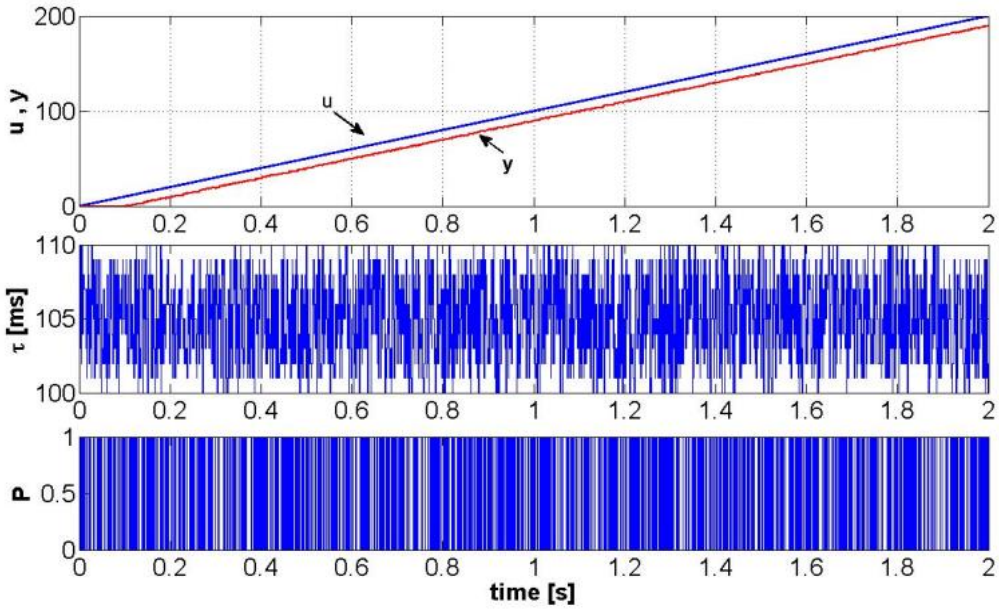

Fig. 2.11 - Simulations results for the NTB with a discrete ramp input on a 2 seconds window

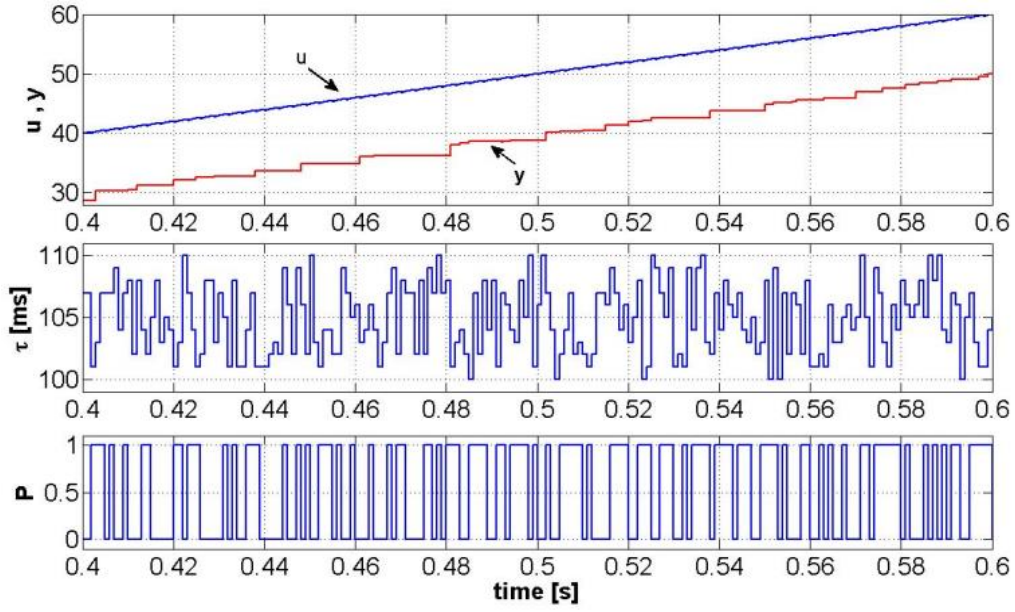

Fig. 2.12 - Simulations results for the NTB with a discrete ramp input on a 0.2 seconds window

For the third scenario a discrete sinusoidal input of 10 rad/s was considered (Fig. 2.13). Due to the significantly increased standard deviation of the delay, signal deformations can be observed here even on a large time scale of 2 s.

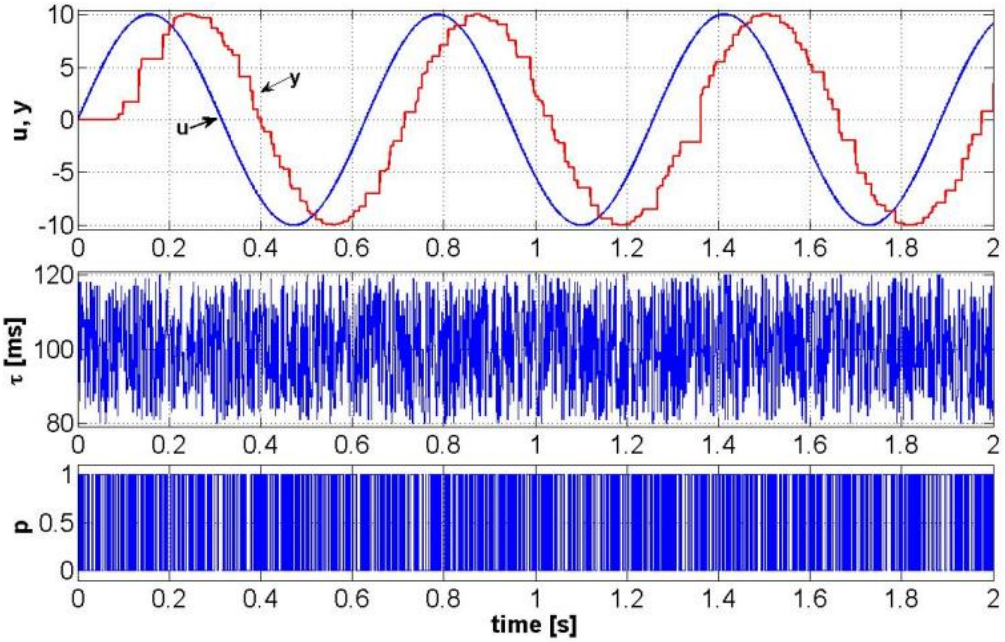

Fig. 2.13 - Simulations results for the NTB with a discrete sinusoidal input on a 2 seconds window

Ultimately, it can be concluded that the NTB implementation manages to reproduce patterns which, from the point of view of signal transmissions, are very close to real TCP/IP network transmissions complemented with an additional handling strategy.

3. CONTROL STRATEGIES USED IN NETWORKED CONTROL SYSTEMS

Several control strategies have been proposed in the literature for NCSs, based on the main issues induced by the network: delay, packet loss and limited communication ([3], [2], [32], [49]). The vast majority of control strategies focus on the network delay issue (delay compensation). Just a few methods try to somehow "compensate" the disturbance effect due packet loss, by considering for example a varying sample rate or through an event based approach. The limited communication aspect is usually overlooked, considering (somehow justified) that the control data needed to be transmitted over the network is relatively small compared to the capacity of data transmission on modern communication networks. Consequently, the discussion will further focus mainly on the time delay problem, and only marginally on the packet loss problem.

The focus on delay compensation in addressing the network induced perturbation is additionally justified by the following aspects: in some situations (e.g. small packet loss ratio) packet loss can be approximately equivalated by an additional delay, packet loss usually does not occur in small (local) networks or industrial networks, some protocols do not involve packet loss (e.g. TCP).

A wide variety of control solutions have been developed for systems with time delays ([50], [51], [52]). However, most of them treat the time delay as being constant, which in the case of NCS is unrealistic – possibly the most fundamental characteristic of network transmissions is the network time varying delay (it is not uncommon to have large variations on relatively small time scales). Attempts to adapt these techniques to NCS through simplifying assumptions (like constant time delay) or by forcing the delay to be constant (through buffering or queuing) lead to poor control performances. This context motivated the need for new control strategies, which emerged as the interest in NCS applications increased.

The main categories of control solutions that are the most often encountered in the specialized literature on NCS are: predictive control, event based control, optimal stochastic control, robust control, observer-based control, queuing/buffering based control, variable sample time based control, adaptive control, Lyapunov based control.

Further one, after a short overview of these methods (Section 3.1), two control solutions developed by the author mainly in [53] and [54] will be presented (Section 3.2, Section 3.3). The state of the art will be from an engineering perspective, focusing more on techniques capable of achieving certain control performances (tracking problem) instead of just ensuring stability (stabilization problem). Additionally, theoretical methods with a high degree of complexity, which (usually) involve a large body of assumptions, and are difficult to test in practice, are intentionally avoided. Finally, the two control solutions developed further in this thesis will be presented at a conceptual level – the subsequent chapter will give a detailed description of these methods, followed by case studies.

3.1. An Overview of Networked Control Strategies

3.1.1. Model Based Predictive Control

Model predictive control has traditionally been developed for slow large-scale process, with complex dynamics and large model uncertainties (e.g. chemical industrial processes). The method consists in predicting at each sample instance the future evolution of the system, with the control signals being generated through an optimization procedure. Because of this, the method is usually computationally demanding. However, recent advances of technology (particularly related to computational power) have made possible to use such methods also for fast process, including NCSs ([55]). Still, most studies focus on small scale networks (or private unshared networks, industrial networks), because the dynamics of large scale shared networks (like the Internet) cannot be modelled, and the evolution of the network's (as a system) behaviour cannot be predicted.

Several types of predictive techniques can be found in the literature in respect with NCSs, which differ through the manner in which the time delay and/or packet loss compensation is integrated into the predictive strategy.

One of the most classical examples is the well-known Smith predictor, which was initially designed for compensating constant time delays ([16] - Vol. I, Section 9.8). More recently, this was extended to an adaptive Smith Predictor ([56]), where the adaptation is done online, through a delay estimator which adopts a delay value at each sample instance based on the RTT delay and packet arrival. Although the experimental results shown on a wide area network transmission are encouraging, the stability is not proven, so there is no indication of what types of delay variations the control structure can handle.

In [57], the standard model based predictive control strategy is extended in order to incorporate time-varying delays. Different delay modelling approaches are presented, but eventually each one of them involves embedding in the prediction strategy of the time delay model (the delay is actually constant on each prediction horizon).Experimental results are shown for a small scale industrial network (CAN).

In [58] the predictive algorithm is used along with an online model identifier, while the prediction horizon varies as function of the network time delay. At each sample instance all the control values computed for the current prediction horizon are sent to the actuator and stored in a buffer, such that when packet losses occur, these previously predicted values are used as control inputs for the plant until new data arrives. The experiments, conducted on an Ethernet based local area network, show that the control solution can successfully compensate the delay effects on such network, and can withstand a certain amount of packet loss (up to 12.5%). However, of more interest would have been to evaluate the system's response to larger delay values, specifically to large area networks.

An interesting approach is given in [59], for dealing with large packet loss ratios (Fig. 3.1). On the controller side, the predicted control values at a given sample instance are all sent to the actuator. If the packet received from the sensors arrives in a certain imposed time limit, it is used for calculating the current value of the control signal. Otherwise, an estimate obtained from previous measurements is used. Additionally, a flag is used for signalling the actuator if the current control value is

computed based on measurements or estimations. On the plant's side, the actuator contains a state machine (Fig. 3.2) which selects for usage either the arrived current control value- if it arrives in the imposed time limit, or other previous received values. The state machine has two modes of operation: synchronized and interrupted. In the synchronized mode the plant's state are considered to be synchronized with the plant's model states. The transition from the synchronized mode to the interrupted mode occurs when on the direct path a packet is lost. In the interrupted model the actuator has to use a previous estimated control value or maintain a constant value if all the estimated values were already used. The transition back to the synchronized model occurs when a new packet is received at the actuator node with the mentioned flag indicating that a control value calculated based on measurement data was transmitted. The results shown suggest that the method is efficient in dealing with large percent of packet loss (up to 90 %!). Still, the distribution of packet loss is uniform, which in case of real communication networks may differ significantly (especially when practically no packets arrived at the receiving node for a large number of consecutive sample periods). Moreover, because the experiments presented are for local area network, the delays are insignificant.

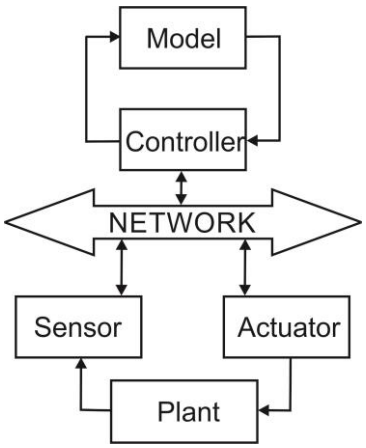

Fig. 3.1 – Model-based predictive NCS (adapted from [59])

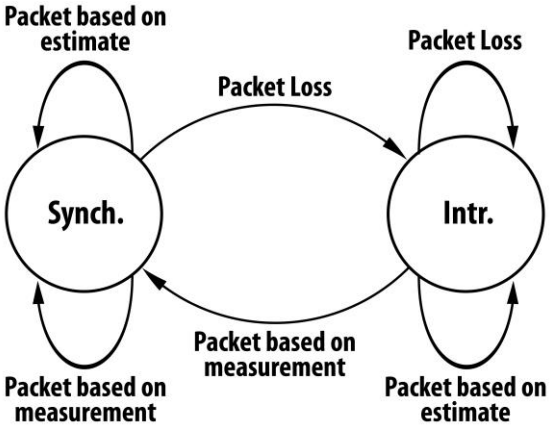

Fig. 3.2 - State machine at the actuator (adapted from [59])

Finally, many other approaches are hybrid- in the sense that they combine a predictive technique with another control approach - this shall be seen in the subsequent sections.

3.1.2. Event Based Control

Motivated by the rapid development of embedded systems, event based control systems have received an increasing amount of attention lately from the control community. Although a lot has been done in this direction, there are relatively few studies in conjunction with NCSs ([60]). This is somehow surprising, because phenomena like multiple consecutive packet loss (i.e. no data arrives at the receiving node during several consecutive sample periods), specific to network transmission, would intuitively lead one to think of an event based approach (event triggered communication – [61]). In this context, two recent studies are further mentioned.

In [62] an event-based predictive controller is preceded by a network compensator (both place remotely), which makes a forward prediction of the plant's evolution for the worst case scenario of the delay evolution. The controller sends all the predicted control values at each sample instance to the actuator, which stores them in a buffer, and adopts the proper control value for each sampling instance. The sensors send with each measurement packet, besides the time-stamp of the current packet, the time stamp of the last successfully arrived packet at the actuator. A new measurement packet is sent only after a new control input arrived or was lost. The stability of the overall systems is proven for a nonlinear model of the process. The solution is validated only through simulations, for uniform distribution of the time delay and packet loss ratio.

A more practical approach is followed in [63], where also an event-based predictive controller is used. The control structure is interesting in its own right, and thus reproduced in Fig. 3.3.

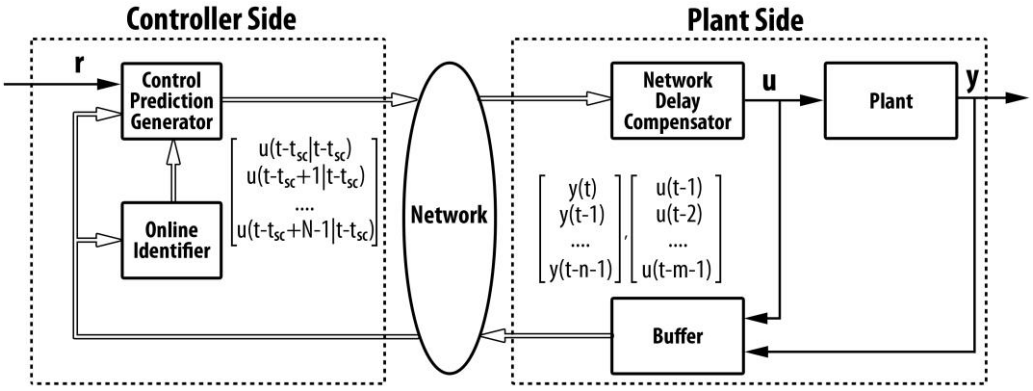

Fig. 3.3 - Network event based predictive control structure (adapted from [63])

The controller is active only when a new measurement data has arrived and generates the set of control values on the given prediction horizon. An online recursive leas-squares parameter estimator is also used, which calibrates the plant model parameters according to the real plant. On the plant's side, a network delay compensator is used, which chooses the control value to use from the predicted control sequence received, based on an objective function which also uses past values

of the plant's output. If no new data arrives on the direct path, the network delay compensator uses the previous received values of the control signal and of the plant's output. The two sequences corresponding to the input and output signals of the plant are queued in a buffer and sent to the controller side. An important advantage of this control structure is that the delay compensation is done by using previous output values of the plant from a buffer – which eliminates issues of delay measurements and synchronization. The control methodology is finally validated through experiments done on an intercontinental network transmission (WAN).

3.1.3. Optimal Stochastic Control

Network transmissions, as part of NCS, are of an intrinsic stochastic nature, which makes an optimal stochastic control approach seem appropriate. However, studies in this direction bring a more involved mathematical framework, while experimental results which can show the attained performance of the control solution are sparse. In this context, only the pioneering work of Nilsson ([64]) will be mentioned, along with future extensions.

In [64] an optimal stochastic control methodology is developed for the NCS (Fig. 3.4), where the process is assumed to be perturbed by white noise, while the delays given by network transmission are considered stochastically independent. The control strategy is based on an optimal state feedback, through the design of a LQ-controller which uses the state provided by an optimal state estimator. The parameters of the optimal controller are determined by minimization of the defined cost function for several possible values of the delays. Finally, the parameters obtained are integrated into an interpolation table. According to the current measured delay value, the interpolation table provides in real-time the parameters used by the LQ-controller. Although the work is limited to delay values below the sampling period, an extension to larger delay values was done in [65], where a Kalman Filter is used as an optimal observer. Further developments have been presented in [66], where the performance of the optimal stochastic control approach, when both time varying delays and packet losses occur during network transmission, is analysed.

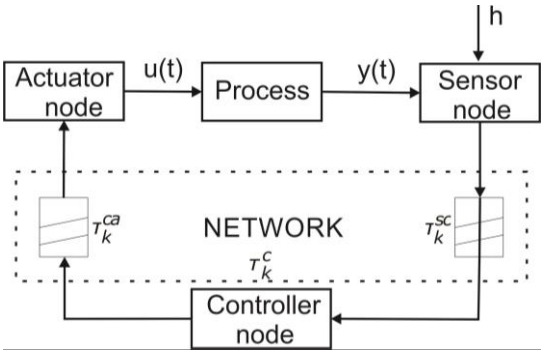

Fig. 3.4 – Distributed control system with induced delay (adapted from [64])

3.1.4. Robust Control

Robust control is a very active area of research, concerned with designing controllers and/or control structures that conserve their performances when dealing with plant model uncertainties or disturbance uncertainties. Because this always

happens to a certain degree in practice, such an approach is always welcomed when feasible. In NCSs, the uncertainties are primarily due to the network, and as a result it can be said for example that the network time delay is time varying or that it is almost constant – but with some uncertainties. Such an approach is followed in many robust networked control strategies, mostly along with state feedback controllers. The disadvantage is that if the network time delay varies in a very large range (as is the case of transmission over the Internet), this would mean large uncertainties, which eventually makes such a control strategy relatively unfeasible (thus the conservative nature) – especially for fast processes. Additionally, most studies focus just on the linear case. While having in mind that the design procedure is complex in respect with other types of strategies (with a possible exception being the optimal stochastic approach), even for linear systems alone, two control solutions will be further presented from the specialized literature.

A reference work in robust networked control is that from [67], where the network time-varying delay was considered as a multiplicative uncertainty. The control structured is illustrated in Fig. 3.5. G represents the process model, K is the controller and W_r is a reference filter. Because the delay (T_u/T_y) was considered bounded and varying around a fixed value, the used delay model has actually two components: a first order Pade approximation for the fixed part of the delay (G_{du}/G_{dy}), and a multiplicative perturbation for the varying part (composed out of a weighting transfer function W_u/W_y and a complex perturbation function Δ_u/Δ_y). The controller K was obtained through μ-synthesis so that it would guarantee stability and the imposed performance in the presence of multiplicative uncertainty (delay uncertainty). A drawback of proposed method is that it is limited to linear systems; e.g. a large spike for the time delay variation would make the control signal increase up to entering in saturation- which happens for all types of control systems in practice – thus a nonlinear component.

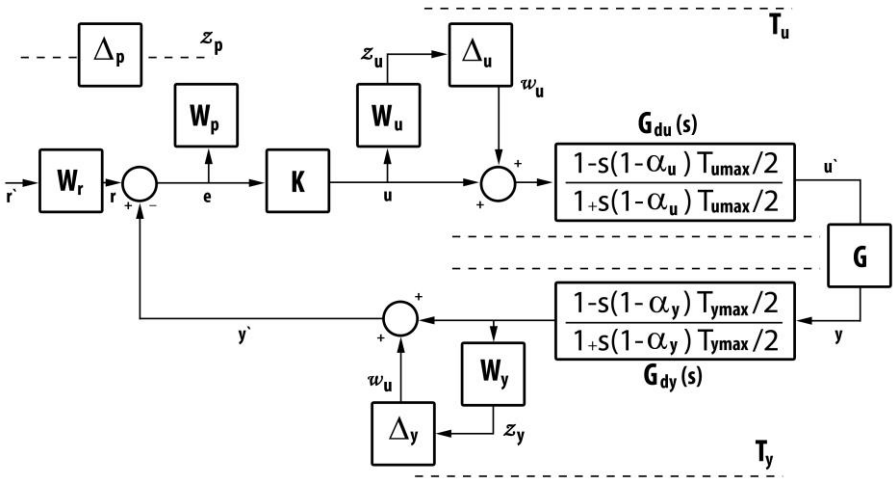

Fig. 3.5 - Networked robust control structure (adapted from [67])

A more recent robust networked control strategy is proposed in [68], based on H_∞ control. As opposed to most studies from the literature, which address only the stability problem, this study addresses the tracking control problem, by augmenting the closed loop system with an exogenous model for the reference. A state feedback

controller is designed which can reject two input disturbances – at the plant and the exogenous reference model, i.e. the tracking error caused by disturbances is attenuated at an imposed level in the H_∞ sense. The design uses Lyapunov-Krasovskii functional (which can deal with time-varying delays in the closed loop model) and LMI based techniques (through which the controller can be easily derived by solving numerically several LMI conditions).The design is extended such that the controller is robust to parametric uncertainties. Finally, a simulation example shows the control performances of the system, for small delay variations (up to 10 ms) and a small ratio of consecutive packet loss.

3.1.5. Queuing/Buffering Based Control

Buffering is often used in networked control strategies for storing control values/measurement values at the actuator/sensor/controller level. Many predictive techniques use a buffer to store the predicted sequence at a given sample instance in case packet drops may occur in the future (this can be regarded as a sort of packet loss compensation) – see the above mentioned predictive control strategies. Alternatively, many studies use queues for forcing the delay to be constant. Some approaches involve placing a queue at the sensor level ([69]) or at the actuator side ([70]), so that a remote observer which estimates the non-delayed state can be designed. In [71] a queuing methodology is proposed (Fig. 3.6): on the remote side a queue is placed in series with an observer, a predictor and a controller; on the local side a queue is placed in series with the actuator, plant and sensor. The queues work based on the FIFO principle (First-In-First-Out) and aid the predictor in determining the future states of the plant. The delay compensation is thus achieved by the combination of the queues with the predictor. Finally, it important to mention that the buffering/queuing approaches which impose a constant time delay are practically maximizing the time delay to its larges value, which in many cases can negatively influence the control performances (e.g. in terms of settling time).

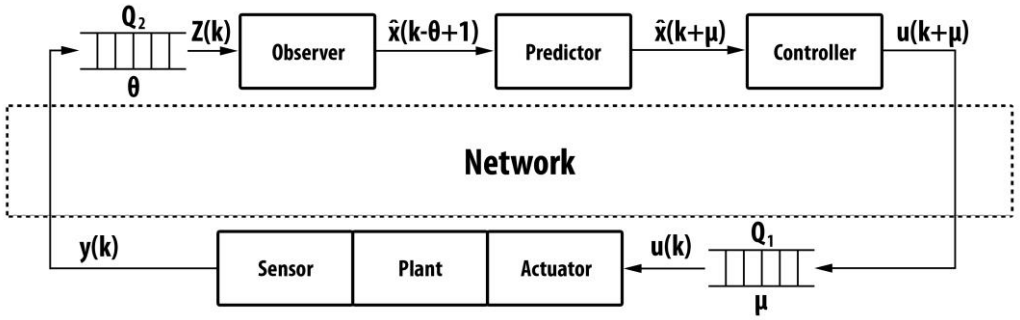

Fig. 3.6 - Predictor-queuing time delay compensation strategy (adapted from [32])

3.1.6. Adaptive Control (Gain Scheduling and Switching Type)

Under the name adaptive control we will refer here to all types of control techniques for which the parameters of the controller vary in time, as dictated by some exogenous signal/signals. One early direction developed in this area is the so called gain-scheduling approach ([72], [12] – Section 12.5), where the parameters (gains) of the controller are changed in time as a function of some measurable signal of interest at the plant level (scheduling signal) that is considered to characterize the

changes in the dynamics of the plant (i.e. it influences the operating point), and which is considered to have slow time variations. Such methods address the problem of controlling systems with slow changing dynamics. A recent direction of high interest in the last decade refers to the case when the plant dynamics has fast time variations, referred to as 'switching', for which switching controllers have to be designed according to specified switching variables ([48] – Part III). As a formal distinction between these two, scheduling control implies (traditionally) a continuous variation of the controller parameters (through tuning rules or interpolation), while switching control implies a discontinuous variation (due a switching signal or/and a switching logic). Referring back to NCSs, the communication network induces a switching behaviour either due to the fast time delays variations, packet losses, or other types of phenomena. In this context, several attempts in the literature focus on designing switched controllers that can face such disturbances.

With the wide use of PID (proportional-integral-derivative) controllers in the industry ([73]), it was only naturally to early consider gain-scheduling (and later on switching) to such controllers. In particular, recent studies consider the case when the plant is characterized by a time-varying delay, and design a gain-scheduling strategy for the PID controller with the delay as the scheduling variable. Such a situation is directly applicable to NCSs, when network transmissions are characterized (ideally) only through time delays, and the delays are lumped into a single round-trip delay at the plant level. For example, in [74] tuning rules are derived for the PID controller, based on multi-objective optimization with the ITAE criterion (integral of time-weighted absolute error) and the inverse of the jitter margin (upper bound for additional delay for which the system maintains stability) as performance objectives, for certain classes of benchmark process models. Another example is the approach from [75], where the gains of a PI controller are determined heuristically according to different values of the QoS (defined by the network throughput and the point-to-point maximal delay bound of the largest packet) and stored in an interpolation (look-up) table, for real-time gain adaptation.

By far, the vast majority of switched controllers are of state feedback type, and in some cases integral state feedback, due to the simplicity and general applicability of such controllers. However, the focus is usually on stability, with few approaches addressing the tracking problem. In [35] a RTT delay dependent switched state feedback integral controller is proposed, with the gains determined offline through numerical optimization. Because on the controller side only the sensor-to-controller delay is available, the controller actually calculates control values for all possible discrete delays (multiples of the sampling period) from an a priori defined set, and sends them to the actuator. At the actuator level, according to the obtained RTT delay (sensor-to-controller delay plus controller-to-actuator delay), the corresponding control values is selected and used further for controlling the plant. Although this solves the issue of synchronization, by using only the RTT delay (and not one way delays) for controller switching, for small sampled periods with large possible delay variations, this would mean that a lot of useless information would be send on the direct pathway with each sample instance – thus an inefficient used of the network bandwidth. A somehow similar approach is that from [76], where the gains of an LQR controller are tuned according to the network delay; more specific, the weights of the LQR controller are tuned using LMI type restrictions so that it would ensure stability for different delay value ranges. Other approaches consider the time varying delay to be unknown or uncertain (for example due to lack of synchronization between components), and instead switch the controller according to a generic or

arbitrary switching signal (specific to some switching logic component of the system in cause) – see for example [77] – Chapters 3, 4.

In many practical situations the states of the process cannot be directly measured, and thus an observer has to be designed for state estimation. In NCSs, the assumption is that usually at the plant level there is little computational power available, and as a result the problem of remote estimation appears, when the observer is place remotely along with the controller. However, this complicates the control problem because now the observer has to reconstruct the state values despite the disturbance effect of the networks (see [66] and [3] for more on remote estimation over networks). In this context, different studies consider networked control structures with remotely placed controllers and observers, with either one or both of them being switched. Recent examples are [78] and [79], where the control structure is based on remotely placed switched state feedback controller and switched Luenberger observer, where the switching is done after the network time delay. In [79], certain subintervals for the delay values are predefined such that the switching occurs only when crossing from one subinterval to the other (this eliminates oscillations of the control signal due to small delay variations, and makes the stability analysis easier because fewer switching modes have to be taken in consideration). Moreover, a switching dwell time (minimum interval before another consecutive switch can occur) is imposed, in order to ensure global stability. The method is finally validated through experimental results, for a NCS over the internet, with delay values up to 120 ms.

Lastly, it is important to mention that a possible drawback in switching based control of NCS, which becomes even more crucial when the switching is delay or packet loss dependent, is the appearance of oscillations during steady state regimes of the plant, due to control signal fluctuations caused by the fact that the network parameters are continuously varying even then. Additionally, fast switching between large values of the controller parameters can cause undesired transient behaviour. For the first problem, the most straightforward (and probably the most effective) solution is to extract an integrator component from the controller, and place it downstream of the controller, so that in steady state the control signal that affects the plant is forced to be constant (see [80] - Chapter 6 for switching and [12] – Section 12.5 for gain-scheduling). Other possible solutions would be filtering the switching signal in order to force it to vary more slowly, or use a granularity approach that implies defining subsets for the delay values and impose switching only between these sets. For the second problem, the solution implies the introduction of some form of bump less transfer between different controller parameters, but at the price of increasing the complexity of the controller ([81], [82]).

3.2. A Control Structure with Observer-based Delay Compensation

A new method for delay compensation in NCSs, inspired from classical control theory (see for example [83]; for a survey on the issue see [84]), considers the delay as additive disturbance acting at the input of the process ([6]). This disturbance is estimated through a so called communication disturbance observer (CDOB), whose output is used to reject its effect from the controller's point of view. While most of the methods mentioned require a model for the time delay, or impose some kind of delay estimation/measurement, the usage of the CDOB based method has the main advantage that no information about the time delay instantaneous values or time delay variation rate is needed - the time delay is treated as an unknown input disturbance. Moreover, the CDOB method avoids any synchronization issues that would appear in delay measurements over the network.

The study from [6] is limited to first order processes. However, in control design practice, many second order benchmark process models can be encountered. In this context, the current study extends the design of the CDOB method for second order processes. Furthermore, an elaborate analysis is made concerning the disturbance estimation and rejection, which implies: setting the optimum gains for the observer in correlation with certain cut-off frequencies, comparing different types of observers (full order and reduced order). Finally, the peaking phenomenon of the observer is discussed as an implementation issue, and the overall control structure is tested in a realistic scenario including time-varying delay and packet loss.

Consider the networked control structure from Fig. 3.7, where the aim is to reject the disturbance effect of the network and the local disturbances, while also ensuring satisfactory process control performances. The process is situated remotely, being separated from the controller through a network, which is considered as a discrete time nonlinear system. At the process level, the local disturbance d is compensated by a local feedback loop composed out of a disturbance observer (DOB) and a disturbance compensator (DCO). At the controller level, a communication disturbance observer (CDOB) and a conventional controller are used. The CDOB compensates the effect of the delay disturbance from the controller's point of view, i.e., due to the CDOB, the controller "looks at the process" as if it is unaffected by communication disturbances.

As a working design hypothesis, the network system is idealized as a time varying delay element. By considering that the plant is linear, the network delays on the feedback path and direct path from Fig. 3.7 can be merged, obtaining a round-trip-time (RTT) delay τ at the input of the process. The RTT is considered as a delay disturbance d_n, defined as the difference between the transmitted control signal u_r and the received control signal u_n ([6]):

$$d_n(t) = u_n(t) - u_r(t) \tag{3.1}$$

with

$$u_n(t) = u_r(t - \tau) \tag{3.2}$$

In this context, the network model from Fig. 3.7 is reduced to a unitary direct path with an additive delay disturbance ($u_n(t)=u_r(t)+d_n(t)$) and a unitary feedback path ($y_n=y_p$).

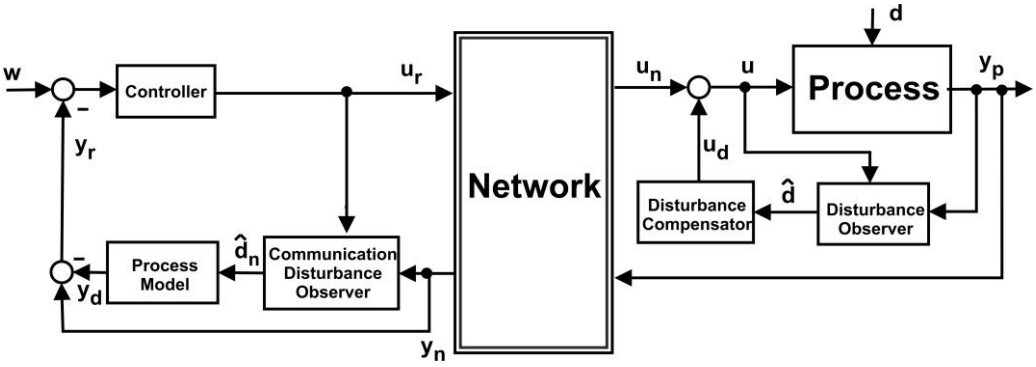

Fig. 3.7 - Observer-based delay compensation structure

3.3. A Control Structure Based on a Switched Delay Compensator

In addressing the control objective (tracking and stabilization), a new networked control structure is proposed here, composed out of a remote placed controller (designed for the local process) and a local switched PD compensator which rejects the network disturbance effect. The structure aims in achieving a balance between design complexity and control performances – a time-invariant controller is proposed for the time-invariant plant, while the switching behaviour of the network is attenuated through a switched compensator. As far as the author knows, such a control structure, designed in a modular manner, has not been reported in the literature in respect with NCSs.

Consider the networked control structure given in Fig. 3.8. Because the control structure consists of both local and remote control elements, it can be regarded also as a particular type of hierarchical networked control structure (as defined in [32]).

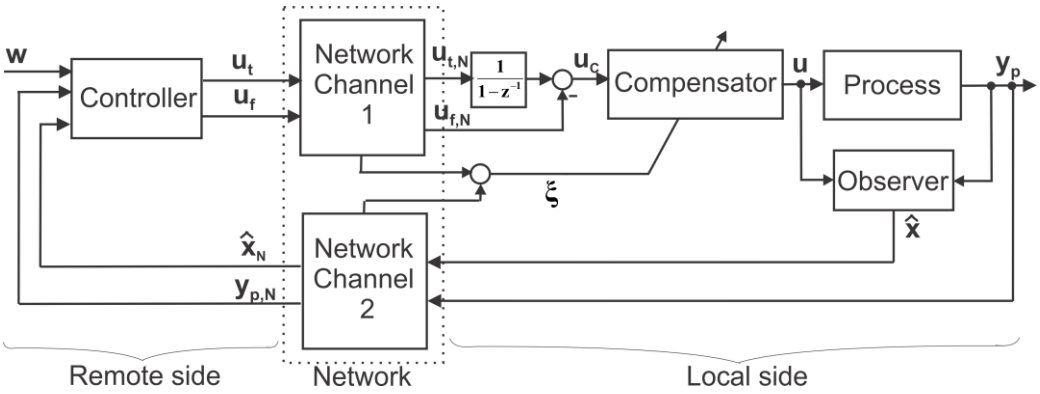

Fig. 3.8 - Networked control structure with a switched delay compensator

On the remote side the controller (designed for the local control structure, i.e. by considering it to be directly coupled to the process) generates two control signals – one for tracking (u_t) and one for feedback stabilization (u_f) – based on the received state and output signals of the process. On the local side a discrete integrator is placed for assuring a null steady state tracking error, while a compensator aims in rejecting the disturbance effect of network transmissions (thus preserving the control system's performances imposed when designing the controller). The compensator is adapted according to a generic signal ξ which is related to the quality of network transmissions (i.e. it can incorporate information regarding the network delay, packet loss, etc.). Additionally, a state observer is placed on the local side for estimating the states of the process which are not directly measurable.

4. DESIGN AND ANALYSIS OF NETWORKED CONTROL STRUCTURES WITH DELAY COMPENSATION

This chapter presents in detail the design and analysis of several networked control structures using different strategies for delay compensation.

A first method considers the delay as additive disturbance acting at the input of the process ([6]). This disturbance is estimated through a communication disturbance observer (CDOB), whose output is used to reject its effect from the controller's point of view. The other two strategies use adaptive delay compensation. The compensator blocks continuously adapt their parameters according to the quality of network transmissions.

4.1. Observer-based Networked Control Structure

The current section describes the design and analysis procedures for the networked control structure from Fig. 3.7. The aim is to obtain a control structure capable of rejecting the disturbance effects of the network and ensuring satisfactory process control performances ([53]).

The design is based on the following strategy:

- First, the local feedback loop is designed (DOB+DCO) for the rejection of the local disturbance.
- Second, a conventional controller is designed for the local control of the plant (the network will be further introduced between the controller and the plant).
- Third, the CDOB is designed which, coupled with a model of the process, rejects the delay disturbance, from the controller's point of view.

The modular approach has two main advantages. First, it reduces the overall complexity of the design process, because each module can be designed independently. Second, from a practical point a view, an existing local control structure can be upgraded to a networked control structure simply by adding additional modules (CDOB).

The design steps for the networked control structure are further presented for the speed control of an electrical drive containing a DC motor, using a 2^{nd} order model for the motor. Although the design is presented for a specific process, the same sequence of steps can be followed for other processes of 2^{nd} order.

4.1.1. Process Modelling

4.1.1.1. The Mathematical Model of the Electrical Drive

The process taken into consideration in the current study is an electrical drive containing a DC motor with fixed field excitation. Fig. 4.1 illustrates the hybrid physical scheme. Based on this scheme the following well known equations hold:

- The voltage balance equation for the electrical subsystem

$$u_A(t) = R_A i_A(t) + L_A \frac{d}{dt}\left(i_A(t)\right) + e(t) \tag{4.1}$$

where u_A is the armature voltage, i_A is the armature current, e is the back EMF, R_A and L_A are the armature resistance and inductance.

- The equation of the generated back EMF is proportional to the motor angular speed ω (due to the constant excitation voltage, the electrical field is considered to be constant)

$$e(t) = k_e \omega(t) \tag{4.2}$$

where k_e is a constant which also includes the value of the electric field.

- The equation of the electromagnetic torque developed by the motor

$$T(t) = k_t i_A(t) \tag{4.3}$$

where k_t is a constant.

- The dynamic equation of motion

$$J \frac{d}{dt}\left(\omega(t)\right) = T - T_l \tag{4.4}$$

where T_l is the external load torque and J is the moment of inertia of the mechanical parts. The initial conditions for equation (4.1) and (4.4) are $i_A(0)=i_{A0}$ and $\omega(0)= \omega_0$.

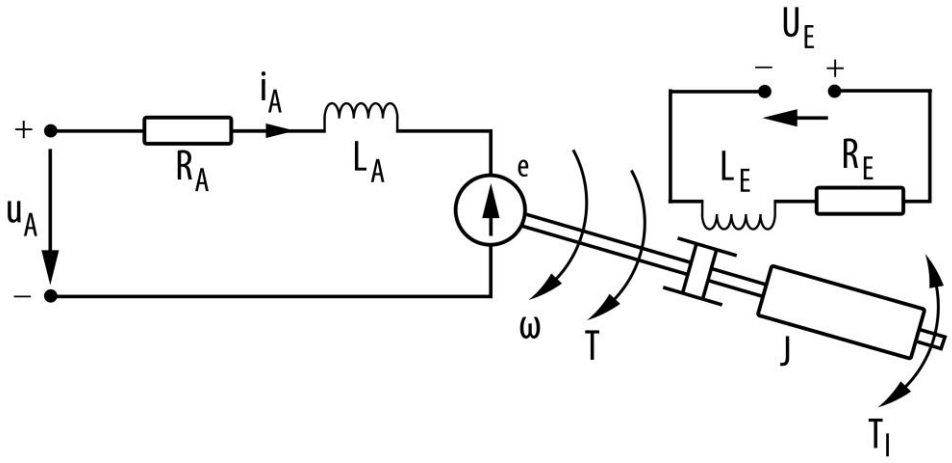

Fig. 4.1 - Equivalent diagram for a DC motor with fixed field excitation

The DC motor is considered a dynamical system with the input-output orientation { u_A,T_l } -> { ω }. Because the model is completely linear by applying the Laplace transform to equations (4.1)-(4.4), the block diagram from Fig. 4.2 is obtained:

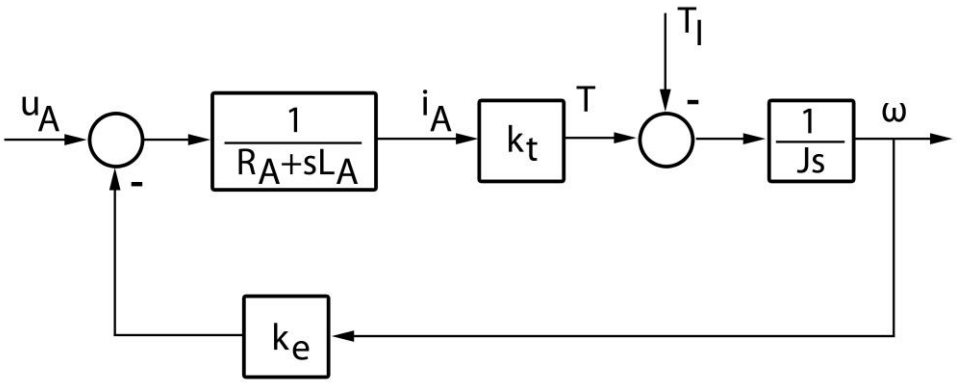

Fig. 4.2 - Block diagram of the DC motor model

The transfer functions model of the system from Fig. 4.2 is

$$\omega(s) = \frac{1/k_e}{T_aT_ms^2 + T_ms + 1}u_A(s) - \frac{(1+T_as)T_m/J}{T_aT_ms^2 + T_ms + 1}T_l(s) \qquad (4.5)$$

Here, $T_a=L_A/R_A$, $T_m=(JR_A)/(k_tk_e)$ are the electrical, respectively electromagnetic time constants of the motor.

The DC motor is controlled through an electronic actuator and the speed is measured using a tachogenerator or a rotary encoder.

By neglecting their dynamics, the actuator and the sensor can be modelled as simple proportional elements:

$$u_A(t) = k_u u(t), \quad \omega_m(t) = k_\omega \omega(t) \qquad (4.6)$$

where k_u and k_ω are the gains of the sensor and the actuator, u is the control signal and ω_m is the measured speed.

Now, for the complete model of the process the following transfer function dependence can be used:

$$\omega_m(s) = \frac{k_\omega k_u/k_e}{T_aT_ms^2 + T_ms + 1}u(s) - \frac{(1+T_as)T_m}{T_aT_ms^2 + T_ms + 1}T_L(s) \qquad (4.7)$$

where $T_L=T_l/J$ is the load disturbance related to the moment of inertia.

4.1.1.2. Estimating the Parameters of the Mathematical Model

The parameters of the mathematical model (4.7) which describes the controlled process can be classified into two categories: gains (k_ω, k_u, k_e) and time constants (T_m and T_a). Thus, the identification procedure can also be divided into two steps: identifying the parameters responsible for the static behaviour of the system (gains), and identifying the parameters responsible for the dynamic behaviour of the

system (time constants). In order to reduce the number of parameters used in identification, the gains k_ω, k_u, k_e will be lumped together under a single gain k_P ($k_P = k_\omega k_u / k_e$).

The DC motor considered in the experiments is controlled within the voltage domain of ±24 V, has a moment of inertia of $5.18 \bullet 10^{-6}$ kg m^2 and it can reach a maximum speed of 4000 rpm. The actuator consists mainly in an H bridge driven in the voltage domain of ±6 V through a PWM circuit, while the speed sensor is a tachogenerator, linear on the entire speed domain.

Fig. 4.3 illustrates this experimental setup. Now that the physical process has been defined, the two step identification procedure can be executed based on offline experimental recordings.

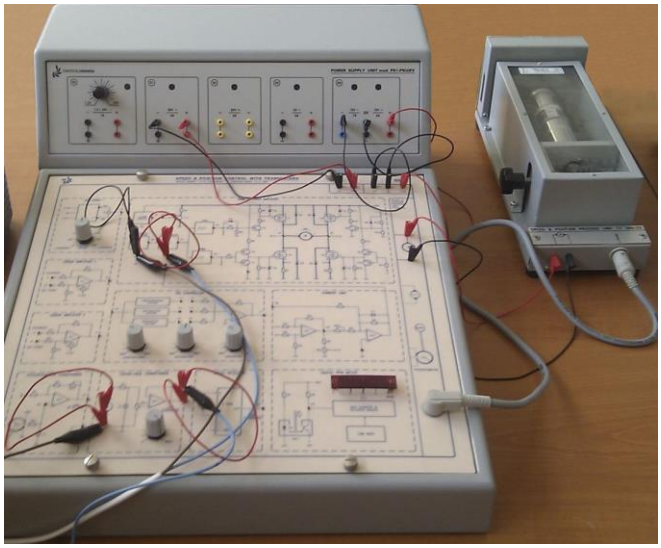

Fig. 4.3 - Experimental setup of the controlled process

The process gain k_P could be easily estimated from the slope of the input-output static characteristic of the physical process, assuming that the process is linear (i.e. the static characteristic is a line that passes through the origin). From the experiments it was observed that the physical process is not linear, having an asymmetric static characteristic with an insensitivity region near zero velocity (Fig. 4.4). The insensitivity region is probably caused by friction forces, while the asymmetry can be caused by the electromagnetic part of motor or the electric drive. A solution in surpassing this inconveniency is to compensate the static nonlinear characteristic of the process with an inverse static characteristic (Fig. 4.5), implemented as an interpolation block on the controller side and connected in series with de process. The resulted characteristic is presented in Fig. 4.6. The x mark symbolize the fact that according to Fig. 4.5 when the control signal u reaches the null value, the signal c takes a sudden jump. In a non-reversible working regime this jump is unimportant. In a reversible working condition the jump induces an impulse into the signal c. Theoretically, this fact can either be expressed by introducing an additional term in (4.7), that generates short period impulses when the control signal becomes u=0, or by manipulating the initial conditions. Because the DC motor acts like a filter towards this impulses, in practice it was observed that their effect was

negligible. So, the $\omega_m(u)$ characteristic was considered linear, with the newly constructed process having a unit static gain (k_P=1). These results were also verified through experiments, where the maximum error of the static nonlinear compensation was below 1%. Thus it can be concluded that the linearization is successful.

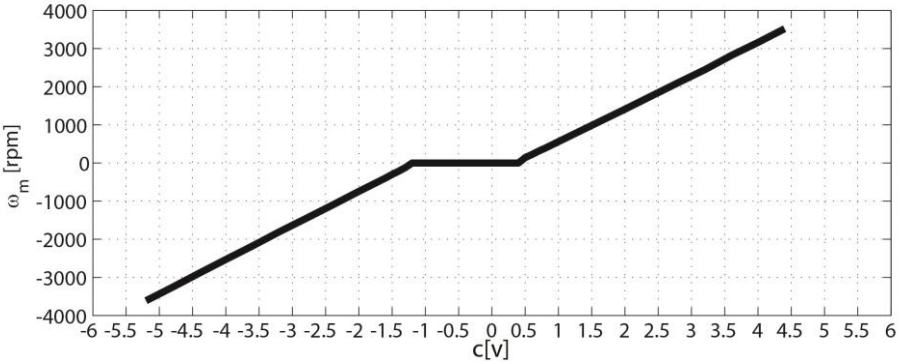

Fig. 4.4 - Static characteristic of the process (c is the control signal for the actuator)

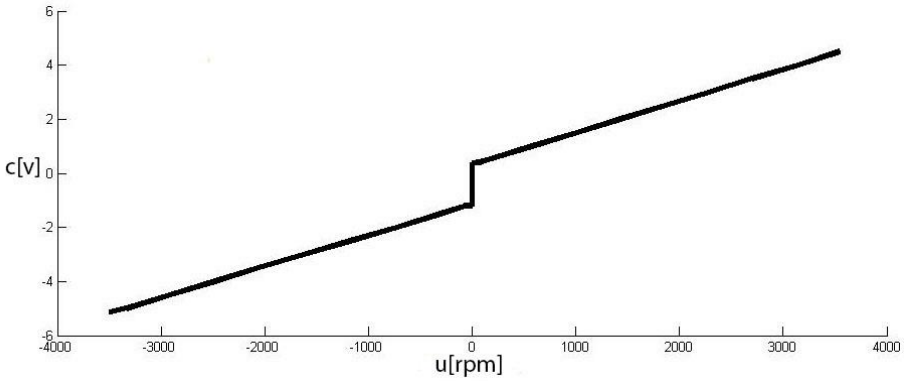

Fig. 4.5 - Inverse characteristic used for linearization (u is the control signal and c is the output of the interpolation block)

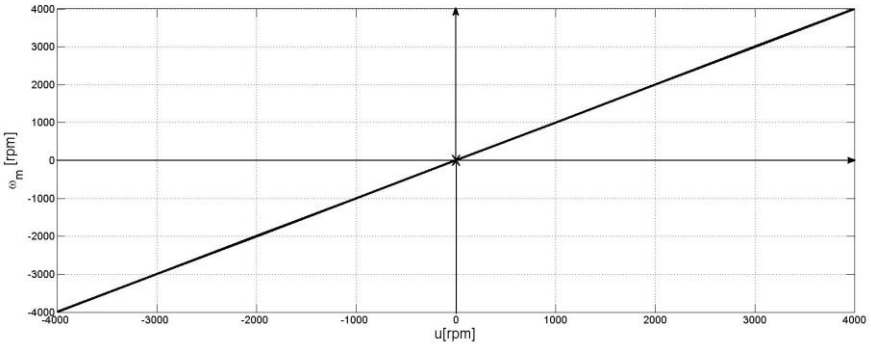

Fig. 4.6 – Static characteristic of the linearized process

Identifying the time constants (the second step) require experiments that would reveal the dynamic behaviour of the process. With this purpose in mind, two kinds of scenarios were used: one that involves step signals and one that involves ramp signals. So, for the first scenario, the control signal has a rectangular waveform (rising step and falling step). Different amplitudes were used in testing the dynamics of the process (both positive and negative values). For the second scenario the control signal has a trapezoidal waveform (rising ramp and falling ramp). Again, different amplitudes were used in testing (positive and negative).

The output and input signals (ω_m, u) were recorded during all the experiments, done according to the above mentioned scenarios. For each experiment both time constants were identified based on the measured output-input signals by using the System Identification Tool from Matlab ([85]). The tool uses the Gauss-Newton method which practically solves a non-linear least squares problem by minimizing the error between the measured output and the model's output. The time constant values obtained for all the considered experiments were averaged. Finally, the average values are T_m=0.157 sec and T_a=0.039 sec, with a standard deviation of about 18%.

As an example, Fig. 4.7 shows the measured response of the physical process compared with the response of the model obtained through simulations for both type of scenarios (rectangular and trapezoidal control signals). As one can see, the simulation results are close to the ones obtained through measurements.

4.1.2. Controller Design

In order to design the controller for the structure from Fig. 3.7 the following assumptions are made:

Assumption 1: The DOB and DCO blocks assure the local disturbance compensation without modifying the dynamics of the main control system represented in Fig. 4.8.

Assumption 2: The CDOB and process model blocks assure the network disturbance compensation, again with an insignificant influence on the behaviour of main control system.

The above assumptions postulates a separability condition that permits the independent design of the controller and the compensation blocks. Based on this principle the controller design is obtained using the simplified structure from Fig. 4.8. For the process dynamics only the first term of the transfer function from (4.7) is of interest

$$H_u(s) = \frac{k_P}{T_a T_m s^2 + T_m s + 1} \tag{4.8}$$

For simplifying the design process, the second order transfer function $H_u(s)$ is approximated by a first order transfer function

$$H_u^*(s) = \frac{k_p}{Ts + 1} = \frac{1}{Ts + 1} \tag{4.9}$$

with the time constant T computed so that the differences of the Magnitude – Frequency Bode plot for the two transfer functions are as small as possible on the

frequency range of interest (0-200 sec^{-1}). By repeated attempts the results from Fig. 4.9 were obtained. These results correspond to a time constant T=0.29 s.

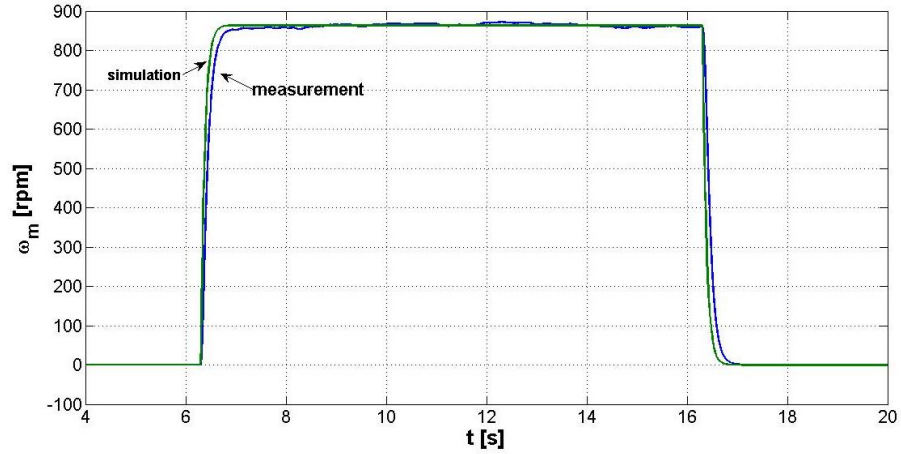

a) rectangular control signal

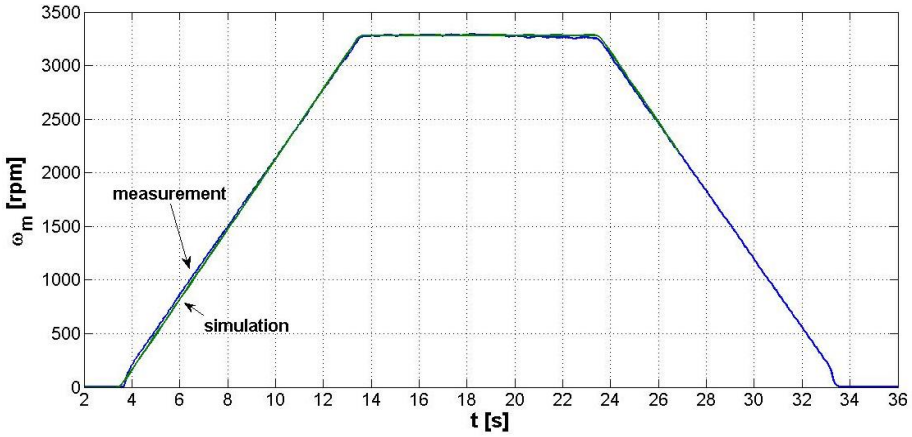

b) trapezoidal control signal

Fig. 4.7 - The process and the model's responses to a rectangular and a trapezoidal control signal

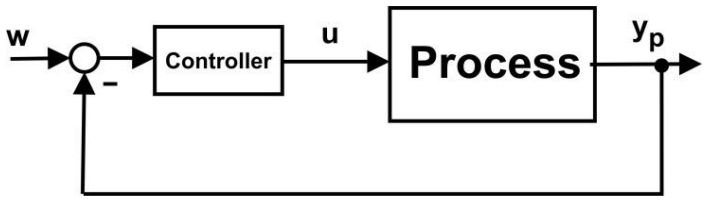

Fig. 4.8 - Local control structure of the undisturbed process

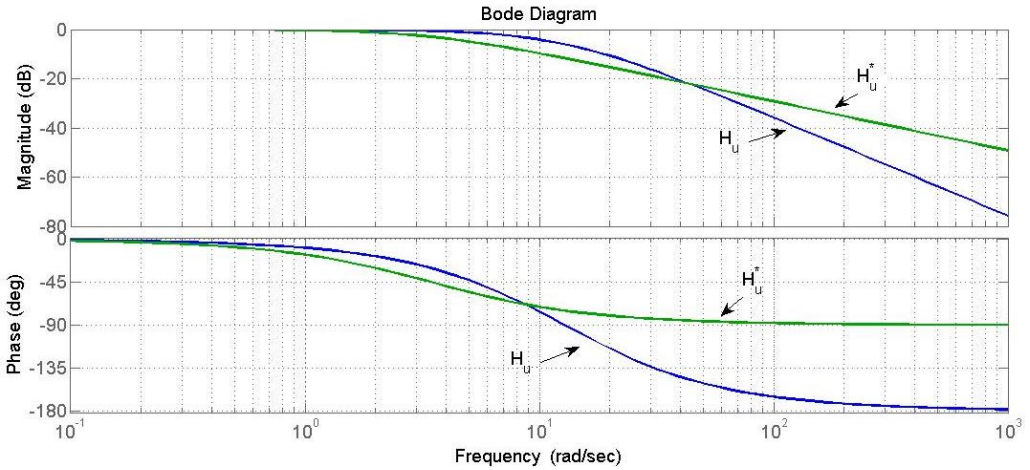

Fig. 4.9 - Bode characteristics for H_u and H_u^*

In order to obtain a null steady state error, a PI controller is adopted for the approximated undisturbed process model (4.9):

$$H_C(s) = K_p + K_i \frac{1}{s} = K \frac{T_i s + 1}{T_i s} \tag{4.10}$$

with $K=K_p$ and $T_i=K_p/K_i$. The time constant T_i is adopted in order to compensate the inertia of the simplified process ($T_i=T=0.29$s) and the gain K is determined by imposing a certain settling time for the resulted closed loop with

$$H(s) = \frac{H_C(s)H_u^*(s)}{1 + H_C(s)H_u^*(s)} = \frac{1}{(T_i / K)s + 1} \tag{4.11}$$

For an imposed settling time of 2.5s, by considering that the settling time is four times the time constant from (4.11) (i.e. less than 2% from the steady state value), it follows that K=0.46.

4.1.3. Disturbance Observer Design

The DOB will be used for load disturbance compensation (a local feedback loop like in Fig. 3.7).

First, the process model (4.7) is brought to the state space form:

$$\begin{bmatrix} \dot{x}_{p1}(t) \\ \dot{x}_{p2}(t) \end{bmatrix} = \begin{bmatrix} 0 & T_m^{-1} \\ -T_a^{-1} & -T_a^{-1} \end{bmatrix} \begin{bmatrix} x_{p1}(t) \\ x_{p2}(t) \end{bmatrix} + \begin{bmatrix} 0 & -1 \\ T_a^{-1} & 0 \end{bmatrix} \begin{bmatrix} u(t) \\ x_a(t) \end{bmatrix}$$
$$y_p(t) = \begin{bmatrix} 1 & 0 \end{bmatrix} \begin{bmatrix} x_{p1}(t) \\ x_{p2}(t) \end{bmatrix} \tag{4.12}$$

where x_{p1} and x_{p2} are the states of the process, $x_a=T_L$ and $y_p=\omega_m$.

Second, due to the fact that the local disturbance x_a cannot be measured and has slow variations in time, it will be considered as an exogenous staircase signal modelled by

$$\dot{x}_a(t) = 0 \tag{4.13}$$

Consequently, for the disturbed process the following observable extended state space model holds:

$$\begin{aligned}
\begin{bmatrix} \dot{x}_{p1}(t) \\ \dot{x}_{p2}(t) \\ \dot{x}_a(t) \end{bmatrix} &= \begin{bmatrix} 0 & T_m^{-1} & -1 \\ -T_a^{-1} & -T_a^{-1} & 0 \\ 0 & 0 & 0 \end{bmatrix} \begin{bmatrix} x_{p1}(t) \\ x_{p2}(t) \\ x_a(t) \end{bmatrix} + \begin{bmatrix} 0 \\ T_a^{-1} \\ 0 \end{bmatrix} u(t) \\
y_p(t) &= \begin{bmatrix} 1 & 0 & 0 \end{bmatrix} \begin{bmatrix} x_{p1}(t) \\ x_{p2}(t) \\ x_a(t) \end{bmatrix}
\end{aligned} \tag{4.14}$$

Third, in order to estimate the disturbance x_a, a reduced order DOB is built for the extended process (4.14). The reduced order DOB is designed as a Luenberger observer, by taking into account that state x_{p1} is available through the measured output y_p of the system ([86]). Thus, by isolating the measurable state of the system, model (4.14) becomes

$$\begin{aligned}
\begin{bmatrix} \dot{x}_{p1}(t) \\ \dot{x}_{p2}(t) \\ \dot{x}_a(t) \end{bmatrix} &= \left[\begin{array}{c|cc} \underbrace{A_{a11}}_{0} & \multicolumn{2}{c}{\underbrace{A_{a12}}_{T_m^{-1} \quad -1}} \\ \hline -T_a^{-1} & -T_a^{-1} & 0 \\ \underbrace{0}_{\underline{A}_{a21}} & \underbrace{0}_{\multicolumn{2}{c}{\underline{A}_{a22}}} & 0 \end{array}\right] \underbrace{\begin{bmatrix} x_{p1}(t) \\ x_{p2}(t) \\ x_a(t) \end{bmatrix}}_{\underline{x}_\beta} + \underbrace{\begin{bmatrix} 0 \\ T_a^{-1} \\ 0 \end{bmatrix}}_{\underline{b}_{a2}} u(t) \\
y_p(t) &= \left[\begin{array}{c|cc} \underbrace{1}_{\underline{c}_{a1}^T} & \multicolumn{2}{c}{\underbrace{0 \quad 0}_{\underline{c}_{a2}^T}} \end{array}\right] \cdot \begin{bmatrix} x_{p1}(t) \\ x_{p2}(t) \\ x_a(t) \end{bmatrix}
\end{aligned} \tag{4.15}$$

The corresponding reduced order Luenberger observer that allows the estimation of $\underline{x}_\beta$ is

$$\begin{aligned}
&\dot{\hat{\underline{x}}}_\beta(t) - \underline{l}_a \, \dot{y}_p(t) = \\
&= (\underline{A}_{a22} - \underline{l}_a \underline{A}_{a12}) \hat{\underline{x}}_\beta(t) + (\underline{A}_{a21} - \underline{l}_a A_{a11}) y_p(t) + (\underline{b}_{a2} - \underline{l}_a b_{a1}) u(t)
\end{aligned} \tag{4.16}$$

where $\underline{l}_a = [l_{a1} \; l_{a2}]^T$ is the internal observer gain.

In order to avoid using the derivative of the measured output y_p, the state of the observer is redefined as:

$$\tilde{\underline{x}}(t) = \hat{\underline{x}}_\beta(t) - \underline{l}_a \, y_p(t) \tag{4.17}$$

Finally, the equations of the reduced order observer become:

$$\dot{\tilde{\underline{x}}}(t) = \left(\underline{A}_{a22} - \underline{l}_a \ \underline{A}_{a12}\right)\hat{\underline{x}}_\beta(t) + \left(\underline{A}_{a21} - \underline{l}_a \ A_{a11}\right)y_p(t) + \left(\underline{b}_{a2} - \underline{l}_a \ b_{a1}\right)u(t) \quad (4.18)$$

respectively

$$\begin{bmatrix} \dot{\tilde{x}}_1(t) \\ \dot{\tilde{x}}_2(t) \end{bmatrix} = \overbrace{\begin{bmatrix} -\dfrac{T_m + T_a l_{a1}}{T_a T_m} & l_{a1} \\ -\dfrac{l_{a2}}{T_m} & l_{a2} \end{bmatrix}}^{\dot{\tilde{\underline{x}}}(t)} \begin{bmatrix} \hat{x}_{p2}(t) \\ \hat{x}_a(t) \end{bmatrix} - \begin{bmatrix} \dfrac{1}{T_a} & \dfrac{1}{T_a} \\ 0 & 0 \end{bmatrix} \begin{bmatrix} x_{p1}(t) \\ u(t) \end{bmatrix} \quad (4.19)$$

Forth, the DCO is designed for closing the local disturbance compensation feedback loop. For simplicity, the DCO will be considered a static gain k_a, while the design procedure is adapted from [6].

The forth design step ends the algorithmic design of the control loop, followed in a last step by the parameters calculation (l_{a1}, l_{a2} and k_a). They will be adopted in order to satisfy the static and dynamic requirements of the local closed loop system.

The compensation loop closes through

$$u(s) = u_n(s) + k_a \hat{x}_a(s) \quad (4.20)$$

Fig. 4.10 illustrates all the interconnections contained by the process model (4.12), the disturbance observer (4.18) and the compensation law (4.20). The notations permit an association with those from Fig. 3.7: $x_a = d, \hat{x}_a = \hat{d}$.

Taking into account that, according to (4.7)

$$\begin{aligned} x_{p1}(s) &= H_u(s)u(s) + H_{xa}(s)x_a(s) \\ &= \underbrace{\frac{1}{T_a T_m s^2 + T_m s + 1}}_{H_u} u(s) - \underbrace{\frac{(1 + T_a s)T_m}{T_a T_m s^2 + T_m s + 1}}_{H_{xa}} x_a(s) \end{aligned} \quad (4.21)$$

Fig. 4.10 permits the immediate deduction of the dependency between the estimate perturbation $\hat{x}_a$ and the real one x_a

$$\hat{x}_a(s) = \underbrace{\frac{T_m l_{a2}(T_a s + 1)}{T_m T_a s^2 + (T_m + l_{a1}T_a - T_a T_m l_{a2})s - l_{a2}T_m}}_{H_a(s)} x_a(s) \quad (4.22)$$

respectively of the dependency $\{u_n, x_a\} \rightarrow \{x_{p1}\}$

$$x_{p1}(s) = \left[H_u(s)u_n(s) + \overbrace{\left(H_u(s)k_a H_a(s) + H_{xa}(s)\right)}^{H_a(s)} x_a(s)\right] \quad (4.23)$$

Explicitly,

$$H_a(s) = \frac{T_m(T_a s + 1)}{T_m T_a s^2 + T_m s + 1} \frac{T_m T_a s^2 + (T_m + l_{a1}T_a - l_{a2}T_m T_a)s + l_{a2}(k_a - T_m)}{T_m T_a s^2 + (T_m + l_{a1}T_a - l_{a2}T_m T_a)s - l_{a2}T_m} \quad (4.24)$$

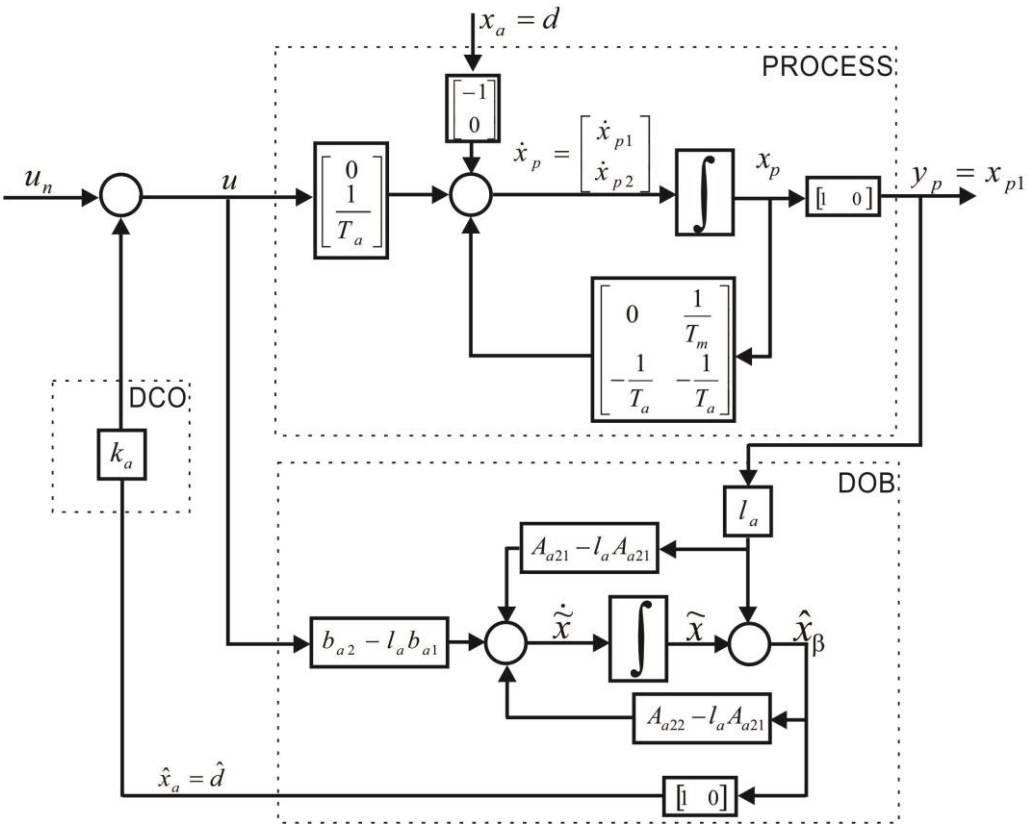

Fig. 4.10 – Local compensation loop

It can be observed that the transfer coefficient k_α of $H_\alpha(s)$ is

$$k_\alpha = \frac{T_m l_{a2}(k_a - T_m)}{-T_m l_{a2}} = T_m - k_a \tag{4.25}$$

In order to assure complete disturbance compensation in steady state conditions k_α should be 0. This leads to

$$k_a = T_m \tag{4.26}$$

In this case

$$H_\alpha(s) = \frac{T_m(T_a s + 1)}{T_m T_a s^2 + T_m s + 1} \frac{T_m T_a s^2 + (T_m + l_{a1} T_a - l_{a2} T_m T_a)s}{T_m T_a s^2 + (T_m + l_{a1} T_a - l_{a2} T_m T_a)s - l_{a2} T_m} \tag{4.27}$$

In reality, condition (4.27) cannot be exactly achieved, only by approximation, and a permanent small stationary error will appear.

The dynamic behaviour on the $x_a \rightarrow x_{p1}$ path, described by $H_\alpha(s)$, depends on the design parameters l_{a1} and l_{a2}. It can be observed that the transfer function $H_\alpha(s)$ corresponds to a band pass filter ($H_\alpha(0)=0$, the degree of the numerator is smaller

than the degree of the denominator). Consequently, the parameters l_{a1} and l_{a2} have to be adopted so that

- the observer should be stable;
- the observer should be faster than the control process;
- pass band bandwidth should be as small as possible.

The poles of the process, p_{p1}=-11.169 s^{-1} and p_{p2}=-14.473 s^{-1}, are identified as the roots of the characteristic polynomial

$$\mu_p(s) = T_m T_a s^2 + T_m s + 1 \tag{4.28}$$

Also, the poles of the control loop, p_{c1}=-1.245 s^{-1} and $p_{c2,3}$=-12.198±7.700j s^{-1}, are identified as the roots of the characteristic polynomial

$$\mu_c(s) = s^3 + \frac{1}{T_a} s^2 + \frac{1 + k_p k}{T_m T_a} s + \frac{k_p k}{T_m T_a T_i} \tag{4.29}$$

The observer poles are adopted as p_{DOB1}=-17 and p_{DOB2}=-20 in order to assure a fast observation process. This leads to l_{a1}=-0.30 and l_{a2}=-13.26. By adopting p_{DOB1} and p_{DOB2} close to each other, the condition to have a small pass band bandwidth is assured.

The amplitude - frequency Bode characteristic for H_a is presented in Fig. 4.11. The figure confirms the band pass nature of $H_a(s)$, rejecting low frequency disturbances. In this case, the observer's poles cannot modify the lower cut-off frequency, but they can modify the amplitude slope at low frequencies, ensuring a better disturbance rejection. As x_a has slow variations in time it can be considered that the designed local disturbance rejection loop should ensure satisfactory performances.

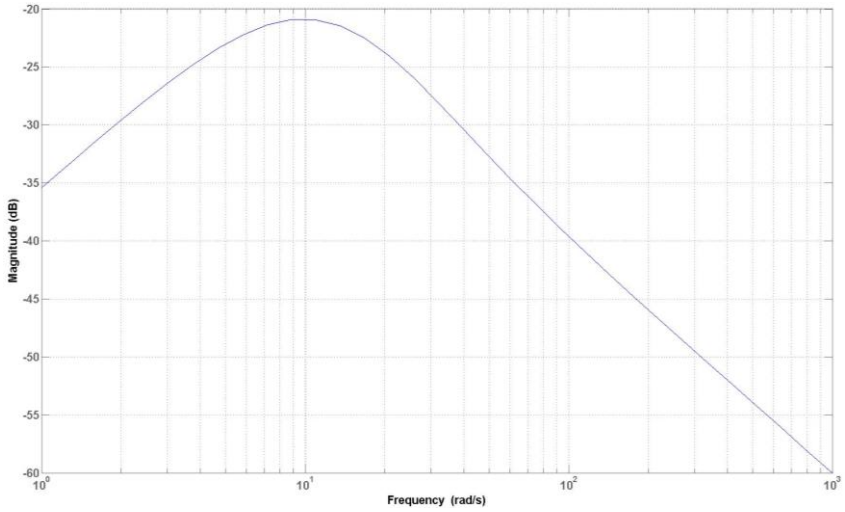

Fig. 4.11 - Amplitude-frequency Bode characteristics for $H_a(s)$.

4.1.4. Communication Disturbance Observer Design

The CDOB will be used for delay disturbance x_n (corresponding to disturbance d_n from Fig. 3.7) compensation. The design procedure is based on [6], but extended to a second order process, hence to a more complicated process.

The observation structure is depicted in Fig. 4.12. Here, x_n is a staircase signal representing an equivalent fictive signal that denote the difference u_n-u_r between two staircase signals associated to the real digital synchronous signals $\{u_r\}$ and $\{u_n\}$.

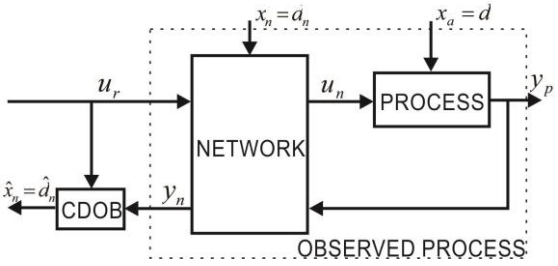

Fig. 4.12 – CDOB observation scheme a).

In this context the scheme from Fig. 4.12 is replaced with the one from Fig. 4.13.

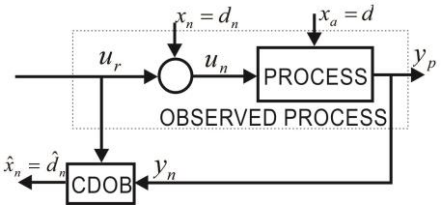

Fig. 4.13 - CDOB observation scheme b).

In order to established the CDOB structure the local perturbation x_a=d is ignored (i.e. x_a=d=0) (Fig. 4.14). Two types of CDOB structures are taken into account (the reason will be described later)

- reduced order CDOB
- full order CDOB

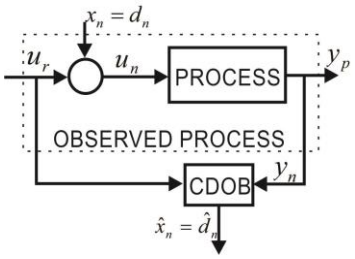

Fig. 4.14 - CDOB observation scheme c).

The mathematical model of the observed process is

$$\begin{bmatrix}\dot{x}_{p1}(t)\\ \dot{x}_{p2}(t)\end{bmatrix}=\begin{bmatrix}0 & T_m^{-1}\\ -T_a^{-1} & -T_a^{-1}\end{bmatrix}\begin{bmatrix}x_{p1}(t)\\ x_{p2}(t)\end{bmatrix}+\begin{bmatrix}0\\ T_a^{-1}\end{bmatrix}u_n(t)$$
$$y_n(t)=\begin{bmatrix}1 & 0\end{bmatrix}\begin{bmatrix}x_{p1}(t)\\ x_{p2}(t)\end{bmatrix} \tag{4.30}$$

The staircase form of signal x_n is considered to be generated by the exogen system

$$\dot{x}_n(t)=0 \tag{4.31}$$

By taking into account that

$$u_n(t)=u_r(t)+x_n(t) \tag{4.32}$$

the extended state space model of the process becomes

$$\begin{bmatrix}\dot{x}_{p1}(t)\\ \dot{x}_{p2}(t)\\ \dot{x}_n(t)\end{bmatrix}=\begin{bmatrix}0 & T_m^{-1} & 0\\ -T_a^{-1} & -T_a^{-1} & T_a^{-1}\\ 0 & 0 & 0\end{bmatrix}\begin{bmatrix}x_{p1}(t)\\ x_{p2}(t)\\ x_n(t)\end{bmatrix}+\begin{bmatrix}0\\ T_a^{-1}\\ 0\end{bmatrix}u_r(t)$$
$$y_n(t)=\begin{bmatrix}1 & 0 & 0\end{bmatrix}\begin{bmatrix}x_{p1}(t)\\ x_{p2}(t)\\ x_n(t)\end{bmatrix} \tag{4.33}$$

The system (4.33) is observable.

4.1.4.1. Reduced Order Communication Disturbance Observer Design

The possibility to design a reduced order CDOB is based on the fact that system (4.33) is observable and the state x_{p1} is the output of the system. Isolating the measurable state, the process model is redefined as

$$\begin{bmatrix}\dot{x}_{p1}(t)\\ \dots\\ \dot{x}_{p2}(t)\\ \dot{x}_n(t)\end{bmatrix}=\left[\begin{array}{c|cc}\underbrace{A_{n11}}_{0} & \underbrace{A_{n12}}_{T_m^{-1}} & \underbrace{}_{0}\\ \dots & \dots & \dots\\ -T_a^{-1} & -T_a^{-1} & T_a^{-1}\\ \underbrace{0}_{\underline{A}_{n21}} & \underbrace{0}_{0} & \underbrace{0}_{\underline{A}_{n22}}\end{array}\right]\underbrace{\begin{bmatrix}x_{p1}(t)\\ \dots\\ x_{p2}(t)\\ x_n(t)\end{bmatrix}}_{\underline{x}_Y}+\underbrace{\begin{bmatrix}0\\ \dots\\ T_a^{-1}\\ 0\end{bmatrix}}_{\underline{b}_{n2}}u_r(t)$$
$$y_n(t)=\left[\begin{array}{c|cc}\underbrace{1}_{\underline{c}_{n1}^T} & \underbrace{0}_{\underline{c}_{n2}^T} & 0\end{array}\right]\cdot\begin{bmatrix}x_{p1}(t)\\ \dots\\ x_{p2}(t)\\ x_n(t)\end{bmatrix} \tag{4.34}$$

The reduced order observer has the following equation

$$\dot{\underline{\bar{x}}}(t) = (\underline{A}_{n22} - \underline{l}_n\ \underline{A}_{n12})\underline{\hat{x}}_Y(t) + (\underline{A}_{n21} - \underline{l}_n\ A_{n11})y_n(t) + (\underline{b}_{n2} - \underline{l}_n\ b_{n1})u_r(t) \quad (4.35)$$

where

$$\underline{\bar{x}}(t) = \underline{\hat{x}}_Y(t) - \underline{l}_n\ y_n(t) \quad (4.36)$$

The observed states vector is defined as $\underline{\hat{x}}_Y = [\hat{x}_{p2}\quad \hat{x}_n]^T$ while the internal observer gain is defined as $\underline{l}_n = [l_{n1}\quad l_{n2}]^T$.

The detailed equations of the observer are

$$\begin{bmatrix}\dot{\bar{x}}_1\\ \dot{\bar{x}}_2\end{bmatrix} = \begin{bmatrix}-\dfrac{T_m + l_{n1}T_a}{T_aT_m} & \dfrac{1}{T_a}\\ -\dfrac{l_{n2}}{T_m} & 0\end{bmatrix}\begin{bmatrix}\hat{x}_2\\ \hat{x}_n\end{bmatrix} - \begin{bmatrix}\dfrac{1}{T_a} & \dfrac{1}{T_a}\\ 0 & 0\end{bmatrix}\begin{bmatrix}x_{p1}(t)\\ u_r(t)\end{bmatrix} \quad (4.37)$$

The characteristic polynomial of the observer is

$$\mu_{CDOB}(s) = det[s\underline{I}_2 - (\underline{A}_{n22} - \underline{l}_n\underline{A}_{n12})] = s^2 + \left(\frac{1}{T_a} + l_{n1}\frac{1}{T_m}\right)s + l_{n2}\frac{1}{T_aT_m} \quad (4.38)$$

Fig. 4.15 illustrates the CDOB integration into the control system. The concept is based on the following assumptions permitted by the system's linearity:

Assumption 3: The load disturbance x_a is omitted.
Assumption 4: The compensation loop for the load disturbance x_a is excluded.

According to the scheme from Fig. 4.15 the estimation of the delay disturbance x_n is given by

$$\hat{x}_n(s) = H_n(s)x_n(s) \quad (4.39)$$

with

$$H_n(s) = -\frac{1}{(T_mT_a / l_{n2})s^2 + (T_m / l_{n2} + l_{n1}T_a / l_{n2})s + 1} \quad (4.40)$$

The transfer $x_n(s) \to \hat{x}_n(s)$ corresponds to a second order low pass filter having the cut-off frequency and the damping coefficient

$$\omega_{0n} = \sqrt{\frac{l_{n2}}{T_aT_m}};\quad \zeta_n = \frac{1}{2\sqrt{l_{n2}}}\left(\sqrt{\frac{T_m}{T_a}} + \frac{1}{l_{n1}}\sqrt{\frac{T_a}{T_m}}\right) \quad (4.41)$$

Considering the hypotheses mentioned above the signal y_r becomes

$$\begin{aligned} y_r(s) &= y_p(s) - y_d(s) = H_u(s)u_n(s) - H_u(s)H_n(s)x_n(s) = \\ &= H_u(s)u_r(s) + H_u(s)[1 - H_n(s)]x_n(s) \end{aligned} \quad (4.42)$$

Explicitly

$$y_r(s) = \frac{1}{T_a T_m s^2 + T_m s + 1} u_r(s) + \frac{1}{T_a T_m s^2 + T_m s + 1} \cdot \frac{s^2 + \left(\frac{1}{T_a} + l_{n1}\frac{1}{T_m}\right)s}{s^2 + \left(\frac{1}{T_a} + l_{n1}\frac{1}{T_m}\right) + l_{n2}\frac{1}{T_a}\frac{1}{T_m}} x_n(s) \tag{4.43}$$

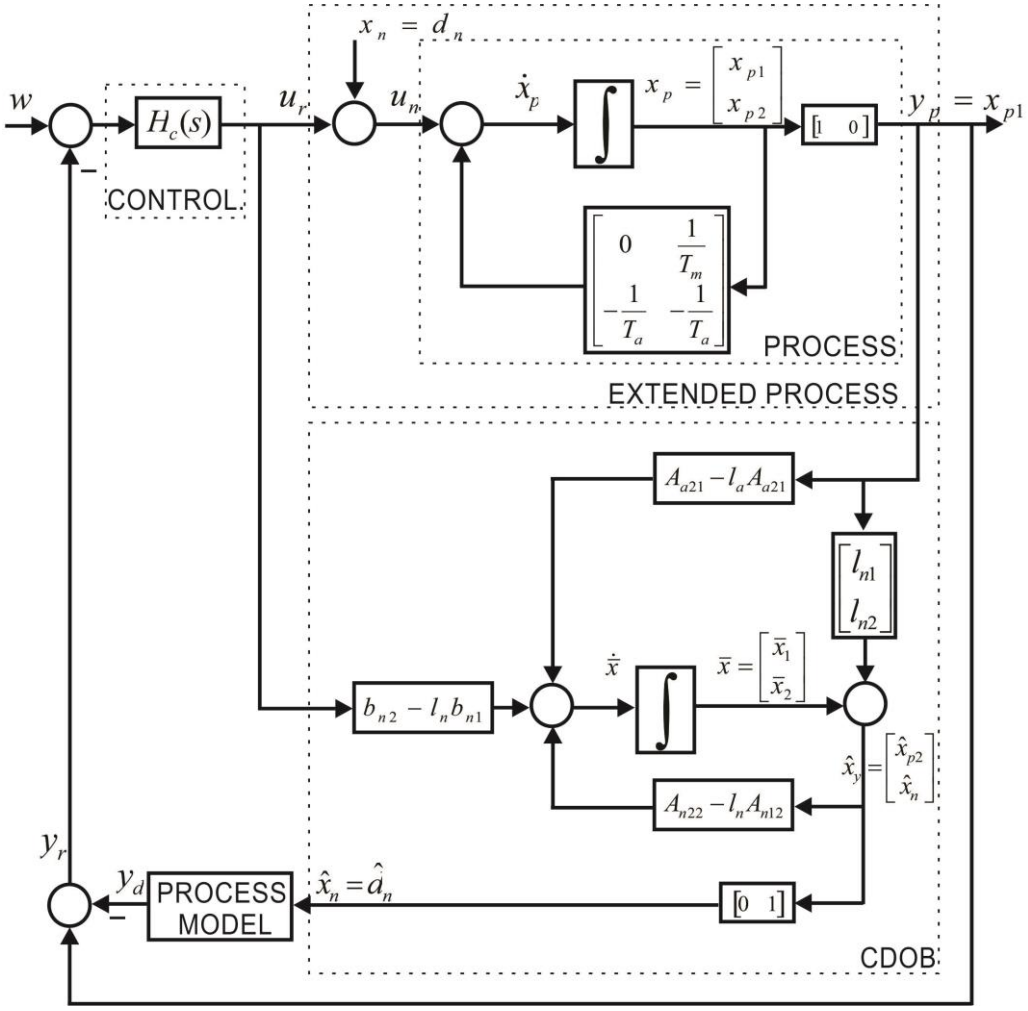

Fig. 4.15 - CDOB compensation loop.

Next, considering the case when the load perturbation is not omitted, the estimated disturbance containing both delay and local disturbances becomes

$$\begin{aligned} \hat{x}_n(s) &= H_n(s)x_n(s) + H_{CDOB}(s)H_{xa}(s)x_a(s) \\ &= H_n(s)x_n(s) + H_n(s)H_\delta(s)x_a(s) \end{aligned} \tag{4.44}$$

where $H_{CDOB}(s)$ is the CDOB transfer function for the $y_n \to \hat{x}_n$ path

$$\hat{x}_n(s) = H_{CDOB}(s)y_n(s); \quad H_{CDOB}(s) = \frac{s^2 + \frac{1}{T_a}s + \frac{1}{T_aT_m}}{s^2 + \left(\frac{1}{T_a} + l_{n1}\frac{1}{T_m}\right)s + l_{n2}\frac{1}{T_a}\frac{1}{T_m}} \quad (4.45)$$

and

$$H_\delta(s) = \frac{(1+T_as)T_m}{l_{n2}} \quad (4.46)$$

Finally, when taking into account the load disturbance and the local compensation loop, the estimated delay disturbance containing also the residual effect of the load disturbance (not compensated locally) becomes

$$\hat{x}_n(s) = H_n(s)x_n(s) + H_\beta(s)H_n(s)x_a(s) \quad (4.47)$$

with

$$H_\beta(s) = (1+T_as)T_m[H_u(s)k_aH_a(s)/H_{xa}(s) + 1] \quad (4.48)$$

4.1.4.2. Full Order Communication Disturbance Observer Design

For comparison purposes, the CDOB will also be designed as a full order observer. The extended process model (4.33) will be used and this time the observer will estimate all three states. The full order CDOB can be written directly as

$$\begin{bmatrix} \dot{\hat{x}}_{p1}(t) \\ \dot{\hat{x}}_{p2}(t) \\ \dot{\hat{x}}_n(t) \end{bmatrix} = \begin{bmatrix} -l'_{n1} & T_m^{-1} & 0 \\ -T_a^{-1} - l'_{n2} & -T_a^{-1} & T_a^{-1} \\ -l'_{n3} & 0 & 0 \end{bmatrix} \begin{bmatrix} \hat{x}_{p1}(t) \\ \hat{x}_{p2}(t) \\ \hat{x}_n(t) \end{bmatrix} + \begin{bmatrix} 0 \\ T_a^{-1} \\ 0 \end{bmatrix} u_r(t) + \begin{bmatrix} l'_{n1} \\ l'_{n2} \\ l'_{n3} \end{bmatrix} x_{p1}(t)$$
$$\hat{y}_n(t) = \begin{bmatrix} 1 & 0 & 0 \end{bmatrix} \begin{bmatrix} \hat{x}_{p1}(t) \\ \hat{x}_{p2}(t) \\ \hat{x}_n(t) \end{bmatrix} \quad (4.49)$$

where the internal observer gain is defined as $\underline{l}'_n = [l'_{n1} \quad l'_{n2} \quad l'_{n3}]^T$

In this case

$$H_n(s) = \frac{-l'_{n3}}{T_aT_ms^3 + T_m(1 + l'_{n1}T_a)s^2 + (l'_{n1}T_m + l'_{n2}T_a + 1)s + l'_{n3}} \quad (4.50)$$

4.1.4.3. Parameter Requirements for the Reduced and Full Order Communication Disturbance Observer

At this stage, the design of the delay disturbance compensation structure reduces to adopting the observer gains so that the estimated disturbance follows the real disturbance as fast as possible, while also assuring the stability of the CDOB.

For this the following conditions have to be met

- the CDOB has to be stable and faster than the control process;
- in open loop, the CDOB has to estimate as good as possible the disturbance x_n and so to contribute to the rejection of the influence of x_n upon y_r as quickly as possible;
- the CDOB has to attenuate as strong as possible the residual effect of the load disturbance x_a.

Considering equations (4.39), (4.44) and (4.47), the above conditions can be redefined as

$$\begin{cases} Condition\ 1: CDOB\ stable\ \&\ faster\ than\ the\ control\ process \\ Condition\ 2: \left|H_n(j\omega)\right| \to 1 \\ Condition\ 3: \left|H_n(j\omega)H_\delta(j\omega)\right| \to 0\ or \\ Condition\ 3': \left|H_n(j\omega)H_\beta(j\omega)\right| \to 0 \end{cases} \tag{4.51}$$

4.1.4.4. Full Order Versus Reduced Order Communication Disturbance Observer - Design Issues

The CDOB design involves the determination of its parameters: $\underline{l}_n$ for reduced order and, respectively, $\underline{l'}_n$ for full order CDOB. The parameters' determination has to take into account the conditions stated in (4.51).

Condition 1 reduces to the requirement that the CDOB poles have to be situated in the left half plane and to the left of the process poles. Based on the root locus method, in this case, it results that the closed loop poles are also placed in the left half plane and the observation process will unessentially influence the control systems' dynamic.

Regarding Condition 2, 3 and 3', it can be observed that the requirements are contradictory. This observation is based on the fact that in Condition 3 and 3' H_n appears as a factor and both H_δ, H_β are of an anticipatory nature.

The CDOB parameters are obtained mainly based on Condition 2, by imposing certain break frequencies for $H_n(s)$. More exactly, for the reduced order CDOB the parameters are determined based on equations (4.41), while for the full order CDOB they are determined by equalling term by term the coefficients of the characteristic polynomial given by denominator of $H_n(s)$ and a desired characteristic polynomial (imposed through the adopted break frequencies). The results are presented in Fig. 4.16 and Fig. 4.17.

Fig. 4.16 presents in a comparative manner the amplitude – frequency characteristics of Hn(s) and the product $H_n(s)H_\beta(s)$. The representation is made for three sets of values for the pair (l_{n1}, l_{n2}), respectively the triplet (l'_{n1}, l'_{n2}, l'_{n3}) determined in order for the amplitude – frequency characteristics of $H_n(j\omega)$ to take the value -3 dB for three different bandwidth frequency: ω_{b1}=37 s^{-1}, ω_{b2}=370 s^{-1}, ω_{b3}=18000 s^{-1}. Once a pair or a triplet of parameters are fixated the transfer function $H_\beta(s)$ can also be determined.

Analysing the three situations, it results that only the first two present any interest (for ω_{b3} the supraunitary amplification from the H_nH_β characteristics represents an effect that contradicts Condition 3' from (4.51)). Also, it can be

observed that when ω_b is too small, because of the characteristic of H_n, Condition 2 cannot be met.

When adopting the suitable value for ω_b, also, a peaking phenomenon - which appears due to numerical errors - has to be taken into account. It is known that this phenomenon affects the performance of high gain observers, especially in their reduced order form. Fig. 4.17 illustrates the manner in which the control system behaves in respect to the value of $\hat{x}_n$ when applying a rectangular pulse as a reference signal w(t) (rising edge at 3.5 s and falling edge at 9.5 s in the case when ω_b=370 s^{-1}, respectively 3 s and 9 s when ω_b=37 s^{-1}). Because of the amplitude difference, when ω_b=370 s^{-1}, the delay disturbance x_n cannot be easily observed (correspond to the darker areas of the plot). It can be observed that the most advantageous situation is when using the full order CDOB and ω_b=37 s^{-1} (the peaking phenomenon is avoided - the full order CDOB manages to produce a smooth estimation of x_n, while the reduced order CDOB still has some noise in the estimation due to numerical errors). This situation corresponds to a full order CDOB having the gains l'_{n1}=102.04, l'_{n2}=410.01 and l'_{n3}=461.43.

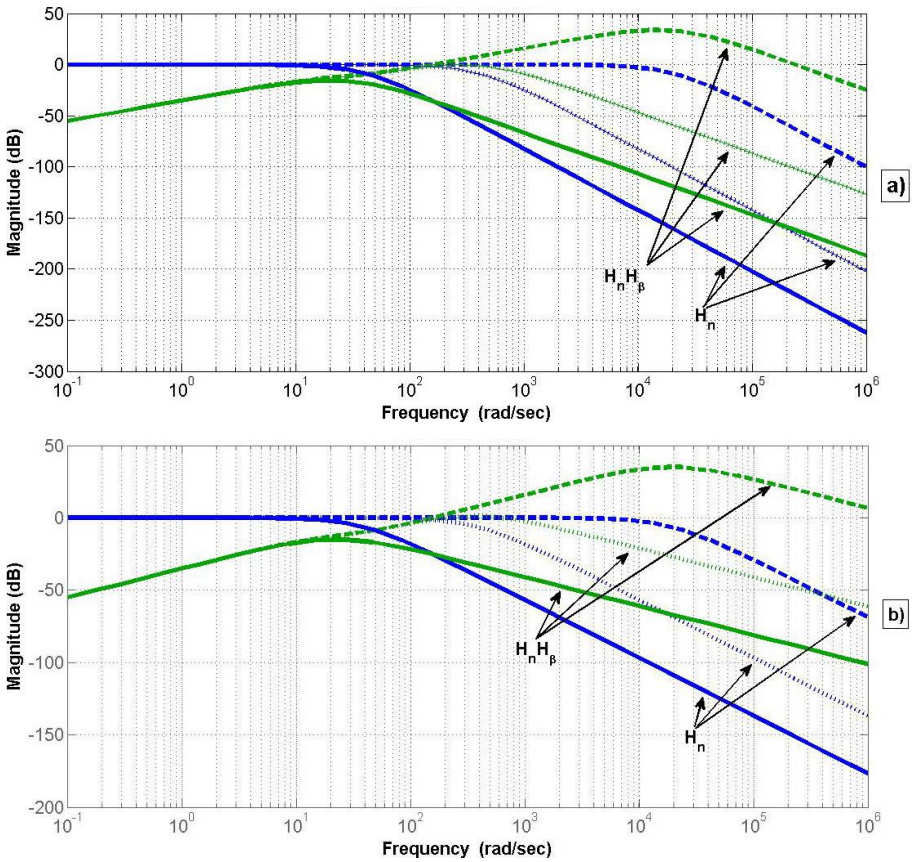

Fig. 4.16 – Amplitude - Frequency characteristics for the H_n and H_nH_β for the full order CDOB (a) and the reduced order CDOB (b), when choosing a bandwidth frequency of ~37 rad/s (solid line), ~370 rad/s (dotted line), and ~18000 rad/s (dashed line).

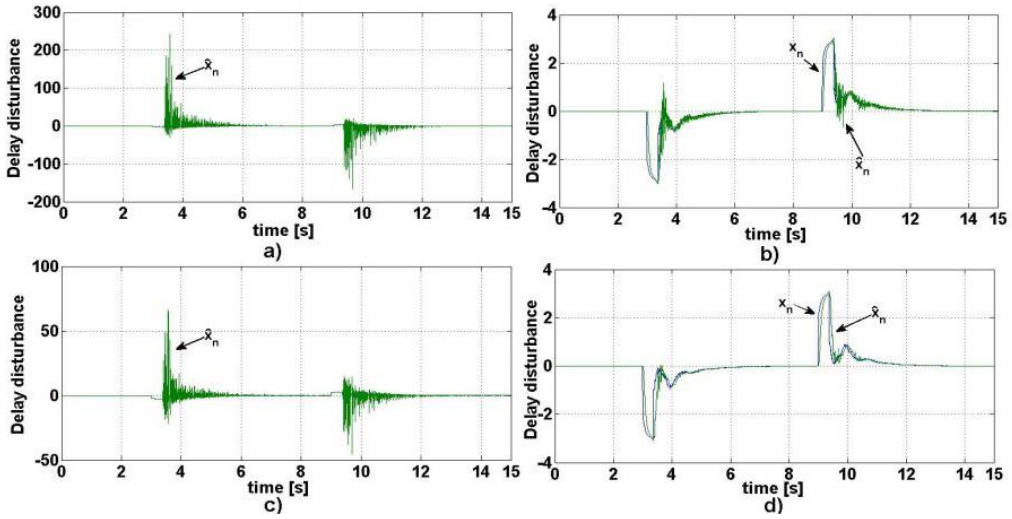

Fig. 4.17 - Estimation of x_n done by the reduced order CDOB (a,b) and full order CDOB (c,d), when choosing the bandwidth frequency of ~370 rad/s (a,c) and ~37 rad/s (b,d).

4.1.5. Stability Analysis

In order to analyse the stability of the proposed networked control structure from Fig. 3.7, first, several simplifying assumptions will be made:

Assumption 5: For simplicity, the local disturbance d and the reference w are assumed to be null.

Assumption 6: The network is idealized as a time-varying delay, equal to the RTT, placed on the direct path. Consequently, the influence of data loss and the communication channels' limited capacity are neglected (the packet loss rate is assumed to be negligible in respect with the sample period, while the digital bandwidth of the channel is assumed to be sufficiently large).

Assumption 7: The RTT delay is assumed to be bounded: $0 \le \tau(t) \le \tau_{max}$.

As remarks:

Remark 1: If certain characteristics for the variations of d and w are known or imposed, then exogenous models could be associated to these inputs, and as a result A5 can be dropped.

Remark 2: An upper bound τ_{max} is always considered in practice. In other words, it is considered that in normal scenarios, when no fault occurs, the delay value cannot be larger than τ_{max}.

Next, for determining the closed loop model associated to the control structure from Fig. 3.7, the following state space models are associated to each element of the control structure:

Process (*P*):
$$\begin{cases} \dot{x}_p(t) = A_p\, x_p(t) + b_p\, u(t) \\ y_p(t) = c_p^T\, x_p(t) \end{cases} \tag{4.52}$$

$$\textit{Controller}\ (\mathrm{C}): \quad \begin{cases} \dot{x}_c(t) = -y_r(t) \\ u_r(t) = K_i\, x_c(t) - K_p\, y_r(t) \end{cases} \tag{4.53}$$

$$\textit{Observer}(\mathrm{O}): \quad \begin{cases} \dot{\underline{x}}_o(t) = \underline{A}_o\, \underline{x}_o(t) + \underline{b}_{oc}\, u_r(t) + \underline{b}_{op}\, y_p(t) \\ \hat{d}_n(t) = \underline{c}_o^T\, \underline{x}_o(t) \end{cases} \tag{4.54}$$

$$\textit{Process model}\ (\mathrm{M_P}): \quad \begin{cases} \dot{\underline{x}}_{mp}(t) = \underline{A}_p\, \underline{x}_{mp}(t) + \underline{b}_p\, \hat{d}_n(t) \\ y_d(t) = \underline{c}_p^T\, \underline{x}_{mp}(t) \end{cases} \tag{4.55}$$

In accordance to Assumption 5, the local feedback loop which includes the DOB was dropped. This means that at the input of the process P we have $u(t)=u_n(t)$.Additionally, because $w(t)=0$, the input to the controller C is $-y_r(t)=-(y_n(t)-y_d(t))$. In accordance to Assumption 6, the Network Block is replaced by a single time-varying delay on the direct path (equal to the RTT), such that $u_n(t)=u_r(t-\tau(t))$ and $y_n(t)=y_p(t)$.

Further on, we associate for the process P and the process model M_p the model (4.12), for the controller C the model (4.10), for the observer O the model (4.49). The closed loop model is given by

$$\dot{\underline{x}}(t) = \underline{A}\,\underline{x}(t) + \underline{A}_d\,\underline{x}(t - \tau(t)) \tag{4.56}$$

where $\underline{x}^T(t)=[\underline{x}_p^T(t)\ \underline{x}_o^T(t)\ \underline{x}_{mp}^T(t)\ x_c(t)]^T$ and

$$\underline{A} = \begin{bmatrix} \underline{A}_p - \underline{b}_p K_p \underline{c}_p^T & \underline{0}_{2x3} & \underline{b}_p K_p \underline{c}_p^T & \underline{b}_p K_i \\ -\underline{b}_{oc}\underline{c}_p^T + \underline{b}_{op} K_p \underline{c}_p^T & \underline{A}_o & \underline{b}_{oc} K_p \underline{c}_p^T & \underline{b}_{oc} K_i \\ \underline{0}_{2x2} & \underline{b}_p \underline{c}_o^T & \underline{A}_p & \underline{0}_{2x1} \\ -\underline{c}_p^T & \underline{0}_{1x3} & \underline{c}_p^T & 0 \end{bmatrix}$$

$$\underline{A}_d = \begin{bmatrix} -\underline{b}_p K_p \underline{c}_p^T & \underline{0}_{2x3} & \underline{b}_p K_p \underline{c}_p^T & \underline{b}_p K_i \\ \underline{0}_{3x2} & \underline{0}_{3x3} & \underline{0}_{3x2} & \underline{0}_{3x1} \\ \underline{0}_{2x2} & \underline{0}_{2x3} & \underline{0}_{2x2} & \underline{0}_{2x1} \\ \underline{0}_{1x2} & \underline{0}_{1x3} & \underline{0}_{1x2} & 0 \end{bmatrix} \tag{4.57}$$

The closed loop system (4.56) is now in standard form for time delay systems, for which several stability methods were investigated in the literature in the last two decades. The methods can be classified according to three categories: delay independent, delay dependent and rate dependent, delay dependent and rate independent. Because in practice the delay is usually bounded in a certain range (Assumption 7), and the rate of the delay variation is usually unknown, here the focus will be on the delay dependent and rate independent case.

The aim is to find the maximum range $[0, \tau_{max}]$ in which the time delay can vary, for which the NCS is still stable; in other words to find the maximum value of τ_{max} for which the system is stable. To this end, the following theorem gives the sufficient condition for stability for a given delay range $[0, \tau_{max}]$. The theorem, along with the proof, is an adaptation of the results from [87].

Theorem 1. The system (4.56) with time-varying delay $\tau(t)$ of upper bound τ_{max} is asymptotically stable if there exist symmetric positive definite matrices $\underline{P}$, $\underline{Q}$, $\underline{Z}$, and matrices $\underline{N}_1$, $\underline{N}_2$, $\underline{S}_1$, and $\underline{S}_2$ such that the following LMI holds:

$$\begin{bmatrix} \underline{P}\underline{A}+\underline{A}^T\underline{P}+\underline{Q}+\underline{N}_1+\underline{N}_1^T & \underline{P}\underline{A}_d+\underline{N}_2^T-\underline{N}_1+\underline{S}_1 & -\underline{S}_1 & \tau_{max}\underline{N}_1 & \tau_{max}\underline{S}_1 & \tau_{max}\underline{A}^T\underline{Z} \\ * & \underline{S}_2+\underline{S}_2^T-\underline{N}_2-\underline{N}_2^T & -\underline{S}_2 & \tau_{max}\underline{N}_2 & \tau_{max}\underline{S}_2 & \tau_{max}\underline{A}_d^T\underline{Z} \\ * & * & -\underline{Q} & \underline{0} & \underline{0} & \underline{0} \\ * & * & * & -\tau_{max}\underline{Z} & \underline{0} & \underline{0} \\ * & * & * & * & -\tau_{max}\underline{Z} & 0 \\ * & * & * & * & * & -\tau_{max}\underline{Z} \end{bmatrix} < 0 \tag{4.58}$$

where $*$ stands for symmetric term in a symmetric matrix.

■

Proof. Consider the following Lyapunov functional candidate[1]

$$V(\underline{x}_t) = \\ = \underline{x}^T(t)\underline{P}\underline{x}(t) + \int_{t-\tau_{max}}^{t} \underline{x}^T(s)\underline{Q}\underline{x}(s)\,ds + \int_{-\tau_{max}}^{0}\int_{t+\theta}^{t} \dot{\underline{x}}^T(s)\underline{Z}\dot{\underline{x}}(s)\,ds\,d\theta \tag{4.59}$$

with $\underline{P}=\underline{P}^T>0$, $\underline{Q}=\underline{Q}^T>0$, and $\underline{Z}=\underline{Z}^T>0$. Based on the Leibniz-Newton formula, the following equations hold for any matrices $\underline{N}_1$, $\underline{N}_2$, $\underline{S}_1$, and $\underline{S}_2$ (weighting matrices):

$$2\left[\underline{x}^T(t)\underline{N}_1+\underline{x}^T(t-\tau(t))\underline{N}_2\right]\cdot \\ \left[\underline{x}(t)-\underline{x}(t-\tau(t))-\int_{t-\tau(t)}^{t}\dot{\underline{x}}(s)\,ds\right]=0 \tag{4.60}$$

$$2\left[\underline{x}^T(t)\underline{S}_1+\underline{x}^T(t-\tau(t))\underline{S}_2\right]\cdot \\ \left[\underline{x}(t-\tau(t))-\underline{x}(t-\tau_{max})-\int_{t-\tau_{max}}^{t-\tau(t)}\dot{\underline{x}}(s)\,ds\right]=0 \tag{4.61}$$

Additionally, the following equation also holds:

[1] $\underline{x}_t\in C([t_a,t_b],R^n)$ is defined by $\underline{x}_t(\theta)=\underline{x}_t(t+\theta)$, with $-\tau_{max}\le\theta\le 0$ and $t\in[t_a+\tau_{max}, t_b]$, and where $C([t_a,t_b],R^n)$ is a Banach space of continuous functions mapping the interval $[t_a,t_b]$ into R^n, with the norm $||\underline{x}_t||=\sup_{[-\tau_{max}\le\theta\le 0]}||\underline{x}_t(\theta)||_2$.

$$-\int_{t-\tau_{max}}^{t}\dot{\underline{x}}^T(s)\,\underline{Z}\,\dot{\underline{x}}(s)\,ds=-\int_{t-\tau(t)}^{t}\dot{\underline{x}}^T(s)\,\underline{Z}\,\dot{\underline{x}}(s)\,ds-\int_{t-\tau_{max}}^{t-\tau(t)}\dot{\underline{x}}^T(s)\,\underline{Z}\,\dot{\underline{x}}(s)\,ds \tag{4.62}$$

Next, by making use of Leibniz's integral rule, the derivative of $V(x_t)$ along the solutions of (4.56) can be written as:

$$\begin{aligned}\dot{V}(\underline{x}_t)=2\underline{x}^T(t)\underline{P}\dot{\underline{x}}(t)+\underline{x}^T(t)\underline{Q}\underline{x}(t)-\underline{x}^T(t-\tau_{max})\underline{Q}\underline{x}(t-\tau_{max})+\\ \tau_{max}\dot{\underline{x}}^T(t)\underline{Z}\dot{\underline{x}}(t)-\int_{t-\tau_{max}}^{t}\dot{\underline{x}}^T(s)\underline{Z}\dot{\underline{x}}(s)ds\end{aligned} \tag{4.63}$$

The further use of equations (4.60) - (4.62), and after some calculations and regrouping yield

$$\begin{aligned}\dot{V}(\underline{x}_t)&\le 2\underline{x}^T(t)\underline{P}\dot{\underline{x}}(t)+\underline{x}^T(t)\underline{Q}\underline{x}(t)-\underline{x}^T(t-\tau_{max})\underline{Q}\underline{x}(t-\tau_{max})\\ &+\tau_{max}\dot{\underline{x}}^T(t)\underline{Z}\dot{\underline{x}}(t)-\int_{t-\tau(t)}^{t}\dot{\underline{x}}^T(s)\,\underline{Z}\,\dot{\underline{x}}(s)\,ds-\int_{t-\tau_{max}}^{t-\tau(t)}\dot{\underline{x}}^T(s)\,\underline{Z}\,\dot{\underline{x}}(s)\,ds\\ &+2\left[\underline{x}^T(t)\underline{N}_1+\underline{x}^T(t-\tau(t))\underline{N}_2\right]\left[\underline{x}(t)-\underline{x}(t-\tau(t))-\int_{t-\tau(t)}^{t}\dot{\underline{x}}(s)\,ds\right]\\ &+2\left[\underline{x}^T(t)\underline{S}_1+\underline{x}^T(t-\tau(t))\underline{S}_2\right]\cdot\\ &\left[\underline{x}(t-\tau(t))-\underline{x}(t-\tau_{max})-\int_{t-\tau_{max}}^{t-\tau(t)}\dot{\underline{x}}(s)\,ds\right]\\ &\le\underline{\zeta}^T(t)\left[\underline{\Gamma}+\overline{\underline{A}}^T\tau_{max}\underline{Z}\,\overline{\underline{A}}+\tau_{max}\underline{N}\underline{Z}^{-1}\underline{N}^T+\tau_{max}\underline{S}\,\underline{Z}^{-1}\underline{S}^T\right]\underline{\zeta}(t)\\ &-\int_{t-\tau(t)}^{t}\underbrace{\left[\underline{\zeta}^T(t)\underline{N}+\dot{\underline{x}}^T(s)\,\underline{Z}\right]\underline{Z}^{-1}\left[\underline{N}^T\underline{\zeta}(t)+\underline{Z}\dot{\underline{x}}(s)\right]}_{>0\quad since\ \underline{Z}>0}ds\\ &-\int_{t-\tau_{max}}^{t-\tau(t)}\underbrace{\left[\underline{\zeta}^T(t)\underline{S}+\dot{\underline{x}}^T(s)\,\underline{Z}\right]\underline{Z}^{-1}\left[\underline{S}^T\underline{\zeta}(t)+\underline{Z}\dot{\underline{x}}(s)\right]}_{>0\quad since\ \underline{Z}>0}ds\end{aligned} \tag{4.64}$$

where

$$\underline{\zeta}(t)=\begin{bmatrix}\underline{x}(t)\\ \underline{x}(t-\tau(t))\\ \underline{x}(t-\tau_{max})\end{bmatrix},\ \underline{N}=\begin{bmatrix}\underline{N}_1\\ \underline{N}_2\\ \underline{0}\end{bmatrix},\ \underline{S}=\begin{bmatrix}\underline{S}_1\\ \underline{S}_2\\ \underline{0}\end{bmatrix},\ \overline{\underline{A}}=\begin{bmatrix}\underline{A}^T\\ \underline{A}_d^T\\ \underline{0}\end{bmatrix}^T,$$
$$\underline{\Gamma}=\begin{bmatrix}\underline{P}\underline{A}+\underline{A}^T\underline{P}+\underline{Q}+\underline{N}_1+\underline{N}_1^T & \underline{P}\underline{A}_d+\underline{N}_2^T-\underline{N}_1+\underline{S}_1 & -\underline{S}_1\\ * & \underline{S}_2+\underline{S}_2^T-\underline{N}_2-\underline{N}_2^T & -\underline{S}_2\\ * & * & -\underline{Q}\end{bmatrix}. \quad (4.65)$$

The last two integral terms can be dropped, and (4.64) becomes

$$\begin{aligned}\dot{V}(\underline{x}_t)&\le\underline{\zeta}^T(t)\left[\underline{\Gamma}+\overline{\underline{A}}^T\tau_{max}\underline{Z}\overline{\underline{A}}+\tau_{max}\underline{N}\underline{Z}^{-1}\underline{N}^T+\tau_{max}\underline{S}\underline{Z}^{-1}\underline{S}^T\right]\underline{\zeta}(t)\\&\le\underline{\zeta}^T(t)\underline{\Omega}\underline{\zeta}(t)\end{aligned} \quad (4.66)$$

The condition $\underline{\Omega}<0$ is equivalent to (4.58) by Schur complements. Thus, if (4.58) holds, then $\dot{V}(\underline{x}_t) < -\varepsilon\,\|\underline{x}_t\|^2$ for a sufficiently small $\varepsilon>0$, and as a result the system (4.56) is asymptotically stable ([88]).

As a final remark, it is important to mention that this is the first time when the stability of the Observer-based delay compensation structure (CDOB based) is proven for the general case involving a time-varying delay; in [89], [6] and subsequent studies the stability was proven only for constant time delay values.

4.1.6. Simulations and Experiments

In this section the designed NCS is tested in simulations and experiments. The controller and process models used are those from Sections 4.1.2, 4.1.1, the DOB and DCO are the ones from Section 4.1.3, while the CDOB used is the full order CDOB designed in Sections 4.1.5, 4.1.6, 4.1.7.

First, assessing the stability of the NCS, the LMI condition (4.58) from Theorem 1 is solved using CVX Toolbox for Matlab ([90]), by formulating the problem as a convex optimization one. A solution of the optimization problem was found (matrices $\underline{P}$, $\underline{Q}$, $\underline{Z}$, $\underline{N}_1$, $\underline{N}_2$, $\underline{S}_1$ and $\underline{S}_2$) for a maximum delay upper bound τ_{max}=0.35 s, thus proving according to Theorem 1 that the system is asymptotically stable. Although the result may still be conservative, it is usually good enough - a network delay range [0 s, 0.35 s] is consistent with real life network transmission scenarios over the Internet.

Next, consider a scenario with pulse reference signals of the form $w(t)=w0\cdot[\sigma(t-t0)-\sigma(t-t1)]$. The adopted sampling period is of 1 ms. This value is sufficient for controlling the process in real-time. In order to emulate the behaviour of real-time TCP/IP networks, the NTB from Section 2.1.1 was used. For the present case study the values of the time varying delay τ and packet loss flag p are generated as uniformly distributed pseudo-random numbers which are in agreement with measurements on a real TCP/IP network ([42] and Appendix 1). Fig. 4.18 shows the time variation of τ and p on a two second time window. The delay values are between 180 ms and 220 ms with an average of 200 ms. The flag p can take two values: 1 for a received packet and 0 for a lost one.

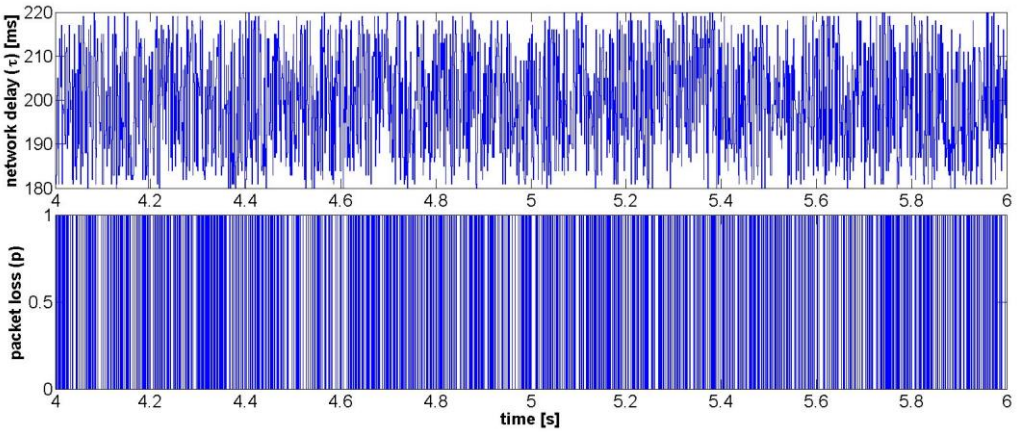

Fig. 4.18 - Generated network delay and network packet loss.

The actual control structure was developed in the Matlab/Simulink environment and implemented on to the dSPACE system. The experimental data was collected on a computer (PC) connected to a dSPACE system. The communication network is emulated also on the dSPACE system through an algorithm which implements the NTB. Fig. 4.19 illustrates the entire structure (experimental setup)

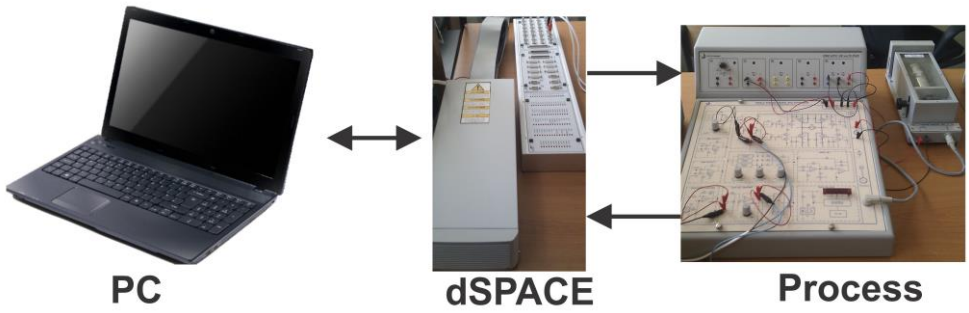

Fig. 4.19 - Experimental setup for the NCS.

As a remark it is important to mention that, besides the results presented, additional experiments were conducted for different delay and packet loss distributions and domain values, and it was observed that the control objective is achieved for delay values of less than 1 s and for packet loss below 30 %.

4.1.6.1. Simulation Results

The results from Fig. 4.20 show the system's response for the considered scenario. The result for local control confirms that the PI controller assures good performances: no overshoot and a settling time closed to the imposed one. When adding the network in the control loop the system becomes oscillatory. The extension of the control system with the CDOB structure leads to a system response close to the response for the local control, while eliminating the oscillations induced by the network. The improved response is due to the CDOB structure's capability to estimate and reject the delay disturbance (Fig. 4.21).

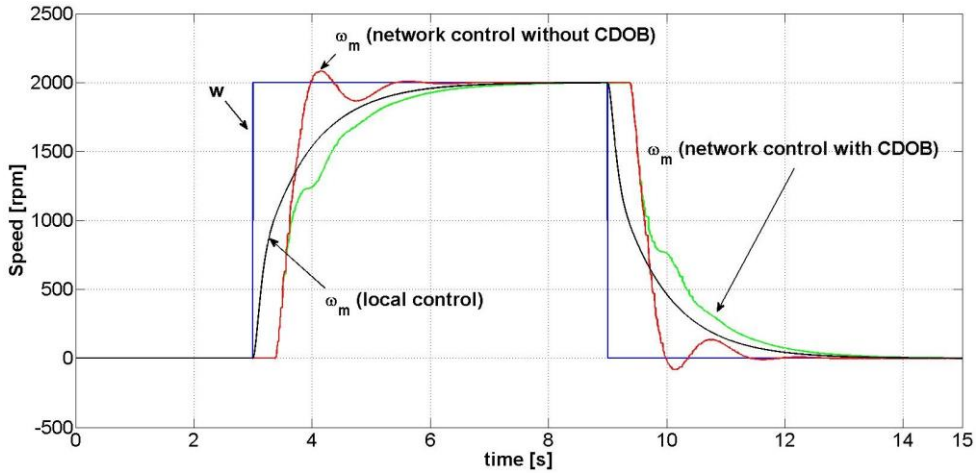

Fig. 4.20 - Comparative simulation results of the control system

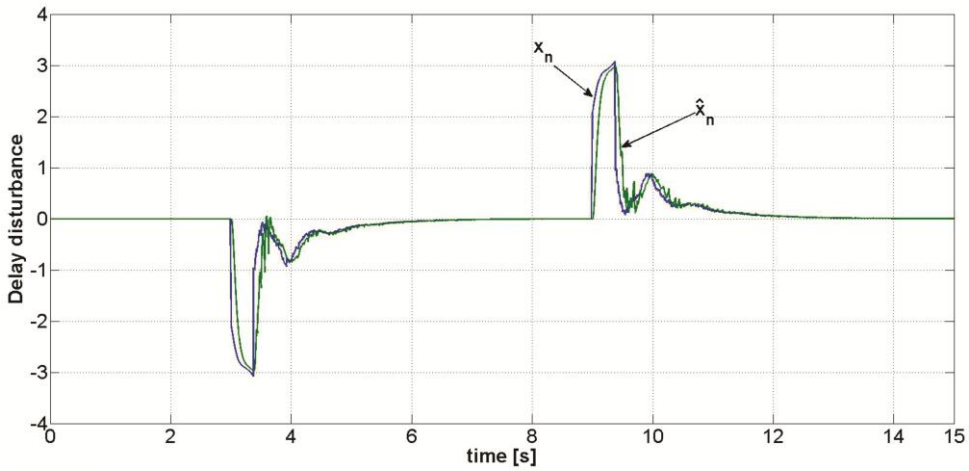

Fig. 4.21 - Delay disturbance (x_n) estimation - simulations.

4.1.6.2. Experimental Results

The results obtained through experiments (Fig. 4.22, Fig. 4.23) are in agreement with the simulation results. Although the oscillations induced by the network in the system's response are larger, when using the CDOB structure the oscillations are still successfully eliminated.

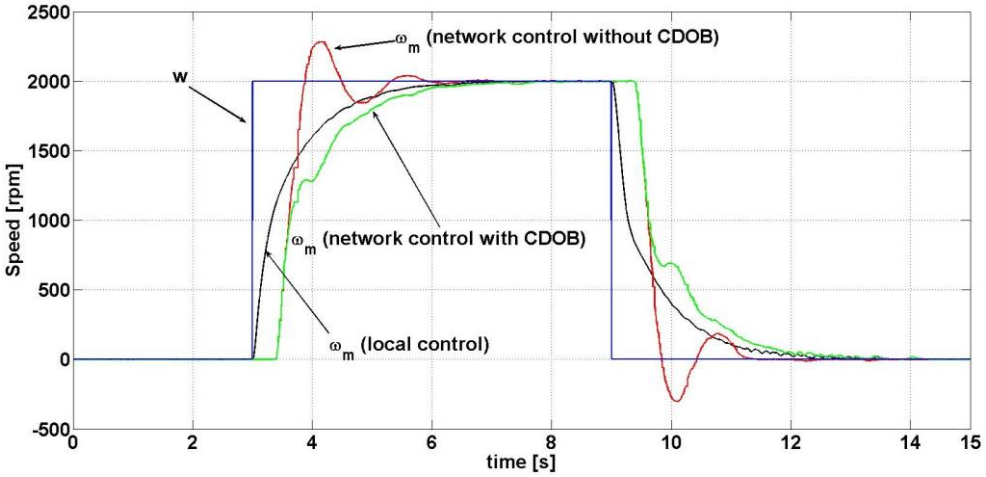

Fig. 4.22 - Comparative experimental results of the control system.

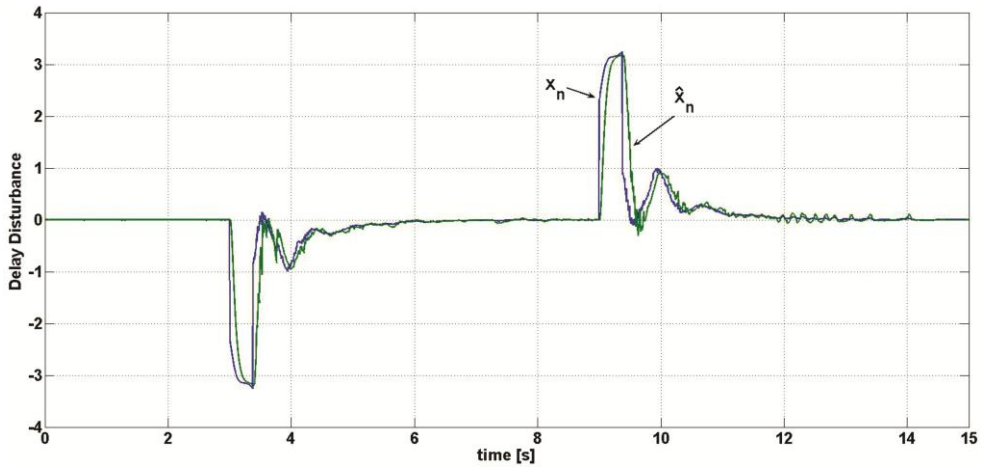

Fig. 4.23 - Delay disturbance (x_n) estimation - experiments.

4.2. Networked Control Structures Using Adaptive Compensation

The following control structures use different adaptive compensation strategies in order to compensate the perturbation effects induced by the network. The adaptive parameters are continuously adjusted according to the information received about the quality of network transmissions. For the first structure, the problem of stabilization is analysed ([91]). The second structure compensates the network disturbances, assuring also some imposed tracking performances ([92], [54]).

4.2.1. Stabilization and Control Synthesis for a Switched Feedback Networked Control Structure

The current section addresses the problem of stability and control synthesis for a NCS which embeds the NTM from Section 2.1.2. The networked control structure from Fig. 4.24 is considered, where the parameters of the controller are adapted according to a vector signal ξ which gives information about the quality of network transmissions.

The formalism of switched systems is approached because the NTM has parameters with a fast time variation (the fast varying parameters will be further considered to be related to the switching signals). Consequently, a switching controller is proposed for the extended plant composed out of the switched NTM and a linear time-invariant (LTI) process model. The stability of the closed-loop switched NCS is investigated for arbitrary switching by using a switched quadratic Lyapunov function. The solutions to both the stability and control design problems are expressed in terms of linear matrix inequalities (LMI). Finally, a numerical example is shown for validating the proposed method.

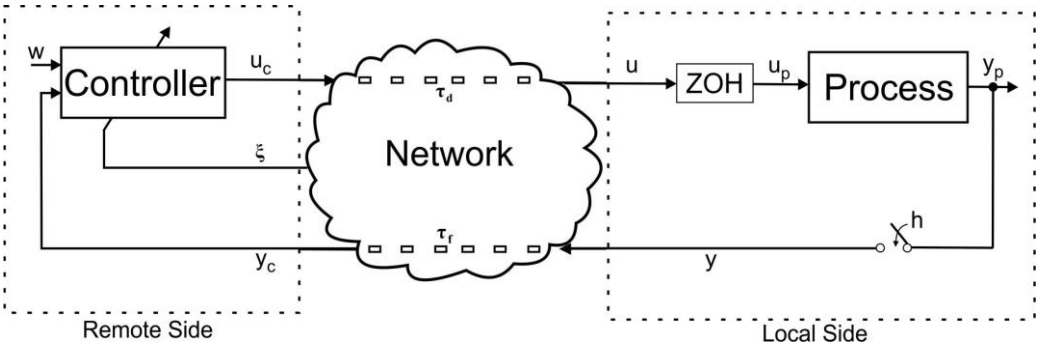

Fig. 4.24 - Switched NCS

4.2.1.1. Problem Formulation

In order to facilitate the design and analysis phases of the NCS, when using a non-inertial controller and when the plant is time invariant, from the stability point of view the network can be considered to be placed on the feedback path. In this context, the closed loop NCS from Fig. 4.25 is equivalent to the one from Fig. 4.24 ([3]). The one way delay τ from Fig. 4.25 represents the round time trip of the network from Fig. 4.24, i.e. $\tau = \tau_f + \tau_d$, and additionally, as a change of notations, $u_c = u$ and $y_c = y_N$.

Let the plant (i.e. the local side subsystem) dynamics be given by the following discrete-time LTI system:

$$\begin{cases} \underline{x}[k+1] = \underline{F}\underline{x}[k] + \underline{G}\underline{u}[k] \\ \underline{y}[k] = \underline{H}\underline{x}[k] \end{cases} \tag{4.67}$$

where $\underline{x} \in \Re^n, \underline{u} \in \Re^m, \underline{y} \in \Re^p$, $\underline{F}$, $\underline{G}$ and $\underline{H}$ are matrices with appropriate dimensions, and ($\underline{F}$,$\underline{G}$) is a controllable matrix pair.

In order to describe network transmission processes (characterized by time varying delays, packet loss and irregular situations as results of exogenous transmission factors) from a signal processing point of view, the switched network model (2.23) is considered.

Due to the switched nature of the extended plant model (i.e. plant model (4.67) coupled with the network model (2.23)), a switching output feedback controller is adopted

$$\underline{u}[k] = \underline{K}_{\underline{\xi}[k]} \cdot \underline{y}_N[k] + \underline{N}_w \cdot w[k] \tag{4.68}$$

where $\underline{K}$ represents a feedback compensator depending on the current values of the switching vector signal $\underline{\xi}[k]=[\alpha[k]\ \delta[k]]^T$. $\underline{N}_w$ is an adapting matrix of the reference signal w.

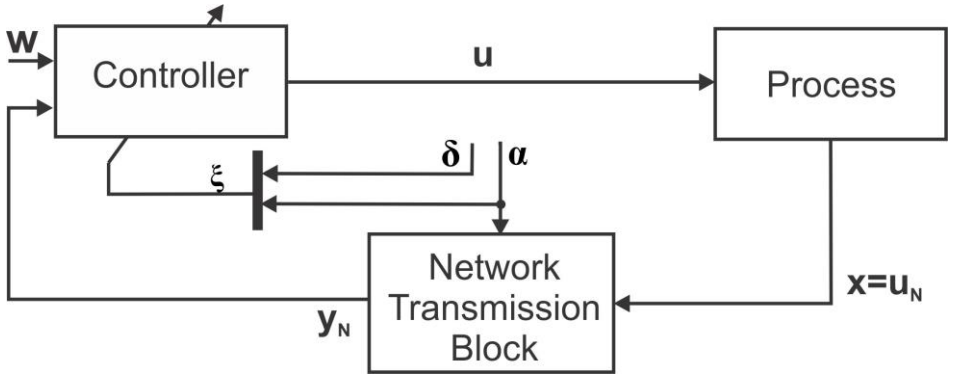

Fig. 4.25 - One-channel Switched NCS

In the current study two problems are investigated:

Problem 1. Stability analysis of the NCS composed of the plant (4.67), network (2.23) and controller (4.68).

Problem 2. Design of the controller (4.68) in order to ensure asymptotic stability of the closed-loop system.

The following assumptions are made:

Assumption 8. The state vector of the controlled process is considered to be measureable.

Assumption 9. Without loss of generality, to simplify the stability analysis, the reference w is assumed to be null ([35]).

Assumption 10. The influence of the communication channels' limited capacity on the network transmissions is neglected (the digital bandwidth of the channel is assumed to be sufficiently large).

Assumption 11. The time-varying delay is not known a priori, but it is assumed that its instantaneous values are available through measurements in real-time.

Assumption 12. As a real-time control constraint, an upper bound τ_{max} is imposed for the time-varying delay. Data packets that arrive with a time delay equal or larger than τ_{max} are considered as lost packets.

4.2.1.2. Stability Analysis and Controller Design

4.2.1.2.1. Closed Loop Model for the Networked Control System

In accordance to Assumption 9 the control loop of the NCS shown in Fig. 4.25 becomes an autonomous system. Its model is obtained as follows.

First, based on Assumption 8, and considering that p equals n, i.e. $\underline{y}=\underline{x}$, also $\underline{H}=\underline{I}_n$, the process model (4.67) reduces to:

$$\underline{x}[k+1] = \underline{F}\underline{x}[k] + \underline{G}\underline{u}[k] \tag{4.69}$$

Second, the process model (4.69) is further coupled with the network model (2.23) through state aggregation $\overline{\underline{x}}_N[k] = \left[\underline{\tilde{x}}_N^T[k]\ \underline{x}^T[k]\right]^T$:

$$\begin{cases} \overline{\underline{x}}_N[k+1] = \tilde{\underline{A}}_{a[k],\delta[k]}\overline{\underline{x}}_N[k] + \tilde{\underline{B}}\underline{u}[k] \\ \underline{y}_N[k] = \tilde{\underline{C}}\overline{\underline{x}}_N[k] \end{cases} \tag{4.70}$$

where

$$\tilde{\underline{A}}_{a[k],\delta[k]} = \begin{bmatrix} \underline{A}_{a[k],\delta[k]} & \underline{B}_{a[k]} \\ \underline{0}_{n\times(r+1)n} & \underline{F} \end{bmatrix}, \tilde{\underline{B}} = \begin{bmatrix} \underline{0}_{(r+1)n\times 1} \\ \underline{G} \end{bmatrix}, \tilde{\underline{C}} = \begin{bmatrix} \underline{C} & \underline{0}_n \end{bmatrix} \tag{4.71}$$

Third, by taking into consideration Assumption 9, the switching feedback controller (4.68) becomes

$$\underline{u}[k] = \underline{K}_{a[k],\delta[k]}\underline{y}_N[k] = \underline{K}_{a[k],\delta[k]}\tilde{\underline{C}}\overline{\underline{x}}_N[k] \tag{4.72}$$

where $\underline{K}_{a[k],\delta[k]}$ is the feedback compensator depending on the current values of $a[k]$ and $\delta[k]$.

Finally, by adding (4.72) to (4.70) - (4.71) the following closed loop autonomous system is obtained:

$$\overline{\underline{x}}_N[k+1] = \left(\tilde{\underline{A}}_{a[k],\delta[k]} + \tilde{\underline{B}}\underline{K}_{a[k],\delta[k]}\tilde{\underline{C}}\right)\overline{\underline{x}}_N[k] = \overline{\underline{A}}_{a[k],\delta[k]}\ \overline{\underline{x}}_N[k] \tag{4.73}$$

4.2.1.2.2. Stability Analysis

Let the switching signal pairs $(a,\delta) \in \Psi=\Omega_1 \times \Omega_2$ be (i,j) at moment k and (u,v) at the consecutive sampling instance $k+1$. Then, the following theorem gives the sufficient condition for asymptotic stability for the closed loop model of the NCS (4.73).

Theorem 2. The autonomous switched linear system (4.73) is asymptotically stable if there exists positive definite symmetric matrices $\{\underline{P}_{i,j} \mid (i,j) \in \Psi\}$, such that

$$\overline{\underline{A}}_{i,j}^T\underline{P}_{u,v}\overline{\underline{A}}_{i,j} - \underline{P}_{i,j} < 0, \qquad \forall((i,j),(u,v)) \in \Psi\times\Psi \tag{4.74}$$

■

Proof. Let us consider the following switched quadratic Lyapunov candidate function of the form ([93], [77])

$$V[k] = \underline{\bar{x}}_N^T[k]\underline{P}_{a[k],\delta[k]}\underline{\bar{x}}_N[k] \tag{4.75}$$

The first order difference of V is given by:

$$\begin{aligned}\Delta V &= V[k+1] - V[k] \\ &= \underline{\bar{x}}_N^T[k+1]\underline{P}_{a[k+1],\delta[k+1]}\underline{\bar{x}}_N[k+1] - \underline{\bar{x}}_N^T[k]\underline{P}_{a[k],\delta[k]}\underline{\bar{x}}_N[k] \\ &= \underline{\bar{x}}_N^T[k]\left[\underline{\bar{A}}_{a[k],\delta[k]}^T\underline{P}_{a[k+1],\delta[k+1]}\underline{\bar{A}}_{a[k],\delta[k]} - \underline{P}_{a[k],\delta[k]}\right]\underline{\bar{x}}_N[k]\end{aligned} \tag{4.76}$$

By considering (4.74), it follows that

$$\underline{\bar{A}}_{a[k],\delta[k]}^T\underline{P}_{a[k+1],\delta[k+1]}\underline{\bar{A}}_{a[k],\delta[k]} - \underline{P}_{a[k],\delta[k]} < 0 \tag{4.77}$$

Consequently, along each state trajectory $\underline{\bar{x}}_N[k]$, $\Delta V < 0$ and the system is asymptotically stable.

□

By using the Schur complement formula ([94]), condition (4.74) of Theorem 2 can be reduced to the following LMI problem:

$$\begin{bmatrix} \underline{P}_{i,j} & \underline{\bar{A}}_{i,j}^T\underline{P}_{u,v} \\ \underline{P}_{u,v}\underline{\bar{A}}_{i,j} & \underline{P}_{u,v} \end{bmatrix} > 0, \forall((i,j),(u,v)) \in \Psi \times \Psi \tag{4.78}$$

The LMI conditions (4.74) and (4.78) can be reformulated based on Theorem 2 from [93] as follows:

Theorem 3. The autonomous switched linear system (4.73) is asymptotically stable if there exist symmetric positive definite matrices $\{\underline{S}_{i,j} \mid (i,j) \in \Psi\}$ and matrices $\{\underline{G}_{i,j} \mid (i,j) \in \Psi\}$ satisfying

$$\begin{bmatrix} \underline{G}_{i,j} + \underline{G}_{i,j}^T - \underline{S}_{i,j} & \underline{G}_{i,j}^T\underline{\bar{A}}_{i,j}^T \\ \underline{\bar{A}}_{i,j}\underline{G}_{i,j} & \underline{S}_{u,v} \end{bmatrix} > 0, \forall((i,j),(u,v)) \in \Psi \times \Psi \tag{4.79}$$

■

4.2.1.2.3. Controller Design

In terms of theorems 2 and 3 compensator $\underline{K}$ was considered a priori known. The design problem of this compensator, i.e. to calculate it so that the theorem conditions are met, is further considered. This means using Theorem 3 also as a design tool, by searching for symmetric positive definite matrices $\{\underline{S}_{i,j} \mid (i,j) \in \Psi\}$ and matrices $\{\underline{G}_{i,j} \mid (i,j) \in \Psi\}$, $\{\underline{K}_{i,j} \mid (i,j) \in \Psi\}$, satisfying

$$\begin{bmatrix} \underline{G}_{i,j} + \underline{G}_{i,j}^T - \underline{S}_{i,j} & \underline{G}_{i,j}^T \left(\underline{\tilde{A}}_{i,j} + \underline{\tilde{B}} \underline{K}_{i,j} \underline{\tilde{C}} \right)^T \\ \left(\underline{\tilde{A}}_{i,j} + \underline{\tilde{B}} \underline{K}_{i,j} \underline{\tilde{C}} \right) \underline{G}_{i,j} & \underline{S}_{u,v} \end{bmatrix} > 0, \forall ((i,j),(u,v)) \in \Psi \times \Psi \quad (4.80)$$

The problem of solving numerically (4.80) leads to a non-convex optimization problem (the optimization problem is not convex in both $\underline{S}_{i,j}$ and $\underline{K}_{i,j}$ – ([94])). In order to make the problem more efficient from the numerical point of view, and also for reducing the conservatism, based on the work from [77] and Theorem 4 from [93], the following theorem can be used:

Theorem 4. The autonomous switched linear system (4.73) is asymptotically stable if there exist symmetric positive definite matrices $\{\underline{S}_{i,j} \mid (i,j) \in \Psi\}$, and matrices $\{\underline{G}_{i,j} \mid (i,j) \in \Psi\}, \{\underline{U}_{i,j} \mid (i,j) \in \Psi\}$ and $\{\underline{V}_{i,j} \mid (i,j) \in \Psi\}$, such that

$$\begin{bmatrix} \underline{G}_{i,j} + \underline{G}_{i,j}^T - \underline{S}_{i,j} & \left(\underline{\tilde{A}}_{i,j} \underline{G}_{i,j} + \underline{\tilde{B}} \underline{U}_{i,j} \underline{\tilde{C}} \right)^T \\ \underline{\tilde{A}}_{i,j} \underline{G}_{i,j} + \underline{\tilde{B}} \underline{U}_{i,j} \underline{\tilde{C}} & \underline{S}_{u,v} \end{bmatrix} > 0, \forall ((i,j),(u,v)) \in \Psi \times \Psi \quad (4.81)$$

and

$$\underline{V}_{i,j} \underline{\tilde{C}} = \underline{\tilde{C}} \underline{G}_{i,j} \quad (4.82)$$

with the feedback gain given by

$$\underline{K}_{i,j} = \underline{U}_{i,j} \underline{V}_{i,j}^{-1} \quad (4.83)$$

■

4.2.1.3. Numerical Example

Consider the DC motor plant from the previous section, described by the following state-space LTI model:

$$\begin{bmatrix} \dot{x}_1(t) \\ \dot{x}_2(t) \end{bmatrix} = \begin{bmatrix} 0 & T_m^{-1} \\ -T_a^{-1} & -T_a^{-1} \end{bmatrix} \begin{bmatrix} x_1(t) \\ x_2(t) \end{bmatrix} + \begin{bmatrix} 0 \\ T_a^{-1} \end{bmatrix} u(t)$$
$$\begin{bmatrix} y_1(t) \\ y_2(t) \end{bmatrix} = \begin{bmatrix} 1 & 0 \\ 0 & 1 \end{bmatrix} \begin{bmatrix} x_1(t) \\ x_2(t) \end{bmatrix} \quad (4.84)$$

where x_1 represents the motor speed, x_2 the armature current, and T_a and T_m are time constants. It should be noted that the model is an idealization of the physical plant, and as a consequence, it does not take into account friction, load torque, or any other energy losses.

The parameters of the continuous time model (4.84) were identified experimentally. Through step response invariant discretization, by using the numerical parameter values and adopting a sample period h=10 ms, the following discrete-time LTI model is obtained

$$\begin{bmatrix} x_1[k+1] \\ x_2[k+1] \end{bmatrix} = \overbrace{\begin{bmatrix} 0.99 & 0.06 \\ -0.23 & 0.77 \end{bmatrix}}^{\underline{F}} \overbrace{\begin{bmatrix} x_1[k] \\ x_2[k] \end{bmatrix}}^{\underline{x}[k]} + \overbrace{\begin{bmatrix} 0.01 \\ 0.23 \end{bmatrix}}^{\underline{G}} u[k]$$
$$\overbrace{\begin{bmatrix} y_1[k] \\ y_2[k] \end{bmatrix}}^{\underline{y}[k]} = \overbrace{\begin{bmatrix} 1 & 0 \\ 0 & 1 \end{bmatrix}}^{\underline{H}} \begin{bmatrix} x_1[k] \\ x_2[k] \end{bmatrix} \tag{4.85}$$

The plant is controlled via a communication network, described by model (2.23), characterized by the parameter r= τ_{max}=4 and the sets

$$\Omega_1 = \{1, 2, 3, 4\},\ \Omega_2 = \{0, 1\} \tag{4.86}$$

These correspond to a packet switched wide area communication network with a maximum round time trip delay of 30 ms.

Next, a closed loop autonomous switched system of the form (4.73) is obtained, where the controller is given by (4.72).

The LMI conditions (4.81) from Theorem 4 reduce to a set of 64 multiple LMIs (i.e. between the elements of the Cartesian product { Ω_1 x Ω_2} there are 64 possible transitions), which are recasted as a single LMI ([94]).The resulting LMI, with the associated equality constraints (4.82), is solved using CVX Toolbox for Matlab ([90]), by formulating the problem as a convex optimization one. The following switched feedback gains are obtained

$$\begin{aligned}
\underline{K}_1 &= \begin{bmatrix} 0.074 & 0.315 \end{bmatrix} && \rightarrow a[k]=1, \delta[k]=0 \\
\underline{K}_2 &= \begin{bmatrix} 0.074 & 0.315 \end{bmatrix} && \rightarrow a[k]=1, \delta[k]=1 \\
\underline{K}_3 &= \begin{bmatrix} 0.036 & 0.170 \end{bmatrix} && \rightarrow a[k]=2, \delta[k]=0 \\
\underline{K}_4 &= \begin{bmatrix} -0.138 & -0.800 \end{bmatrix} && \rightarrow a[k]=2, \delta[k]=1 \\
\underline{K}_5 &= \begin{bmatrix} 0.008 & 0.053 \end{bmatrix} && \rightarrow a[k]=3, \delta[k]=0 \\
\underline{K}_6 &= \begin{bmatrix} -0.107 & -0.615 \end{bmatrix} && \rightarrow a[k]=3, \delta[k]=1 \\
\underline{K}_7 &= \begin{bmatrix} -0.891 & -0.960 \end{bmatrix} && \rightarrow a[k]=4, \delta[k]=0 \\
\underline{K}_8 &= \begin{bmatrix} -1.126 & -1.291 \end{bmatrix} && \rightarrow a[k]=4, \delta[k]=1
\end{aligned} \tag{4.87}$$

which stabilize the system.

Further on, a simulation example is presented. Consider the scenario given by an arbitrary variation of the switching signals *a* and δ as shown in Fig. 4.26. The initial conditions for the plant states are $x_1(0)=2\pi\ s^{-1}$=60 rpm and $x_2(0)=10^{-2}$ A =10 mA. In order to show that Assumption 2 holds, a non-null reference is adopted: w=20 rpm (taking into account that *u* is a scalar signal, $\underline{N}_w$ can be adopted as 1). Fig. 4.26 also illustrates the transient regime for the two states of the plant: x_1 and x_2.

During the transient regimes all the feedback gains from (4.87) were activated. It can be observed that the switching controller manages to stabilize the system, which reaches the equilibrium point x_1= 20 rpm and x_2= 0 A after 0.4 s. The small oscillations of x_2 are caused by the feedback gain switching, in the attempt to stabilize the system at each variation of the network parameters.

Note that the scope of this very simple scenario was to illustrate how an initial imbalance is stabilized by the modelled NCS.

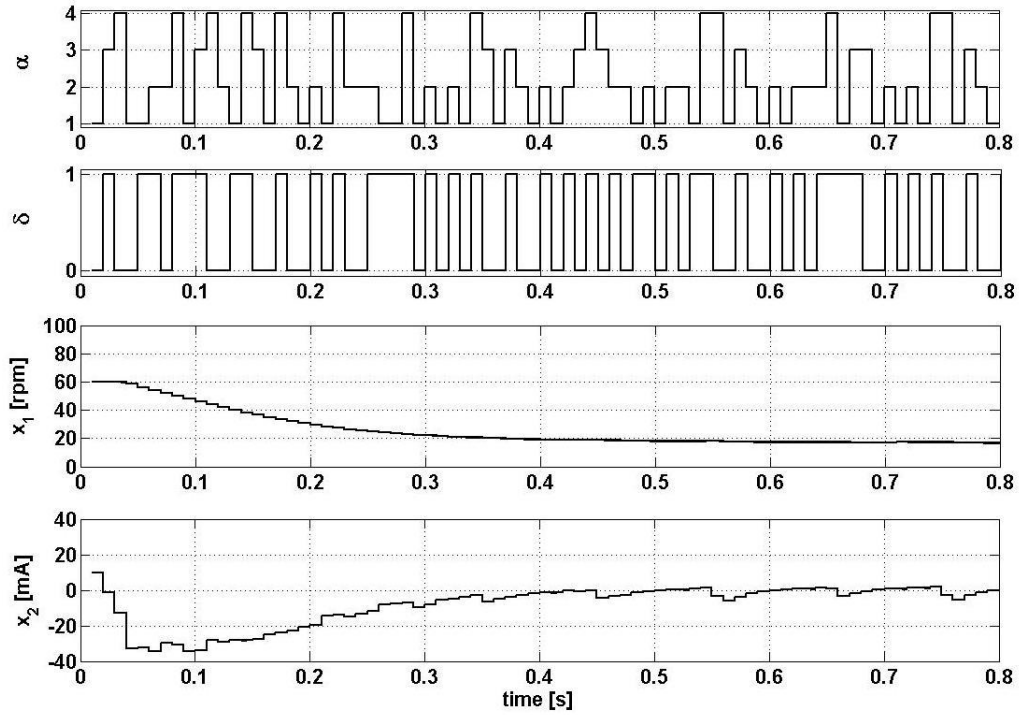

Fig. 4.26 - Simulation results

4.2.2. Design and Analysis of a Networked Control Structure with a Switched PD Compensator

Current section presents in details the design and analysis phases for the networked control structure from Fig. 3.8.

4.2.2.1. Problem Formulation

The controller and the compensator for the NCS from Fig. 3.8, have to be capable of stabilizing the system, to ensure good tracking performances and to reject the disturbance effect of the network.

In order to simplify the analysis and design stages, several assumptions will be made:

Assumption 13: the process is a $\{u\}\rightarrow\{y_p\}$ oriented SISO linear time-invariant system, controllable and observable;

Assumption 14: stabilization and output tracking for the controlled processes can be achieved through state feedback plus integral control;

Assumption 15: network transmissions are characterized by time-varying delays, packet losses and irregular situations, and the network can be regarded as a switched linear system;

Assumption 16: the disturbance effect of network transmissions can be compensated by a switched PD type compensator;

Assumption 17: the tracking reference signal *w* is a stepwise signal, and can be modelled as the output of a first order exogenous system.

Based on the above mentioned assumptions, the networked control structure from Fig. 3.8 can be reconfigured and brought to the form shown in Fig. 4.27. Finally, it is important to state some additional remarks:

Remark 3: a control structure where the network is placed on both paths (like in Fig. 3.8) and where the controller is non-inertial and the plant is time-invariant (the case stated by the above hypothesis) is equivalent - from the point of view of stability analysis - with one where the network is placed only on the feedback path (like in Fig. 4.27) – [3], [95];

Remark 4: placing the compensator (PD type) on the local side has the advantage that it can receive cumulative information regarding the quality of network transmissions on both pathways (ξ), thus being able to reject the overall network disturbance effect on the control loop;

Remark 5: in the control structure from Fig. 4.27 the integrator is placed after the switched PD compensator in order to eliminate any steady state oscillations caused by variations of ξ even when the output of the process reaches steady state (such a solution has been proposed in the literature initially for gain-scheduling [96], and recently for switching controllers [80]);

Remark 6: while one may argue that the observer should be placed remotely for avoiding an increase computational burden on the local side, here it was considered that it is more important that the estimation error should not be influenced by transmission errors (thus also improving the stability in respect with the rate of packet loss – [3]).

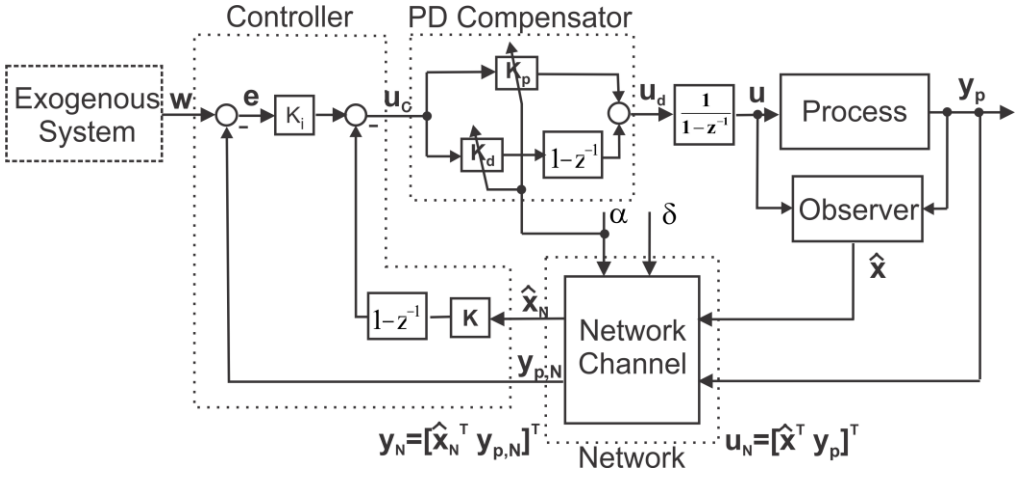

Fig. 4.27 - One-channel NCS

Next, throughout the rest of the section, the networked control structure from Fig. 4.27 will be used as reference.

4.2.2.2. Control System Design

This section presents a methodology for designing the controller, observer and compensator of the NCS from Fig. 4.27. The entire design procedure uses a zero-order hold equivalent model of the continuous-time plant SISO model of the form:

$$\begin{cases} \underline{x}[k+1] = \underline{F}_d x[k] + \underline{G}_d u[k] \\ y_p[k] = \underline{H}_d^T \underline{x}[k] \end{cases} \tag{4.88}$$

where $\underline{x} \in \Re^{n_p}$, $u \in \Re$, $y_p \in \Re$, $\underline{F}_d$ is a $n_p \times n_p$ matrix, $\underline{G}_d$ and $\underline{H}_d$ are $n_p \times 1$ vectors, $(\underline{F}_d, \underline{G}_d)$ is a controllable pair and $(\underline{F}_d, \underline{H}_d^T)$ is an observable pair (Assumption 13).

4.2.2.2.1. Controller and Observer Design

The state feedback integral controller is designed as if it were directly coupled to the process (i.e. for the control structure from Fig. 4.27, without the network block, PD compensator blocks, and observer block). The compensators $\underline{K}$ and K_i are thus designed through the classical pole allocation method.

The state observer is considered to be of Luenberger type ([86]), having the model

$$\begin{cases} \underline{\hat{x}}[k+1] = \underline{F_d}\hat{x}[k] + \underline{G}_d u[k] + \underline{L}\left(y_p[k] - \hat{y}_p[k]\right) \\ \hat{y}_p[k] = \underline{H}_d^T \underline{\hat{x}}[k] \end{cases} \tag{4.89}$$

Because the observer is placed on the local side (Fig. 4.27), and is directly coupled to the process, the compensator $\underline{L}$ can also be designed through pole allocation.

4.2.2.2.2. Compensator Design

As the control structure from Fig. 4.27 illustrates, the compensator adopted for rejecting the disturbance effect of the network is of PD type. If the network disturbance is reduced to the time-varying network delay component (thus idealizing the network as simple synchronous multi-channel time-varying delays), then it can be easily shown (based on frequency characteristics) that the PD transfer element improves the phase margin of the systems, which was initially deteriorated by the presence of network delays in the control loop. Moreover, for coping with time-varying network delays, the parameters of the PD compensator – K_d and K_p – are permanently switched according to the RTT network time delay τ (see Remark 4).

Next, the main issue consists in determining the switching logic which associates a parameter pair (K_d, K_p) to each value of the delay τ. Two main approaches can be identified in the literature in respect with this issue. One hand, for low-order benchmark process models, (quasi-) analytical tuning rules are derived (e.g. [97]). On the other hand, this problem of control synthesis can be augmented to the stability problem, and then a LMI based method can be adopted, so that the obtain solution provides information regarding stability, along with the control parameters of interest

(e.g. [93], [98]). While the first approach – referring to (quasi-) analytical tuning rules – is usually difficult to apply for non-benchmark type process models (e.g. high order, nonlinear, etc.), the second approach has the drawbacks that it is not always applicable (non-convex problems) and it is usually very conservative, i.e. in many cases no feasible solution can be found.

As a different approach, here the switching logic is considered to be given by the following two functions:

$$K_p = f_K(\tau), \quad T_d = f_T(\tau), \tag{4.90}$$

where T_d is the equivalent time constant of the PD transfer element, defined as

$$T_d = \frac{K_d}{K_p} \tag{4.91}$$

As a result, it should be noted that the new parameters of interest become actually K_p and T_d. The two functions are determined as follows.

The time constant T_d can be considered to vary linearly with τ, by considering that qualitatively the PD action compensates the time delay. Thus, the function f_T can have an analytical form, given by

$$f_T(\tau) = \lambda \cdot \tau, \quad \lambda \in (0,1) \tag{4.92}$$

where λ is a constant parameter.

For the gain K_p an analytical function f_K is harder to grasp directly. Considering that τ can take only a finite number of possible values from Ω_1, a tabulated function f_K can be adopted instead, i.e. a function that contains support values of the form $\{(\tau, K_p) \mid \tau \in \Omega_1\}$. The support values K_p for each τ are obtained as the solution of an optimization problem in respect with the structure given by Fig. 4.28. The top side marked structure refers to a simplified version of the NCS from Fig. 4.27, where the network is idealized as time delay elements. The bottom side marked structure refers to a reference model, in which the delay is placed outside the control loop. The output y_r of the reference model is considered as a reference trajectory, imposing some kind of performance profile. Thus, the optimization problem aims in minimizing the error ε between the reference trajectory y_r and the output of the control system y_p, for a given input reference signal w, for each frozen value of τ. By considering an ISE (integral of square error) type objective function, the optimization problem can be stated as

$$\underbrace{min}_{K_p \in [K_{p,min},\ K_{p,max}]} J(K_p), \quad J(K_p) = \sum_{k=1}^{m} \varepsilon^2[k], \tag{4.93}$$

where m is the maximum sample index chosen so that a steady state regime is practically reached, and $[K_{p,min}, K_{p,max}]$ is the allowed range of K_p.

For relatively large values of τ, improved results can be obtained with an IPTSE (integral of powered time-weighted square error) type objective function, for which the optimization problem is formulated as

$$\underbrace{\min}_{K_p \in [K_{p,min},\ K_{p,max}]} J(K_p), \quad J(K_p) = \sum_{k=1}^{m} k^{\chi} \varepsilon^2[k], \tag{4.94}$$

with $\chi>1$.

Both optimization problems – (4.93) and (4.94) – can be framed as classical nonlinear least squares problems with constraints, for which several efficient methods exist in the literature ([99]).

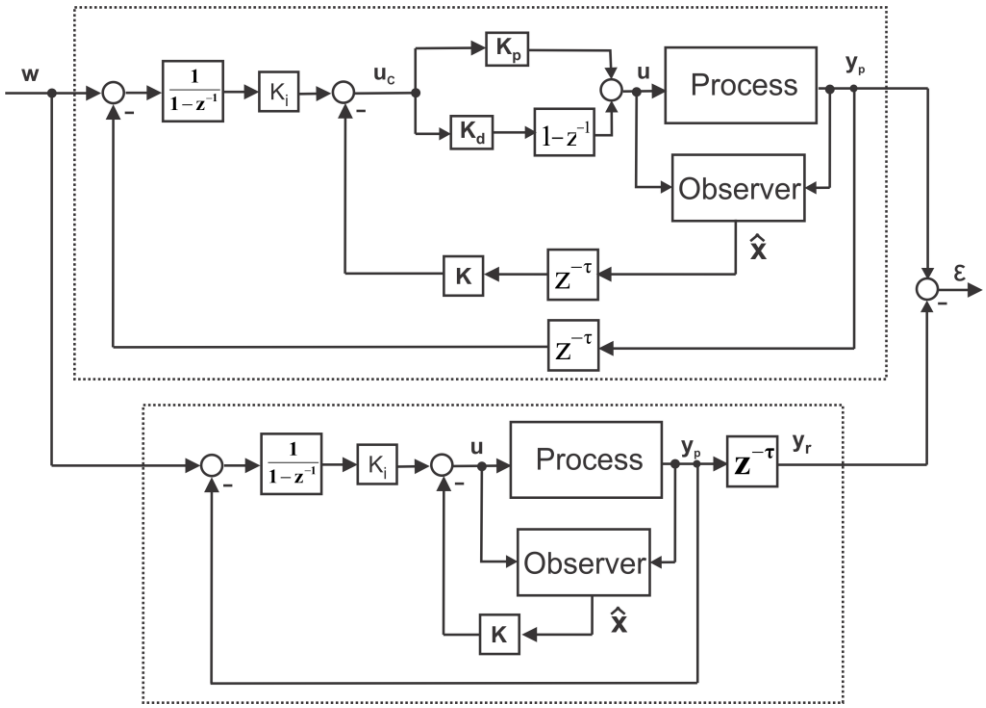

Fig. 4.28 - Control structure used for tuning the PD compensator through offline optimization.

4.2.2.3. Stability Analysis

In order to analyse the stability of the NCS from Fig. 4.27, a closed loop autonomous model is first assembled. The model is obtained by coupling the network model with an extended state space process model that aggregates the process state vector with scalar states corresponding to the PD compensator, auxiliary integrator and derivative components, respectively the exogenous system. The model is obtained through the following steps:

- a state space model is associated to the integrator component:

$$\begin{aligned} x_i[k+1] &= x_i[k] + h\,u_d[k] \\ u[k] &= x_i[k] + h\,u_d[k] \end{aligned} \tag{4.95}$$

where h is the sampling period;

- a state space model is associated to the PD compensator:

$$\begin{aligned} x_d[k+1] &= -K_d\, h^{-1} u_c[k] \\ u_d[k] &= x_d[k] + \left(K_p + K_d h^{-1}\right) u_c[k] \end{aligned} \tag{4.96}$$

- a state space model is associated to the derivative component

$$\begin{aligned} x_{di}[k+1] &= K_i\, w[k] + \underline{K}_2\, y_N[k] \\ u_c[k] &= x_{di}[k] - \underline{K}_1\, y_N[k] \end{aligned} \tag{4.97}$$

with $K_1=[\underline{K}\ -K_i]$ and $K_2=[-\underline{K}\ 0]$;

- a scalar state variable for the exogenous system is introduced as $x_w[k]=w[k]$, with the state space model

$$\begin{aligned} x_w[k+1] &= x_w[k] \\ w[k] &= x_w[k] \end{aligned} \tag{4.98}$$

- the extended state space process model is obtained by defining the aggregated state vector

  $x_e[k] = \left[\hat{x}^T[k]\ x^T[k]\ x_i[k]\ x_d[k]\ x_{di}[k]\ x_w[k]\right]^T$, which leads to

$$\underline{x}_e[k+1] = \underline{F}_e\, \underline{x}_e[k] + \underline{G}_e\, \underline{y}_N[k] \tag{4.99}$$

$$\underline{F}_e = \begin{bmatrix} \underline{F}_d - \underline{L}\underline{H}_d^T & \underline{L}\underline{H}_d^T & \underline{G}_d & \underline{G}_d h & \underline{G}_d\left(K_p h + K_d\right) & \underline{0}_{n_p\times 1} \\ \underline{0}_{n_p\times n_p} & \underline{F}_d & \underline{G}_d & \underline{G}_d h & \underline{G}_d\left(K_p h + K_d\right) & \underline{0}_{n_p\times 1} \\ \underline{0}_{1\times n_p} & \underline{0}_{1\times n_p} & 1 & h & K_p h + K_d & 0 \\ \underline{0}_{1\times n_p} & \underline{0}_{1\times n_p} & 0 & 0 & -K_d h^{-1} & 0 \\ \underline{0}_{1\times n_p} & \underline{0}_{1\times n_p} & 0 & 0 & 0 & K_i \\ \underline{0}_{1\times n_p} & \underline{0}_{1\times n_p} & 0 & 0 & 0 & 1 \end{bmatrix} \tag{4.100}$$

$$\underline{G}_e = \begin{bmatrix} -\underline{G}_d\left(K_p h + K_d\right)\underline{K}_1 \\ -\underline{G}_d\left(K_p h + K_d\right)\underline{K}_1 \\ -\left(K_p h + K_d\right) \\ K_d \underline{K}_1 h^{-1} \\ \underline{K}_2 \\ \underline{0}_{1\times n} \end{bmatrix}$$

- the extended process model is further coupled with the network model (2.23) through the state aggregation $\bar{\underline{x}}_N[k] = \left[\tilde{\underline{x}}_N^T[k]\ \underline{x}_e^T[k]\right]^T$, resulting the closed loop autonomous switched linear system:

$$\bar{\underline{x}}_N[k+1] = \bar{\underline{A}}_{a[k],\delta[k]}\, \bar{\underline{x}}_N[k] \tag{4.101}$$

where

$$\begin{aligned}\bar{\underline{A}}_{a[k],\delta[k]} &= \begin{bmatrix} \underline{A}_{a[k],\delta[k]} & \underline{B}_{a[k]}\underline{B}_1 \\ \underline{G}_{e,a[k]}\underline{C} & \underline{F}_{e,a[k]} \end{bmatrix}, \\ \underline{B}_1 &= \begin{bmatrix} \underline{I}_{n_p} & \underline{H}_d^T & 0 & 0 & 0 & 0 \end{bmatrix}.\end{aligned} \tag{4.102}$$

The fact that the PD parameters (K_d, K_p) are switched according to the switching signal $\alpha[k]$ was taken into account here through the matrices $\underline{F}_{e,\alpha[k]}$ and $\underline{G}_{e,\alpha[k]}$.

Next, consider the switching signal pairs $(a,\delta) \in \Psi=\Omega_1 x \Omega_2$ to be (i,j) at moment k and (u,v) at the consecutive sampling instance $k+1$. Then, the following theorem gives a sufficient condition for asymptotic stability for the closed loop model of the NCS (4.101).

Theorem 5. The autonomous switched linear system (4.101) is asymptotically stable if there exists positive definite symmetric matrices $\{\underline{P}_{i,j} \mid (i,j) \in \Psi\}$, such that

$$\bar{\underline{A}}_{i,j}^T \underline{P}_{u,v} \bar{\underline{A}}_{i,j} - \underline{P}_{i,j} < 0, \forall((i,j),(u,v)) \in \Psi \times \Psi \tag{4.103}$$

■

Proof. Let us consider the following switched quadratic Lyapunov candidate function of the form:

$$V[k] = \bar{\underline{x}}_N^T[k] \underline{P}_{a[k],\delta[k]} \bar{\underline{x}}_N[k] \tag{4.104}$$

used already in [93], but for a switched linear system with a single switching signal.

The difference of V is given by:

$$\begin{aligned}\Delta V &= V[k+1] - V[k] \\ &= \bar{\underline{x}}_N^T[k+1] \underline{P}_{a[k+1],\delta[k+1]} \bar{\underline{x}}_N[k+1] - \bar{\underline{x}}_N^T[k] \underline{P}_{a[k],\delta[k]} \bar{\underline{x}}_N[k] \\ &= \bar{\underline{x}}_N^T[k] \left[\bar{\underline{A}}_{a[k],\delta[k]}^T \underline{P}_{a[k+1],\delta[k+1]} \bar{\underline{A}}_{a[k],\delta[k]} - \underline{P}_{a[k],\delta[k]} \right] \bar{\underline{x}}_N[k]\end{aligned} \tag{4.105}$$

By considering (4.103), it follows that

$$\bar{\underline{A}}_{a[k],\delta[k]}^T \underline{P}_{a[k+1],\delta[k+1]} \bar{\underline{A}}_{a[k],\delta[k]} - \underline{P}_{a[k],\delta[k]} < 0 \tag{4.106}$$

Consequently, along each state trajectory $\Delta V < 0$ and the system is asymptotically stable.

□

By using the Schur complement formula, condition (4.103) of Theorem 5 can be reduced to the following LMI problem:

$$\begin{bmatrix} \underline{P}_{i,j} & \bar{\underline{A}}_{i,j}^T \underline{P}_{u,v} \\ \underline{P}_{u,v} \bar{\underline{A}}_{i,j} & \underline{P}_{u,v} \end{bmatrix} > 0, \forall((i,j),(u,v)) \in \Psi \times \Psi \tag{4.107}$$

4.2.2.4. Illustrative Example

Consider the same DC motor plant used in previous examples having the zero-order hold model given by

$$\begin{bmatrix} x_1[k+1] \\ x_2[k+1] \end{bmatrix} = \overbrace{\begin{bmatrix} 0.99 & 0.06 \\ -0.23 & 0.77 \end{bmatrix}}^{\underline{F}_d} \overbrace{\begin{bmatrix} x_1[k] \\ x_2[k] \end{bmatrix}}^{\underline{x}[k]} + \overbrace{\begin{bmatrix} 0.01 \\ 0.23 \end{bmatrix}}^{\underline{G}_d} u[k]$$
$$y[k] = \overbrace{\begin{bmatrix} 1 & 0 \end{bmatrix}}^{\underline{H}_d^T} \begin{bmatrix} x_1[k] \\ x_2[k] \end{bmatrix} \tag{4.108}$$

where x_1 represents the motor's speed, x_2 the armature current, and the sample rate is h=10 ms.

The plant is controlled via a communication network described by model (2.23) characterized by the parameter $r = \tau_{max} = 6$ and the sets $\Omega_1 = \{1, 2, 3, 4, 5, 6\}$ and $\Omega_2 = \{0, 1\}$. These correspond to a packet switched wide area communication network with a maximum RTT delay of 50 ms.

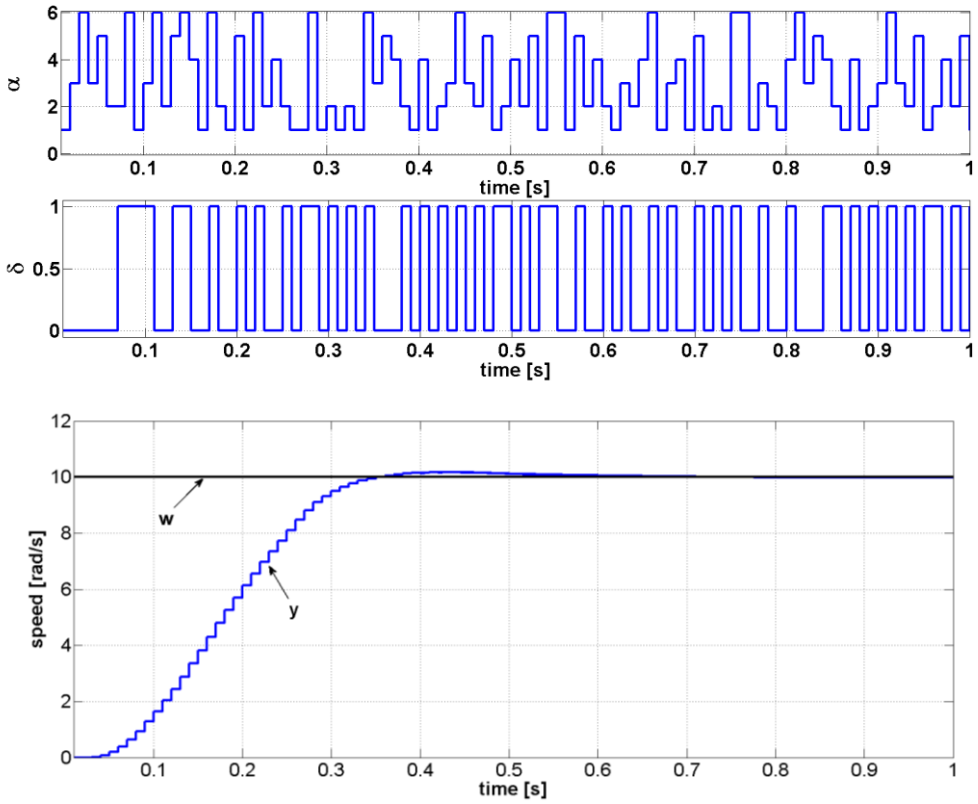

Fig. 4.29 - Simulations results.

The controller and the PD compensator were designed according to Section 4.2.2.2, and the following parameters were obtained: λ=0.2, K_i=32.54, $\underline{K}$=[4.35 1.01], and the set of triplets (τ, K_p, K_d) - {(1, 0.77, 0.0023), (2, 0.63, 0.0038), (3, 0.53, 0.0048), (4, 0.46, 0.0055), (5, 0.40, 0.0060), (6, 0.35, 0.0063)}. Then, the stability of the closed loop system of the form (4.101) was assessed. The multiple LMI conditions (4.107) are recasted as a single LMI, which is solved using CVX Toolbox for Matlab ([90]), by formulating the problem as a convex optimization one. A solution of the optimization problem was found (a set of $\underline{P}_{i,j}$ matrices), thus proving according to Theorem 5 that the system is stable.

Next, a scenario involving arbitrary variations of the switching signals α and δ (Fig. 4.29 – top) is adopted. The initial conditions for the plant states are null. A step reference signal is adopted w[k]=10 σ[k] rad/s. Fig. 4.29 - bottom shows the response of the control system from Fig. 4.27, which is characterized by a settling time of 0.33s, a null steady state error and no overshoot.

5. CONCLUSIONS

5.1. Summary and Contributions

The main contributions of the thesis are:

- Identification and definition in a systematic manner of network transmission issues, highlighting the possible irregular situations that appear in packet switched digital networks when using connectionless protocols (Chapter 1);
- Development of handling strategies for the irregular situations in order to assure optimal control performances (based on the principle of always using the latest available information) (Chapter 2);
- Development of a nonlinear network transmission model which captures from an input-output perspective the behaviour of a real packet switched network, characterized by time varying delays, packet loss and irregular situations, along with the imposed handling strategies (Chapter 2);
- Determination of a time-based switched linear system associated with the nonlinear network transmission model, as a theoretical tool for systems analysis, and an implementation algorithm as a network emulator for testing and validating of possible networked control solutions in both simulations and experiments (Chapter 2);
- Extension of a novel observer based delay compensation method for NCSs, recently proposed in the literature, for second order benchmark process models, which involves a more elaborate analysis and design approach due to additional degrees of freedom (design phase) and also because of the practical limitations identified in practice (testing and validation phase) (Chapter 4);
- Stability analysis and control synthesis for a networked control structure which includes the network transmission model proposed by the author, a linear plant and a switched state feedback controller (Chapter 4);
- Design and analysis of a new networked control structure with a switched PD time-delay compensator and a state observer placed locally (collocated along with the plant), the network transmission model proposed by the author and a remotely placed state feedback controller (Chapter 4).

The thesis begins with a short introduction on NCS, identifying the possible issues that emerge during network transmissions and further states the motivation and objectives of the study.

The analysis of a NCS imposes the use of a mathematical model for network transmissions. Most models found in the specialized literature only partially capture the characteristics of network transmissions (time-varying delays, packet loss, irregular situations, and handling strategies). To fill this gap a new nonlinear state-space model for network transmissions is proposed, which correctly describes the network dynamics from an input-output perspective. In order to further facilitate the

analysis and syntheses of NCS the nonlinear network transmission model is brought to the form of a time based switched linear system. Additionally, a simple algorithm is associated to the network transmission model, which can be used as a network emulator for testing and validation of NCS through simulations and experiments. A wide variety of network transmission scenarios can be prescribed to the algorithm, either by generating the corresponding inputs for the algorithm (time delay, packet loss) or by using a priori measured data from real networks.

The design of NCS imposes new control strategies for dealing with the network induced disturbances. An outline of several control strategies used for NCSs is presented. Alternative control structures are further proposed for the stabilization and tracking problems, with an efficient complexity versus performance design.

The first structure is based on local and remote placed observers to compensate the shortcomings associated with time delays and packet loss in NCSs, in order to meet the tracking control objective. The CDOB based method, recently proposed in the literature for first order processes, is extended here for second order benchmark processes. The additional degrees of freedom involve an elaborate design, and require a more extensive analysis in order to set the observers' parameters (cut-off frequencies). The analysis also captures a peaking phenomenon (no previously shown in the literature), which, from a practical point of view, limits the range of the design parameters. Moreover, a comparative analysis is conducted for determining which type of observer ensures the best performances (full order versus reduced order). The full order CDOB proved to be more efficient. Finally, the design NCS is tested through both simulations and experiments, using the proposed network emulator.

The second structure, addresses the stabilization problem for an NCS, and includes the recently proposed time-based switched linear system associated to the network transmissions. The obtained closed-loop NCS model is defined as a switched linear system with multiple switching signals. By adopting a switched quadratic Lyapunov function, used also as a tool for designing a switched state feedback controller, the asymptotic stability of the switched NCS is proved under arbitrary switching. The stability and control design problems are formulated in terms of LMI-based conditions. Lastly, a numerical example shows the main steps of the stabilization approach.

The third networked control structure, is based on a remote placed controller and a local delay compensator, and addresses the tracking control objective. The closed loop model, which includes the time-based switched linear system associated to the network transmissions, is also defined as a switched linear system. A control design methodology is presented, which combines both analytical and numerical technics (pole placement, tuning rule, numerical optimization). The stability of the closed loop system is proven for arbitrary switching by using a switched quadratic Lyapunov function. Next, an example illustrates the effectiveness of the control solution. As a remark, it is important to highlight the twofold advantage of placing the delay compensator locally. Firstly, this permits a compensation of the RTT delay (instead of just OWD). Secondly, because only the RTT delay needs to be measured the synchronization issue is eliminated because the measurements are always done in respect with the same clock.

5.2. Suggestions of Future Research

Some of the possible future research directions are:

- A straightforward extension for the network transmission model would imply the development of a stochastic model that correlates different network parameters with the time delay and packet loss flag values;
- The observer based delay compensation structure can be extended for different types of observers, like the unknown input observer.

APPENDIX 1– A MOTIVATING EXAMPLE

In order to motivate the current study a telecontrol application example is presented that illustrates the destabilizing effect of the time delays and information loss that occur in network transmissions on a NCS ([100]). The system's controller has the additional burden of compensating the effect of the network. In this context, an efficient approach is to add an additional compensator block which would reject the disturbances caused by data transmissions over the network. Additionally, because network transmissions behave in a time-varying manner (time varying delay and a time varying rate of packet loss), the compensator has to work adaptively, by continuously tuning to these variations.

Based on the above considerations, the example uses the generic control structure presented in Fig. A1.1. The controller block is first designed in order to dictate the dynamic behaviour of the process assuming instantaneously and flawless transmissions over the communication channels. A compensator is then connected in series with the controller, and has the role of compensating the transmission delays and information loss. The compensator's behaviour is continuously adapted through an Adaptation Mechanism block according to the varying behaviour of network transmissions.

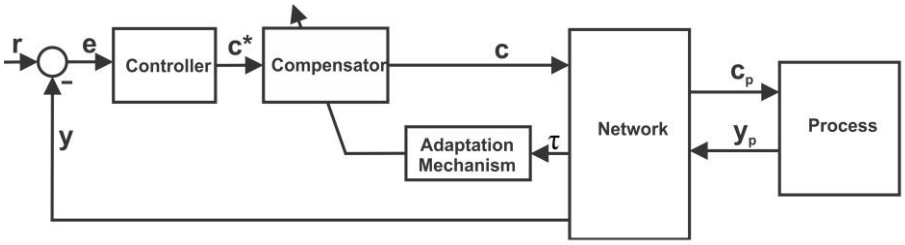

Fig. A1.1 - Adaptive control structure for a NCS

A1.1. Experimental Framework and Scenario

The telecontrol application uses the same experimental setup presented in Fig. 4.19. The goal is to control the motor's speed and reject the effect of network delays and packet loss.

The controller was developed in the Matlab/Simulink environment and implemented on to the dSPACE system. The experimental data was collected on a computer connected to the dSPACE system.

The communication network is emulated on the dSPACE system through the algorithm presented in Chapter 2 and uses a priori measurements from a real TCP/IP network. Basically, the algorithm applies two types of operations to the input signals of the communication network: a time shift (time delay) and a signal deformation (packet loss).

To obtain the time delay measurements for different types of TCP/IP networks, a software module based on client server architecture was designed and implemented on two hardware machines running a real time operating system. The

machines' internal clocks were synchronized using GPS clocks directly connected to each machine and a software product implementing the network time protocol version 4. UDP packets of 512 bytes were used to transfer control information between the two network nodes to assure enough space even for complex control data structure. The software also registers the information about data packets loss and implements the corrections for the irregular situations described in Chapter 2.

Data used for experiments was collected from two networks: a continental wide area network (WAN1) and an intercontinental wide area network (WAN2). Time delays were estimated over a period of 20 s. For WAN1 time delays have an average of 11 ms with maximum value of 160 ms (Fig. A1.2). For WAN2 time delays were significantly lager, around 97 ms (Fig. A1.3).

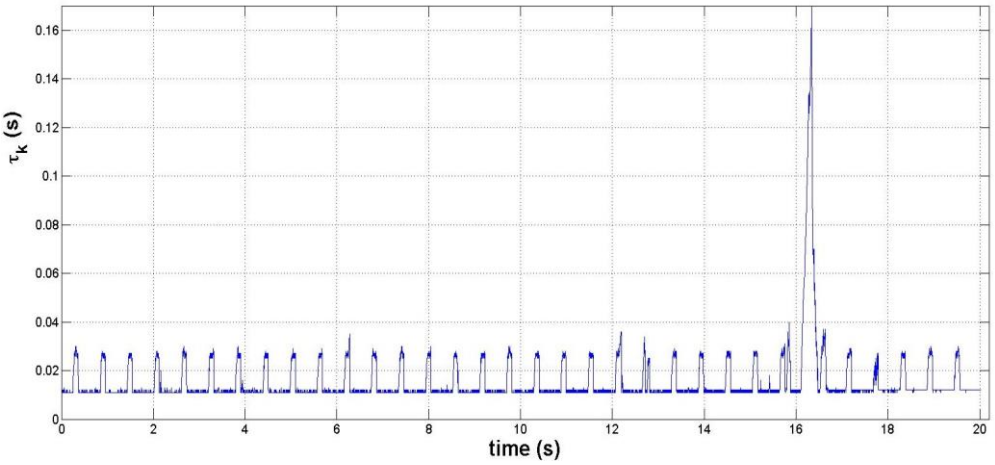

Fig. A1.2 - Network delay measurements – WAN1

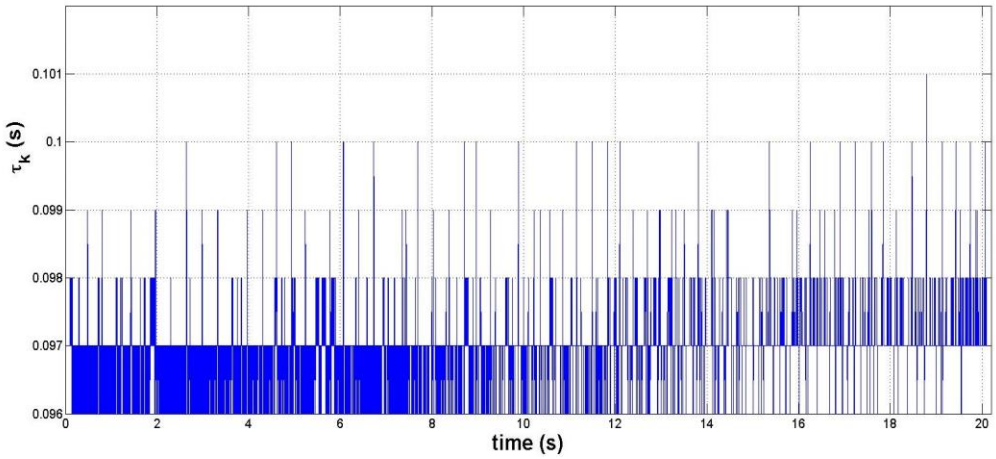

Fig. A1.3 - Network delay measurements – WAN2

A1.2. The Control Structure and Design Issues

The control structure implemented for the telecontrol application corresponds to the one from Fig. A1.1 and is illustrated in Fig. A1.4. Here the gains of the PI controller are $Kp^*=1.2$ and $Ki^*=3$. An adaptive PD compensator, of gains Kp, Kd and interpolative blocks I-Kp and I-Kd, is used. The input-output characteristics (as functions of time delay) of these two interpolative blocks are shown Fig. A1.5. Additionally to Fig. A1.1, a new interpolative block was added (ISC block) with the inverse static characteristic of the process (electric drive + DC motor + tachogenerator), which has the role of compensating the static nonlinearity of the process (the linearization details are presented in Chapter 4). The Network System block embeds the algorithm and measurements described in Chapter 2.

In designing the entire control structure the following three steps were executed:

First, an inverse nonlinear static characteristic was built that would compensate the static nonlinearity of the process (the static characteristic of the process was determined from experimental measurements). This inverse static characteristic was implemented through an interpolation block and placed in series with the process (up-stream).

Second, the PI controller was designed with the Ziegler–Nichols tuning method for the linearized process (the inverse static characteristic in series with the actual process) without the Network System block.

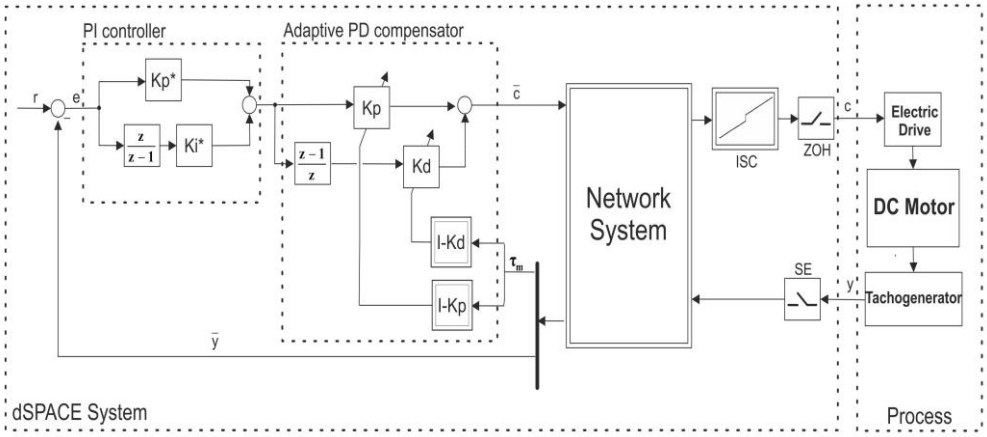

Fig. A1.4 - Telecontrol scheme for speed control of a DC motor (c is the voltage command signal, y is the measured speed, r is the prescribed speed, e is the control error, ZOH is a zero order holder, SE is a sample element and ISC is an inverse static characteristic)

Third, the adaptive PD compensator was designed. As it can be observed from Fig. A1.5, the parameters of the PD compensator are adapted continuously through two interpolation blocks based on the actual measurements of the network delay. These two interpolative blocks contain actually static characteristics which were built based on the parameter values determined for different constant delay values in the interval [0 - 2] seconds (support points for the interpolative blocks I-K_p and I-K_d). This range was adopted based on measurements like the ones from Fig. A1.2 and Fig. A1.3.

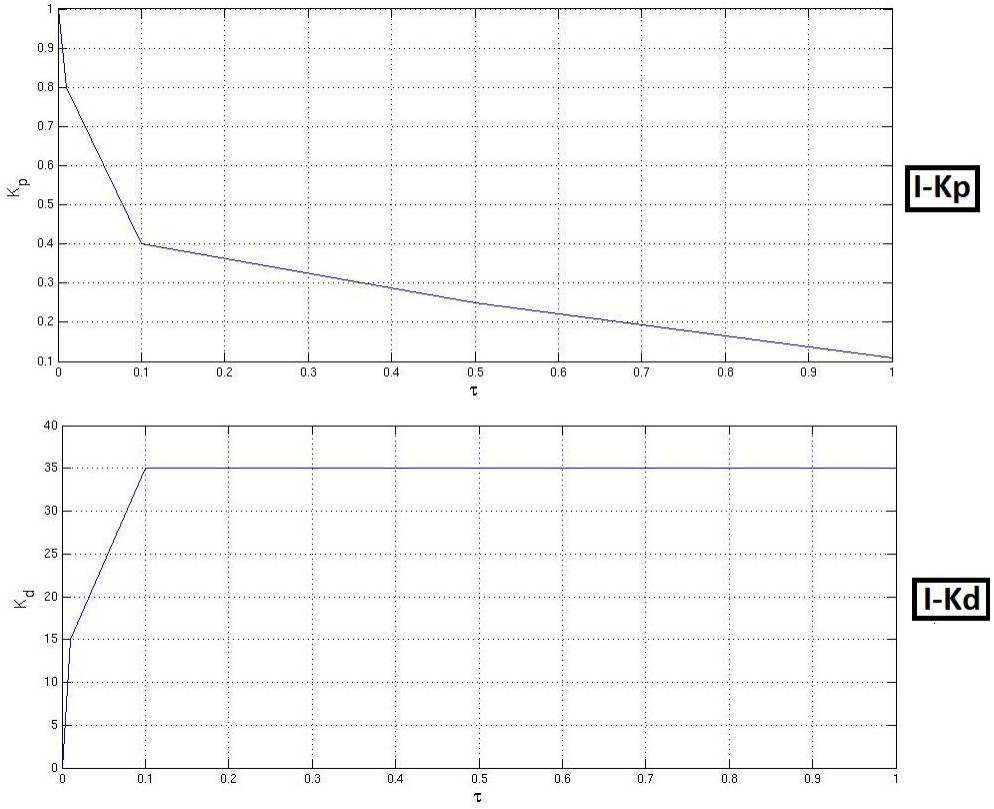

Fig. A1.5 - Input-output characteristic of the interpolative blocks I-Kd and I-Kp

It is important to mention, also, that a further adjustment of the adaptation algorithm consisted in multiplying by two the estimated network delay τ_m at the input of the compensator blocks. Based on the measurements, this multiplication was made under the assumption that the transmission channels on the direct path and on feedback path are similar. Thus, the time delay on the direct path at a given moment was considered to be equal to the latest estimated delay τ_m on the feedback path.

The entire control system uses the sample time h= 1 ms, considered also in the measurements from the network. This small sample period imposed the use of UDP as a transport protocol for the Network System. Moreover, due to the 1 ms sample time and the delay variation interval of [0 - 2] seconds all the irregular situations described in Chapter 2 occur.

A1.3. Experimental Results

For the telecontrol application previously described two experimental scenarios were considered: one for the continental wide area network (WAN1) and one for the intercontinental wide area network (WAN2). In each scenario the behaviour of the system was tested with and without the adaptive PD compensation.

Fig. A1.6 shows the system's response for the WAN1 scenario when there is no adaptive PD compensation. The delays and packet loss induced by the network

transmission lead to oscillations in the system's response which are finally damped by the control structure (the stationary error becomes zero). The overshoot is relatively large – about 20% and further adjustment of Kp^*, Ki^* have a small influence.

Fig. A1.7 presents the system's response for WAN1 when the adaptive PD compensation is used. The compensation eliminates the oscillations completely (no overshoot), but with the price of slightly increasing the settling time.

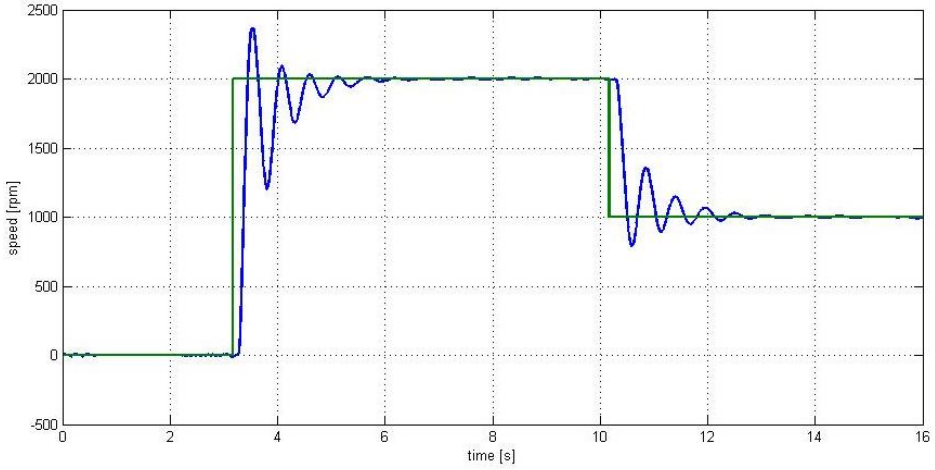

Fig. A1.6 - Response of the telecontrol system without adaptive PD compensation, when using WAN1

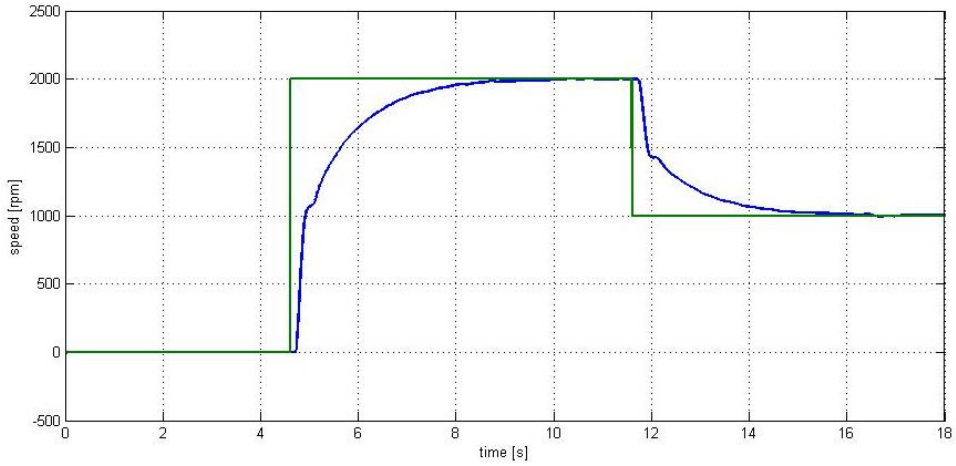

Fig. A1.7 - Response of the telecontrol system with the adaptive PD compensation, when using WAN1

In the WAN2 scenario the results become even more relevant. When the adaptive PD compensators are not included in the control structure, the system enters a state of permanent oscillations (Fig. A1.8) – the control objective is not achieved.

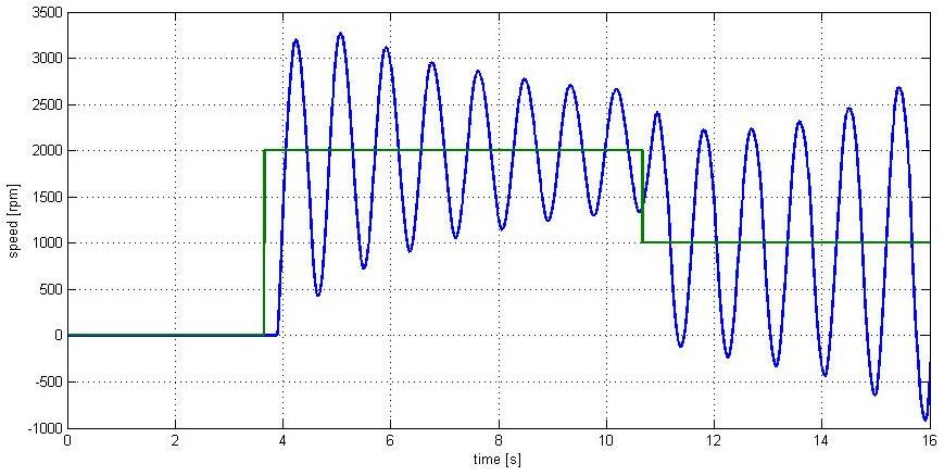

Fig. A1.8 - Responses for the NCS without the adaptive PD compensators, when using WAN2

Fig. A1.9 shows the system's response when the adaptive PD compensators are used.

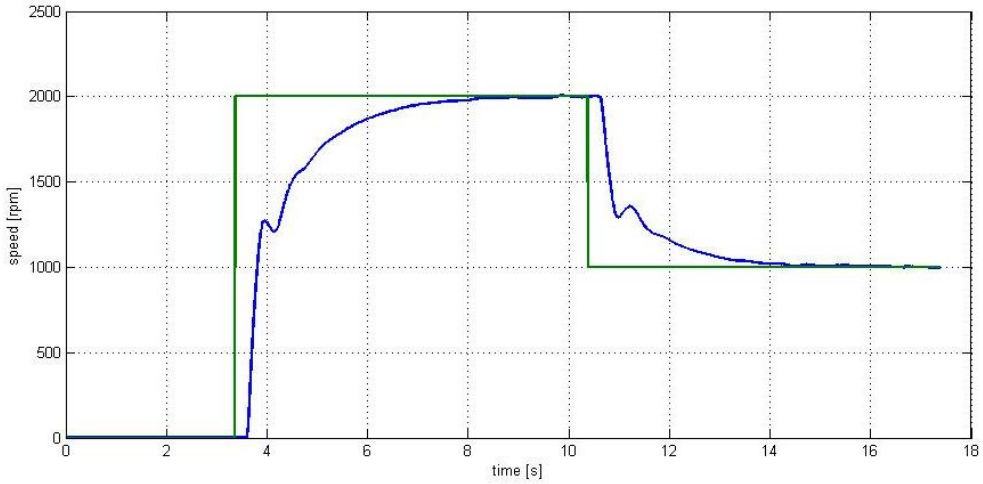

Fig. A1.9 - Responses for the NCS with the adaptive PD compensators, when using WAN2

Similar to the previous scenario, the compensation is successful and the oscillations are eliminated.

REFERENCES

[1] W. Zhang, "Stability Analysis of Networked Control Systems," Case Western Reserve University, Cleveland, Ph.D. Thesis 2001.

[2] S. Zampieri, "Trends in Networked Control Systems," in *Proceedings of the 17th IFAC World Congress*, Seoul, 2008, pp. 2886-2894.

[3] J. P. Hespanha, P. Naghshtabrizi, and Y. Xu, "A survey of Recent Results in Networked Control Systems," *Proc. IEEE*, vol. 95, no. 1, pp. 138-162, January 2007.

[4] S.Y. Nof, Ed., *Springer Handbook of Automation*.: Springer-Verlag, 2009, ch. 13, pp. 237-248.

[5] J. Leen and D. Heffernan, "Expanding Automotive Electronic Systems," *IEEE Computer*, vol. 35, no. 1, pp. 88-93, 2002.

[6] K. Natori, T. Tsuji, K. Ohnishi, A. Hace, and K. Jezernik, "Time-Delay Compensation by Communication Disturbance Observer for Bilateral Teleoperation Under Time-Varying Delay," *IEEE Transactions on Industrial Electronics*, vol. 57, no. 3, pp. 1050–1062, March 2010.

[7] J. Arata et al., "A remote surgery experiment between Japan and Thailand over Internet using a low latency CODEC system," in *Proc. of the IEEE International Conference on Robotics and Automation*, Rome, 2007, pp. 953-959.

[8] P. Seiler and R. Sengupta, "Analysis of communication losses in vehicle control problems," in *Proc. of American Control Conference*, Arlington, 2001, pp. 1491-1496.

[9] P. F. Hokayem and C.T. Abdallah, "Inherent Issues in Networked Control Systems: A Survey," in *Proc. American Control Conference*, Boston, 2004, pp. 4897–4902.

[10] B. M. Wilamowski and J.D. Irwin, Eds., *Industrial Communication Systems*.: CRC Press, 2011.

[11] T. Kailath, *Linear Systems*.: Prentice Hall, 1980.

[12] H. Khalil, *Nonlinear Systems*.: Prentice Hall, 2002.

[13] J.J. Slotine and W. Li, *Applied Nonlinear Control*.: Prentice Hall, 1991.

[14] G.F. Franklin, J.D. Powell, and M. Workman, *Digital Control of Dynamic Systems*.: Pearson Education, 2005.

[15] G.F. Franklin, J.D. Powell, and A. Emami-Naeini, *Feedback Control of Dynamic Systems*.: Prentice Hall, 2009.

[16] W.S. Levine, Ed., *Control Handbook*, 2nd ed.: CRC Press, 2010.

[17] D. Hristu-Varsakelis and W.S. Levine, Eds., *Handbook of Networked and Embedded Control Systems*. Boston: Birkhauser, 2005.

[18] K. Davis. (2010, Jan.) Understanding Latency in Network Systems, Tutorial. [Online]. www.netqos.com

[19] (2013, Apr.) What is Network Latency and Why Does It Matter? [Online]. http://www.o3bnetworks.com/media/40980/white%20paper_latency%20matters.pdf

[20] (2013, Apr.) Latency and Network Jitter. [Online]. http://www.latencystats.com/blog/latency-and-network-jitter

[21] (2013, Apr.) Latency on a Switched Ethernet Network. [Online]. http://www.ruggedcom.com/pdfs/application_notes/latency_on_a_switched_ethernet_network.pdf

[22] CISCO. (2013, Apr.) Design Best Practices for Latency Optimization. [Online]. http://www.cisco.com/application/pdf/en/us/guest/netsol/ns407/c654/ccmigration_09186a008091d542.pdf

[23] K. J. Åström and B. Wittenmark, *Computer-Controlled Systems*.: Prentice Hall, 1997, pp. 38-41.

[24] P.M. Colom, "Analysis and Design of Real-Time Control Systems with Varying Control Timing Constraints," Polytechnic University of Catalonia, Barcelona, Ph.D. Thesis 2002.

[25] D.L. Mills, *Computer Network Time Synchronization: the Network Time Protocol on Earth and in Space*, 2nd ed.: CRC Press, 2011.

[26] D. Dzung, M. Naedele, T.P. Von Hoff, and M. Crevatin, "Security for Industrial Communication System," *Proc. of the IEEE*, vol. 93, no. 6, pp. 1152-1177, 2005.

[27] G.N. Nair and R.J. Evans, "Exponential Stabilisability of Finite-Dimensional Linear Systems with Limited Data Rates," *Automatica*, vol. 39, no. 4, pp. 585-593, 2003.

[28] S.C. Tatikonda, "Control under Communication Constraints," Massachusetts Institute of Technology, Cambridge, PhD Thesis 2000.

[29] N. Elia and S.K. Mitter, "Stabilization of Linear Systems with Limited Information," *IEEE Transactions on Automatic Control*, vol. 46, no. 9, pp. 1384-1400, 2001.

[30] A. S. Tanenbaum and D.J. Wetherall, *Computer Networks*, 5th ed.: Prentice Hall, 2010.

[31] C. Aubrun, D. Simon, and Y.Q. Song, "QoC-aware Dynamic Network QoS Adaptation," in *Co-Design Approaches for Dependable Networked Control Systems*.: Wiley - ISTE, 2010, pp. 105–148.

[32] Y. Tipsuwan and M.-Y. Chow, "Control methodologies in networked control systems," *Control Engineering Practice*, vol. 11, pp. 1099–1111, 2003.

[33] M.G. Rivera and A. Barreiro, "Analysis of networked control systems with drop and variable delays," *Automatica*, vol. 43, pp. 2054-2059, 2007.

[34] W.-A. Zhang and L. Yu, "Modelling and control of networked control systems with both networked-induced delay and packet-dropout," *Automatica*, vol. 44, pp. 3206-3210, 2008.

[35] H. Li, Z. Sun, M.-Y. Chow, and F. Sun, "Gain-Scheduling-Based State Feedback Integral Control of Networked Control Systems," *IEEE Transactions on Industrial Electronics*, vol. 58, no. 6, pp. 2465-2472, June 2011.

[36] Y. Shi and B. Yu, "Robust mixed H2/Hinf control of networked control systems with random time delays in both forward and backward communication links," *Automatica*, vol. 47, pp. 754-760, 2011.

[37] C. Han, H. Zhang, and M. Fu, "Optimal filtering for networked systems with Markovian communication delays," *Automatica*, vol. 49, pp. 3097-3104, 2013.

[38] J. Wu and T. Chen, "Design of networked control systems with packet dropouts," *IEEE Transactions on Automatic Control*, vol. 52, no. 7, pp. 1314-1319, July 2007.

[39] Y. Liang, T. Chen, and Q. Pan, "Optimal linear state estimator with multiple packet dropouts," *IEEE Transactions on Automatic Control*, vol. 55, no. 6, pp. 1428-1433, June 2010.

[40] R. Yang, P. Shi, and G.-P. Liu, "Filtering for discrete-time networked nonlinear systems with mixed random delays and packet dropouts," *IEEE Transactions on Automatic Control*, vol. 56, no. 11, pp. 2655-2660, November 2011.

[41] N. Elia and J. Eisenbeis, "Limitations of linear control over packet drop networks," *IEEE Transactions on Automatic Control*, vol. 56, no. 4, pp. 826-841, April 2011.

[42] **O. Stefan**, T.-L. Dragomir, A. Codrean, and I. Silea, "Issues of identifying, estimating and using delay times in telecontrol systems based on TCP/IP networks," in *Proc. 2nd IFAC Symposium on Telematics Applications*, Timisoara, 2010, pp. 143-148.

[43] **O. Stefan**, A. Codrean, and T.-L. Dragomir, "A Nonlinear State Space Model of Network Transmissions in a Network Control System," *Journal of Control Engineering and Applied Informatics*, vol. 13, no. 4, pp. 58-63, 2011.

[44] A. Cervin, D. Henriksson, B. Lincoln, J. Eker, and K.-E. Årzén, "How Does Control Timing Affect Performance? Analysis and Simulation of Timing Using

Jitterbug and TrueTime," *IEEE Control Systems Magazine*, vol. 23, no. 3, pp. 16-30, 2003.

[45] (2011, June) Simulink Documentation. [Online]. http://www.mathworks.com/help/simulink/index.html

[46] R. Shorten, F. Wirth, O. Mason, K. Wulff, and C. King, "Stability Criteria for Switched and Hybrid Systems," *SIAM Review,* vol. 49, no. 4, pp. 545-592, 2007.

[47] W. Zhang, M.S. Branicky, and S.M. Phillips, "Stability of Networked Control Systems," *IEEE Control Systems Magazine*, vol. 21, no. 1, pp. 84-99, 2001.

[48] D. Liberzon, *Switching in Systems and Control*. Boston: Birkhäuser, 2003, ch. 1.

[49] L. Zhang, H. Gao, and O. Kayanak, "Network-Induced Constraints in Networked Control Systems - A Survey," *IEEE Transactions on Industrial Informatics*, vol. 9, no. 1, pp. 403-416, 2013.

[50] K. Gu, V. Kharitonov, and J. Chen, *Stability of time-delay systems*. Boston: Birkhauser, 2003.

[51] S.-I. Niculescu, *Delay Effects on Stability: A Robust Control Aproach*. New York: Springer, 2001.

[52] J.-P. Richard, "Time delay systems: An overview of some recent advances and open problems," *Automatica*, vol. 39, pp. 1667-1694, 2003.

[53] A. Codrean, **O. Stefan**, and T.-L. Dragomir, "Design, analysis and validation of an observer-based delay compensation structure for a Network Control System," in *Mediterranean Conference on Control & Automation*, Barcelona, 2012, pp. 928-934.

[54] **O. Stefan**, A. Codrean, and T.-L. Dragomir, "A Network Control Structure with a Switched PD Delay Compensator and a Nonlinear Network Model," in *American Control Conference*, Washington, 2013, pp. 758-764.

[55] C.F. Caruntu, "Networked Predictive Control for Fast Processes," "Gheorghe Asachi" Technical University of Iasi, Iasi, PhD Thesis 2011.

[56] C.-L. Lai and P.-L. Hsu, "Design the Remote Control System With the Time-Delay Estimator and the Adaptive Smith Predictor," *IEEE Transactions on Industrial Informatics*, vol. 6, no. 1, pp. 73-80, February 2010.

[57] C. F. Caruntu and C. Lazar, "Networked Predictive Control for Time-varying Delay Compensation with an Application to Automotive Mechatronic Systems," *Journal of Control Engineering and Applied Informatics*, vol. 13, no. 4, pp. 19-25, 2011.

[58] P. LoonTang and C.W. de Silva, "Compensation for Transmission Delays in an Ethernet-Based Control Network Using Variable-Horizon Predictive Control,"

IEEE Transaction on Control System Technology, vol. 14, no. 4, pp. 707-718, 2006.

[59] A. Onat, T. Naskali, E. Parlakay, and O. Mutluer, "Control Over Imperfect Networks: Model-Based Predictive Networked Control Systems," *IEEE Transactions on Industrial Electronics*, vol. 58, no. 3, pp. 905–913, March 2011.

[60] X. Wang and M.D. Lemmon, "Event-Triggered in Distributed Networked Control Systems," *IEEE Transactions On Automatic Control*, vol. 56, no. 3, pp. 586-601, 2011.

[61] M. Lemmon, "Event-Triggered Feedback in Control, Estimation and Optimization in Network Control Systems," in *Lecture Notes in Control and Information Sciences*, A. Bemporard, M. Heemels, and M. Johansson, Eds.: Springer, 2010, pp. 293-358.

[62] P. Varutti and R. Findeisen, "Event-based NMPC for Networked Control Systems over UDP-like Communication Channels," in *American Control Conference*, San Francisco, 2011, pp. 3166-3171.

[63] W. Hu, G. Liu, and D. Rees, "Event-Driven Network Predictive Control," *IEEE Transactions on Industrial Electronics*, vol. 54, no. 3, pp. 1603-1613, 2007.

[64] J. Nilsson, "Real-time control systems with delay," Lund Institute of Technology, Lund, Ph.D. Thesis 1998.

[65] B. Lincoln and B. Bernhardsson, "Optimal Control over Networks with Long Random Delays," in *Symposium on Mathematical Theory of Networks and Systems*, 2000.

[66] L. Schenato, B. Sinopoli, M. Franceschetti, K. Poolla, and S.S. Sastry, "Foundations of Control and Estimation Over Lossy Networks," *Proceedings of the IEEE*, vol. 95, no. 1, pp. 163-187, 2007.

[67] F. Goktas, "Distributed control of systems over communication networks," University of Pennsylvania, Ph.D. Thesis 2000.

[68] H. Gao and T. Chen, "Network-based H∞ Output Tracking Control," *IEEE Transactions on Automatic Control*, vol. 53, no. 3, pp. 655-667, 2008.

[69] H. Chan and U. Ozguner, "Closed-loop control of systems with communication network with queues," *International Jurnal of Control*, vol. 62, no. 3, pp. 493-510, 1995.

[70] A. Seuret, F. Michaut, J,-P. Richard, and T. Divoux, "Networked Control using GPS synchronization," in *American Control Conference*, Minneapolis, 2006, pp. 4195-4200.

[71] R. Luck and A. Ray, "Experimental verification of a delay compensation algorithm for integrated communication and control systems," *International Jurnal of Control*, vol. 59, no. 6, pp. 1357-1372, 1994.

[72] K.J. Åström and B. Wittenmark, *Adaptive Control*, 2nd ed.: Dover, 2008.

[73] K.J. Åström and T. Hagglund, *PID Controllers: Theory,Design and Tuning*, 2nd ed.: The Instrumentation Systems and Automation Society, 1995.

[74] L.M. Eriksson and M. Johansson, "PID Controller Tuning Rules for Varying Time-Delay Systems," in *American Control Conference*, New York, 2007, pp. 619-625.

[75] M.-Y. Chow and Y. Tipsuwan, "Gain Adaptation of Networked DC Motor Controllers Based on QoS Variations," *IEEE Transactions on Industrial Electronics*, vol. 50, no. 5, pp. 936-943.

[76] G. Nikolakopoulos, A. Panousopoulou, and A. Tzes, "Switched Feedback Control for Wireless Networked Systems," in *Networked Control Systems: Theory and Applications*, F.-Y. Wang and D. Liu, Eds.: Springer, 2008, ch. 6.

[77] L. Hetel, "Robust stability and control of switched linear systems," Institut National Polytechnique de Lorraine, Nancy, PhD Thesis 2007.

[78] S. Miani and A.C. Morassutti, "Switching controllers for networked control systems with packet dropouts and delays in the sensor channel," in *IFAC Workshop on Estimation and Control of Networked Systems*, 2008, pp. 334-339.

[79] A. Kruszewski, W.-J. Jiang, E. Fridman, J.P. Richard, and A. Toguyeni, "A Switched System Approach to Exponential Stabilization Through Communication Network," *IEEE Transactions on Control Systems Technology*, vol. 20, no. 4, pp. 887-900, 2012.

[80] K. Wulff, "Quadratic and Non-Quadratic Stability Criteria for Switched Linear Systems," National University of Ireland, Maynooth, Ireland, Ph.D. Thesis 2005.

[81] S.-Y. Cheong and M.G. Safonov, "Slow-Fast Controller Decomposition Bumpless Transfer for Adaptive Switching Control," *IEEE Transactions on Automatic Control*, vol. 57, no. 3, pp. 721-726, 2012.

[82] I. Malloci, L. Hetel, J. Daafouz, C. Iung, and P. Szczepanski, "Bumpless transfer for switched linear systems," *AUtomatica*, vol. 48, pp. 1440-1446, 2012.

[83] M. Hou and P.C. Müller, "Design of Observers for Linear Systems with Unknown Inputs," *IEEE Transactions on Automatic Control*, vol. 37, no. 6, pp. 871-875, June 1992.

[84] A. Radke and Z. Gao, "A Survey of State and Disturbance Observers for Practitioners," in *American Control Conference*, Minneapolis, 2006, pp. 5183-5188.

[85] (2011, January) System Identification Toolbox. [Online]. http://www.mathworks.com/products/sysid/

[86] D. G. Luenberger, "An Introduction to Observers," *IEEE Transactions on Automatic Control*, vol. 16, no. 6, pp. 596-602, December 1971.

[87] Y. He, Q.-G. Wang, C. Lin, and M. Wu, "Delay-range-dependent stability for systems with time-varying delay," *Automatica*, vol. 43, pp. 371-376, 2007.

[88] J.K. Hale and S.M. Verduyn Lunel, *Introduction to Functional Differential Equations*.: Springer, 1993.

[89] K. Natori, R. Oboe, and K. Ohnishi, "Stability Analysis and Practical Design Procedure of Time Delayed Control Systems with Communication Disturbance Observer," *IEEE Transactions on Industrial Informatics*, vol. 4, no. 3, pp. 185-197, 2008.

[90] M. Grant and S. Boyd. (2011, April) CVX: Matlab Software for Disciplined Convex Programming. [Online]. http://cvxr.com/cvx/

[91] **O. Stefan**, A. Codrean, and T.-L. Dragomir, "Stability analysis and control synthesis for a Network Control System using a nonlinear Network Transmission Model-a switched system approach," in *IEEE International Conference on Control Applications*, Dubrovnik, 2012, pp. 885-890.

[92] **O. Stefan**, A. Codrean, and T.-L. Dragomir, "Design and analysis of a network control structure with a switched PD compensator," in *International Conference on Methods and Models in Automation and Robotics*, Międzyzdroje, 2012, pp. 403-408.

[93] J. Daafouz, P. Riedinger, and C. Iung, "Stability Analysis and Control Synthesis for Switched Systems: A switched Lyapunov function approach," *IEEE Transactions on Automatic Control*, vol. 47, no. 11, pp. 1883-1887, November 2002.

[94] S. Boyd, L. E. Ghaoui, E. Feron, and V. Balakrishnan, *Linear Matrix Inequalities in System and Control Theory*. Philadelphia: SIAM, 1994.

[95] M.B.G. Cloosterman et al., "Controller synthesis for networked control systems," *Automatica*, vol. 46, pp. 1584-1594, 2010.

[96] I. Kaminer, A.M. Pascoal, P.P. Khargonekar, and E.E. Coleman, "A velocity algorithm for the implementation of gain scheduled controllers," *Automatica*, vol. 31, pp. 1185-1191, 1995.

[97] L. Eriksson, "PID Controller Design and Tuning in Networked Control Systems," Helsinki University of Technology, Espoo, Ph.D. Thesis 2008.

[98] L. Hetel, J. Daafouz, J.P. Richard, and M. Jungers, "Delay-dependent sampled-data control based on delay estimates," *Systems & Control Letters*, vol. 60, pp. 146-150, 2011.

[99] Å. Björck, *Numerical Methods for Least Squares Problems*. Philadelphia: SIAM, 1996.

[100] **O. Stefan**, A. Codrean, T.-L. Dragomir, and I. Silea, "Time delay and information loss compensation in a network control system for a DC motor," in *IEEE International Symposium on Applied Computational Intelligence and Informatics*, Timisoara, 2011, pp. 131-135.